EFFICIENT ANALYSIS OF INTERCONNECT NETWORKS WITH FREQUENCY DEPENDENT LOSSY TRANSMISSION LINES

Ling Y. Li

A Thesis
Submitted to the Faculty of Graduate Studies
in Partial Fulfillment of the Requirements
for the Degree of

Doctor of Philosophy

Department of Electrical and Computer Engineering
The University of Manitoba
Winnipeg, Manitoba, Canada

March 2005

THE UNIVERSITY OF MANITOBA

FACULTY OF GRADUATE STUDIES

*****

COPYRIGHT PERMISSION

"Efficient Analysis of Interconnect Networks with Frequency Dependent Lossy Transmission Lines"

BY

Ling Y. Li

A Thesis/Practicum submitted to the Faculty of Graduate Studies of The University of Manitoba in partial fulfillment of the requirement of the degree

Of

DOCTOR OF PHILOSOPHY

Abstract

Model order reduction techniques, such as the moment matching based Padé approximation methods, have recently been introduced as new computer-aided design tools for the analysis of interconnect networks. Techniques based on model order reduction have demonstrated a high computational efficiency in solving interconnect problems as compared with conventional simulation methods.

This thesis presents a multipoint Padé approximation based method to analyze interconnect networks containing frequency-dependent multiconductor transmission lines. The proposed method yields reduced-order frequency–domain and time-domain solutions of the interconnect problems by using all the moment sets available at all frequency expansion points. Since the computation effort associated with multipoint moment matching techniques is proportional to the number of expansion points, a new algorithm for the selection of expansion points is developed. As a result, the proposed multipoint Padé approximation method requires a smaller number of expansion points for the same accuracy as compared with existing multipoint moment matching techniques, yielding a reduction in computation time.

In order to accurately and efficiently generate moments associated with frequency-dependent lossy transmission lines, a modified matrix exponential method is introduced. Recursive formulas are derived for fast computation of the transmission line moments and can readily be incorporated in existing moment matching techniques. The proposed method is further extended to handle interconnects characterized by measured or

simulated frequency-dependent transmission line parameter data. The accuracy and efficiency of the proposed method are demonstrated through its applications to numerical simulation for a variety of interconnect examples, including the simulation of transients on frequency-dependent power transmission lines.

Acknowledgements

I would like to express my sincere appreciation to my supervisors, Prof. G. E. Bridges and Prof. I. R. Ciric, for their informed guidance, consistent encouragement, endless patience and generous financial support throughout the course of this study. I could not have imagined having better advisors for my Ph.D. studies and the time that I spent with them at the University of Manitoba will be enjoyable memory in my life.

I would like to thank Dr. R. Achar for many helpful suggestions on this research. I would also like to thank Dr. L. Shafai and Dr. N. Sepehri who served on my advisory committee.

The University Graduate Fellowship, the Edward R. Toporeck Graduate Fellowship in Engineering, and the UMSU Scholarship, awarded through the University of Manitoba, are appreciated. Financial support from the Manitoba Hydro is also acknowledged.

I would like to dedicate this thesis in memory of my father, and to my mother for her constant support and encouragement.

My special thanks go to my wife for her understanding and patience during the process of this thesis work.

Table of Contents

List of Figures

List of Tables

Chapter 1. Introduction

1.1. OBJECTIVES AND MOTIVATION

This thesis presents an efficient approach to transient and frequency-domain analysis of interconnects modeled as lossy coupled transmission lines. Interconnects are often found in a variety of electric circuit structures such as VLSI chips, multi-chip modules, electronic packaging, printed circuit boards, as well as power transmission systems, and are used to connect electrical components for signal propagation. Typically, interconnects are modeled with large linear networks, which may contain hundreds or thousands of lumped resistances, capacitances, inductances, and/or distributed elements, such as transmission lines. As a result, interconnect analysis generally requires the solution of extremely large linear networks [1]-[4]. In addition, at relatively high signal speed, the electrical length of interconnects becomes a significant fraction of the operating wavelength and high-frequency effects of interconnects such as ringing, signal delay, distortion, reflections and crosstalk can no longer be neglected. The accurate prediction of interconnect performance under these conditions requires that distributed quasi-TEM models, such as lossy coupled transmission lines, be simulated directly, without using lumped element approximations. Consequently, the use of conventional simulation tools, such as SPICE [5] or ASTAP [6], to perform interconnect analysis could be computationally inefficient or even prohibitive.

Driven by the need to accurately obtain solutions of interconnect problems at reasonable computational cost, the development of efficient model-order reduction techniques for interconnect analysis has become recently a topic of active research in the area of electronic design automation. The reduced-order model of a linear system can capture, with acceptable engineering accuracy, the important features of the original large system over the frequency bandwidth of interest. This results in significant savings in computational expense since the size of the reduced-order model is much smaller than the original system. The advances in this field have been reported in the literature and are summarized in reference [2].

The motivation behind the work conducted by the author of this thesis is to develop more efficient model order reduction techniques to analyze general interconnect networks containing distributed transmission lines.

1.2. LITERATURE REVIEW

In this section, the model order reduction techniques proposed by various researchers are briefly discussed. These techniques can be classified into two main groups: moment-matching Padé approximation methods and Krylov-subspace based methods.

Moment–matching Padé Approximations

The need for the development of alternative analysis tools for large interconnect networks has led to the introduction of moment matching techniques, such as the Asymptotic Waveform Evaluation (AWE) algorithm [7]. Pillage and Rohrer first proposed AWE in late 80's as an efficient technique for approximating the waveform response of general linear lumped circuits [8], [9]. AWE approximates a linear network

response from a Taylor series expansion of the network frequency response. The CPU cost required is approximately equal to that for one frequency point analysis of the network. The moments, which result from coefficients of the expansion, are matched via Padé approximation [10] to a reduced-order rational function model containing only a relatively small number of dominant poles and residues. The resultant reduced-order model can be used to compute the time-domain and frequency-domain responses of the linear network with considerably less CPU cost than conventional simulation methods. The AWE algorithm has been extended to analyze networks containing both lumped elements and lossy coupled transmission lines [11], [12], and applied to interconnect networks with nonlinear terminations [13], [14]. In combination with electromagnetic computation methods, moment matching techniques have also been applied to solve many applied electromagnetic field problems [15]-[19].

Although moment-matching techniques have successfully been applied to a variety of electrical engineering problems, it is observed that moment matching techniques that are based on a single frequency point expansion can, in general, extract only a small set of dominant poles and the approximations obtained will be accurate only near the expansion point. This is due to the numerical instability of the Hankel matrix which is used to determine the coefficients of the denominator polynomial of the reduced-order rational function. Thus, this deficiency of the AWE algorithm prevents the application of single-point moment matching techniques from accurately characterizing networks that contain distributed transmission line models, where high-frequency effects are significant and usually require a larger number of poles for an accurate analysis.

In order to achieve accurate and efficient simulations of interconnects in the presence of distributed transmission line models, the Complex Frequency Hopping (CFH), a multipoint moment matching technique, has been introduced [20]. By using multiple point expansions in the complex frequency plane and using a single point Padé approximation at each expansion point, CFH provides an accurate approximation for a desired frequency range. A binary search algorithm is typically used for selecting the expansion points on the imaginary axis and the poles extracted from each expansion are then selectively collected to construct a unified network transfer function. In [21], a technique of generating a set of approximate transfer functions over the entire frequency range of interest is proposed. Employing again a binary search technique, this multiple transfer function based approach reduces the number of necessary expansion points and an inverse fast Fourier transform (IFFT) or a set of poles/residues extracted from the resultant transfer functions is used to obtain the transient response. The CFH multipoint moment matching technique has also been applied to full wave interconnect models and to electromagnetic analysis [22]-[25].

In order to improve the accuracy of CFH, a method based on multipoint Padé approximation was proposed in [26]. In this method, the location and the number of expansion points are determined from currently existing pole information, as in [20], and then all the moments generated at the expansion points are matched to a single transfer function. The multiple point expansion techniques can produce more accurate approximations over a wide frequency range than single-point moment matching and have proven useful in analysis of high-speed interconnect networks. Nevertheless, the

computational cost of the multipoint moment matching techniques is relatively higher and proportional to the number of frequency expansion points.

Krylov Subspace Based Methods

As an alternative to the direct moment matching based model reduction techniques such as AWE, the Krylov subspace based reduced-order modeling methods have been recently introduced for the efficient simulation of linear systems. They include Padé via Lanczos (PVL) [27], and Arnoldi [28], [29] algorithms. Unlike the moment-matching Padé approximation methods, which construct the reduced-order model using extracted dominant poles of a given system, the Krylov subspace algorithms perform model order reduction based on extracting the leading eigenvalues of the system. Since Krylov subspace based algorithms match moments implicitly to obtain reduced order transfer functions, they circumvent the numerical ill-conditioning that is associated with model reduction techniques that utilize a direct moment matching processes, such as in the AWE algorithm. This enables the Krylov subspace methods to produce a higher-order approximation as compared with the AWE. Although the Krylov subspace based techniques are well conditioned, their applications have mainly been limited to lumped systems, like RLC networks, and the extension of the existing Krylov subspace techniques to handle distributed systems in general is not always straightforward [30]. For example, these techniques are not readily applied to networks that are characterized with measured or tabulated data.

Another important issue associated with model order reduction is the passivity preservation [31]-[36]. Passivity implies that a network cannot generate more energy than

it absorbs, and, thus, no passive termination of the network will cause the system to become unstable. Preserving passivity of an original system can greatly reduce the probability of an unstable simulation. PRIMA (Passive Reduced-order Interconnect Macromodeling Algorithm) [31] was introduced as a Krylov subspace method and is capable of providing passive, stable reduced-order models of RLC circuits. On the other hand, the passivity of a reduced-order model generated from moment matching based Padé approximation methods is not necessarily ensured, while the stability can be maintained by removing unstable poles in a post-processing phase [7]. Nevertheless, by applying the correction or compensation procedures such as those presented in [37]-[40] to a reduced-order model that is generated from moment-matching based Padé approximation methods, it is possible to enforce the non-passive reduced-order model to be passive and, thus, to mitigate any potential instability from the transient simulation.

Other Methods

Instead of generating a global reduced-order model for interconnect network consisting of lumped elements and distributed elements, several techniques have recently been presented for the development of macromodels of distributed transmission lines [41]-[46]. In [41], [42], a discrete model for multiconductor interconnects with frequency dependent parameters was developed using compact difference approximations [47] and then PRIMA was applied to generate a passive reduced-order model for the transmission line system. The Matrix Padé approximation (MPA) method was proposed for the analysis of distributed multiconductor transmission lines [43], [44]. This method is based on the matrix rational approximation of exponential functions in describing the

Telegrapher's equations. In MPA, the coefficients needed in the macromodel are computed analytically using a closed-form Padé approximation of the exponential matrix. As a result, it can generate high-order approximations and preserve passivity of the reduced-order model. A comparative study of the MPA and the generalized method of characteristics [48] was conducted and the results were reported in [49]. It was noticed that the waveforms obtained by using the MPA might exhibit early-time oscillations for long line simulation and it was suggested in [49] to use higher order macromodels for accuracy improvement. In [45], an optimal matrix rational approximation (OMRA) technique has been proposed to control the macromodel impulse response beyond the maximum frequency of interest and thus to minimize early-time oscillations observed when using the MPA. A performance and accuracy comparison between OMRA and MPA can also be found in [50]. Very recently, a new segmentation-based technique was presented for the transient analysis of multiconductor transmission lines [46]. In this method, poles and residues are extracted analytically from half T-ladder networks, which approximate the multiconductor transmission lines. In order to efficiently develop reduced-order models of transmission line systems, the dominant poles are selected by applying selective rules to all poles extracted. However, a number of redundant poles may be involved in using this method. Also, like the MPA, this method might require higher order approximations to generate accurate waveforms in the case of long line simulation.

1.3. OUTLINE AND CONTRIBUTIONS

The research work presented in this thesis is focused on the development of techniques in the scope of multipoint Padé approximations based on moment matching

for efficient simulation of interconnect networks with frequency-dependent lossy transmission lines. The reason for choosing a multipoint moment matching scheme is mainly due to its applicability to general distributed systems as well as its simple mechanism of error-control. The significance of the research work is that the proposed method can be applied to calculate, in a more efficient manner as compared with conventional techniques, the frequency and transient responses of interconnect networks consisting of linear lumped components and dispersive transmission lines. In addition, macromodels of multiport linear networks can be developed by using the proposed method. Passivity enforcement, if needed, can be done by means of compensation techniques in the post processing stage, as suggested in the literature [37]-[40].

In chapter two, the basic definitions and formulations used in moment matching based Padé approximation techniques are presented. The general process of moment generation and moment matching is described. The performance of reduced-order model solutions using moment matching based Padé approximation is outlined. After various existing moment matching techniques are reviewed, a new method is introduced in chapter three for efficient simulation of interconnect networks that can include lossy coupled multi-conductor transmission lines. The proposed method is based on multipoint Padé approximations which employ all the moment sets available at all updated expansion points and can be used to efficiently obtain a closed-form solution of the interconnect network. As multipoint expansion methods involve the solution of the network equation at extra frequency expansion points and, thus, require a relatively higher computation cost when compared with the single-point expansion methods, it is very important to reduce the number of expansion points as much as possible. With this

objective, an improved algorithm for the selection of the frequency expansion points is presented, which results in a smaller number of expansion points being required for the same accuracy and yields a reduction in CPU cost. The performance of the new algorithm is investigated through several numerical examples. In chapter four, a review of existing techniques for the generation of moments associated with a distributed transmission line model is given. They include the eigenvalue moment method and the matrix exponential method. In order to improve the computation efficiency, a modified matrix exponential method is introduced for the generation of the moments for frequency-dependent lossy transmission lines. The proposed method yields the same accuracy as the original matrix exponential method [20], but has a computational efficiency which is comparable to that of the eigenvalue moment method [11]. A recursive procedure for calculating the moments for multiconductor transmission lines with frequency-dependent parameters is presented. The accuracy and efficiency of the proposed method are demonstrated by numerical examples. Chapter five focuses on application of the proposed multipoint moment matching method to transient simulation of interconnect networks containing frequency-dependent lossy transmission lines. As the frequency-dependent transmission line parameters can be obtained from electromagnetic simulation software or directly from measurements at a set of discrete frequency points, curve-fitting techniques that approximate the tabulated line parameters and integrate them into the existing moment matching simulation are described. An example of simulating an interconnect network containing frequency-dependent transmission lines is considered. Also in chapter five, transients on frequency-dependent power transmission lines are analyzed using multipoint Padé approximations. Due to the strong wideband frequency dependency of

power transmission line parameters, the multipoint Padé approximations may yield ill-conditioned matrices and cannot directly be applied to simulating transients. To overcome this difficulty, an improved multipoint Padé approximation method is introduced. The new method is then used to analyze frequency dependent power transmission line examples, including a single-phase power transmission line and a three-phase power transmission line. Comparisons of the numerical results obtained by using the improved multipoint method with those obtained by using conventional methods and/or commercial simulation programs are provided.

Chapter 2. Moment Matching Techniques

This chapter begins with the introduction of the general concepts of moment matching techniques. This is accomplished by first describing the Asymptotic Waveform Evaluation (AWE), which is a single point moment matching based algorithm. The general mathematical formulation used in the process of moment matching is presented. In view of the limitations of the AWE, a more elaborate multipoint moment matching techniques will be presented in the next chapter.

2.1. NETWORK EQUATIONS

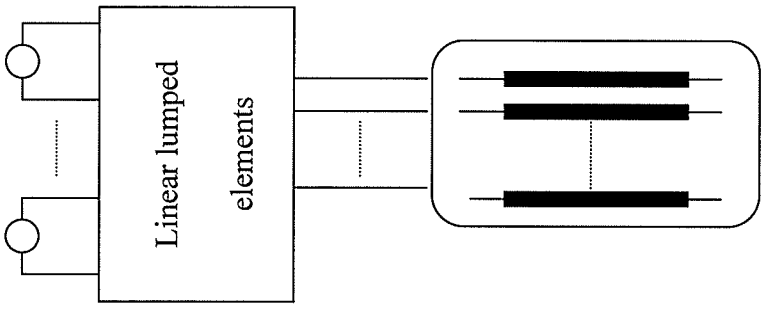

Fig. 2. 1. Linear network containing lumped components and arbitrary linear subnetworks.

Consider a linear network containing lumped components and arbitrary linear subnetworks, as shown in Fig. 2.1. The arbitrary subnetworks may contain distributed

components such as multiconductor transmission lines. Without loss of generality, the modified nodal admittance (MNA) matrix equation [51] of the network with an impulse input excitation can be written as,

$$\boldsymbol{C}\frac{d}{dt}z(t)+\boldsymbol{G}z(t)+\sum_{\kappa=1}^{N_s}\boldsymbol{D}_\kappa \boldsymbol{i}_\kappa(t)-\boldsymbol{b}\delta(t)=0 \tag{2.1}$$

where the entries of vector z(t) are node voltage waveforms, independent voltage source currents, linear inductor currents, and port currents; $\boldsymbol{C}$ and $\boldsymbol{G}$ are constant matrices whose entries are determined by the lumped linear components; $\boldsymbol{b}$ is a constant vector with entries determined by the independent voltage and current sources; $\boldsymbol{D}_\kappa=[d_{i,j}]$, $d_{i,j}\in\{0,1\}$, $i\in\{1,2,\cdots,N_t\}$, $j\in\{1,2,\cdots N_\kappa\}$, with a maximum of one nonzero entry in each row or column, is a selector matrix that maps $\boldsymbol{i}_\kappa$, the vector of currents entering the linear subnetwork κ, into the node space $\Re^{N_t}$ of the network; N_t is the total number of variables in the MNA formulation; N_κ is the number of external terminals of the linear subnetwork κ ; N_s is the number of linear subnetworks; and $\delta(t)$ is the unit impulse function.

The first, second, and fourth terms in (2.1) cover the network's lumped components and independent sources. The third term describes currents at subnetwork terminals and then maps them into the rest of the network through the matrix $\boldsymbol{D}_\kappa$.

A general way to describe the frequency domain equation of the transmission line subnetwork κ is in the form

$$\boldsymbol{A}_\kappa \boldsymbol{V}_\kappa(s)+\boldsymbol{B}_\kappa \boldsymbol{I}_\kappa(s)=0 \tag{2.2}$$

Where V_κ and I_κ represent the Laplace-domain terminal voltage and currents of the subnetwork κ, respectively. In the special case where the subnetwork κ consists of a multi-conductor transmission lines system, A_κ and B_κ can be described in terms of the line parameters.

Taking the Laplace transform of (2.1) and using (2.2), we can write compactly

$$\begin{bmatrix} sC+G & D_1 & D_2 & \cdots & D_{N_s} \\ A_1 D_1^T & B_1 & 0 & \cdots & 0 \\ A_2 D_2^T & 0 & B_2 & \cdots & 0 \\ \vdots & \vdots & \vdots & \cdots & 0 \\ & & & \cdots & 0 \\ A_{N_s} D_{N_s}^T & 0 & 0 & \cdots & B_{N_s} \end{bmatrix} \begin{bmatrix} Z(s) \\ I_1(s) \\ I_2(s) \\ \vdots \\ I_{N_s}(s) \end{bmatrix} = \begin{bmatrix} b \\ 0 \\ 0 \\ \vdots \\ 0 \end{bmatrix} \tag{2.3}$$

or

$$[Y(s)]X(s) = E \tag{2.4}$$

where

$$X(s) = \begin{bmatrix} Z(s) & I_1(s) & I_2(s) & \cdots & I_{N_s}(s) \end{bmatrix}^T$$

$$E = \begin{bmatrix} b & 0 & 0 & \cdots & 0 \end{bmatrix}^T$$

and the superscript T denotes the matrix transpose.

The formulation of the network equation can be illustrated by considering an example circuit shown in Fig. 2.2. In this case, the matrices and vectors defined in (2.3) are given by

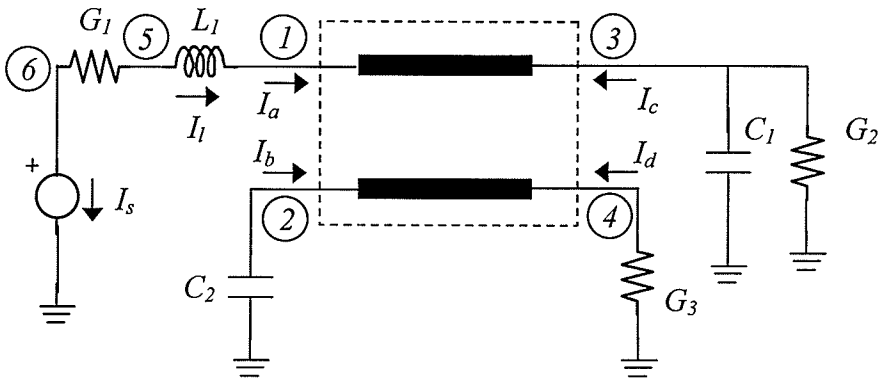

Fig. 2.2. An example circuit containing lumped components and a transmission line subnetwork.

$$\boldsymbol{C} = \begin{bmatrix} 0 & 0 & 0 & 0 & 0 & 0 & 0 & 0 \\ 0 & C_2 & 0 & 0 & 0 & 0 & 0 & 0 \\ 0 & 0 & C_1 & 0 & 0 & 0 & 0 & 0 \\ 0 & 0 & 0 & 0 & 0 & 0 & 0 & 0 \\ 0 & 0 & 0 & 0 & 0 & 0 & 0 & 0 \\ 0 & 0 & 0 & 0 & 0 & 0 & 0 & 0 \\ 0 & 0 & 0 & 0 & 0 & 0 & -L_1 & 0 \\ 0 & 0 & 0 & 0 & 0 & 0 & 0 & 0 \end{bmatrix}$$

$$\boldsymbol{G} = \begin{bmatrix} 0 & 0 & 0 & 0 & 0 & 0 & -1 & 0 \\ 0 & 0 & 0 & 0 & 0 & 0 & 0 & 0 \\ 0 & 0 & G_2 & 0 & 0 & 0 & 0 & 0 \\ 0 & 0 & 0 & G_3 & 0 & 0 & 0 & 0 \\ 0 & 0 & 0 & 0 & G_1 & -G_1 & 1 & 0 \\ 0 & 0 & 0 & 0 & -G_1 & G_1 & 0 & 1 \\ -1 & 0 & 0 & 0 & 1 & 0 & 0 & 0 \\ 0 & 0 & 0 & 0 & 0 & 1 & 0 & 0 \end{bmatrix}$$

$$\boldsymbol{D}_1 = \begin{bmatrix} 1 & 0 & 0 & 0 \\ 0 & 1 & 0 & 0 \\ 0 & 0 & 1 & 0 \\ 0 & 0 & 0 & 1 \\ 0 & 0 & 0 & 0 \\ 0 & 0 & 0 & 0 \\ 0 & 0 & 0 & 0 \\ 0 & 0 & 0 & 0 \end{bmatrix}$$

$$\boldsymbol{X}(s) = [\boldsymbol{Z}(s) \quad \boldsymbol{I}_1(s)]^T$$

$$\boldsymbol{I}_1(s) = [I_a \quad I_b \quad I_c \quad I_d]^T$$

$$\boldsymbol{Z}(s) = [V_1 \quad V_2 \quad V_3 \quad V_4 \quad V_5 \quad V_6 \quad I_l \quad I_s]^T$$

$$\boldsymbol{b} = [0 \quad 0 \quad 0 \quad 0 \quad 0 \quad 0 \quad 0 \quad 1]^T$$

$\boldsymbol{A}_1$ and $\boldsymbol{B}_1$ are 4×4 matrices and are related to the terminal voltages and currents of the subnetwork in the form

$$\boldsymbol{A}_1 \begin{bmatrix} V_1 \\ V_2 \\ V_3 \\ V_4 \end{bmatrix} + \boldsymbol{B}_1 \begin{bmatrix} I_a \\ I_b \\ I_c \\ I_d \end{bmatrix} = 0$$

Several techniques are available for computations of $\boldsymbol{A}_\kappa$ and $\boldsymbol{B}_\kappa$ for the distributed transmission line subnetwork κ. The modified matrix exponential method, which can be used to efficiently generate $\boldsymbol{A}_\kappa$ and $\boldsymbol{B}_\kappa$ for distributed transmission line models with frequency-dependent parameters, will be proposed in chapter four.

2.2. MODEL ORDER REDUCTION

A solution for $\boldsymbol{X}(s)$ over a frequency band can be obtained by repeatedly solving the matrix equation (2.4) at a sufficiently large number of frequency points within the band. This is computationally too expensive and even prohibitive as soon as the size of matrix $\boldsymbol{Y}$ reaches a few hundreds. A more efficient way to deal with this problem is to use model order reduction techniques.

Consider any component of the solution vector $X_l(s)$. The actual transfer function for the output can be represented in a rational function form as

$$X_l(s) = H(s) = \frac{P(s)}{Q(s)} \tag{2.5}$$

where $P(s)$ and $Q(s)$ are polynomials in s with the degree of the numerator less than or equal to the degree of the denominator. Applying a partial fraction decomposition on (2.5) yields

$$H(s) = c + \sum_{j=1}^{N_p} \frac{k_j}{s - p_j} \tag{2.6}$$

where p_j is the jth pole of the system, k_j is the jth residue associated with the specific output, N_p is the total number of system poles, and the constant c represents the direct coupling between the input and the output. By applying the inverse Laplace transform to (2.6), the time-domain impulse response of the output is expressed in closed form in terms of poles and residues as

$$h(t) = c\delta(t) + \sum_{j=1}^{N_p} k_j e^{p_j t} \tag{2.7}$$

As we are interested in analyzing a large network containing distributed components as well as lumped elements, the numerical computation of all the system poles becomes

impractical when the number of unknowns of the network reaches a few hundreds. An efficient alternative is to approximate the actual (high-order) network transfer function $H(s)$ with a reduced-order model that exhibits closely the same frequency characteristics as the actual one.

2.3. MOMENT MATCHING FORMULATION

A reduced-order network transfer function can be realized using moment matching techniques. Moment matching techniques generally consist of two main steps: moment generation and moment matching. In the process of moment generation, a set of linear network unknowns is expanded in a single or multiple Taylor series. The coefficients of the expansion(s) are known as *moments* because they are related to the time moments of the transfer function. For illustration, consider the network matrix equation (2.4); the unknown vector $\boldsymbol{X}(s)$ can be expanded in a Taylor series about a complex frequency point $s = s_k$ as

$$\boldsymbol{X}(s) = \sum_{n=0}^{\infty} \boldsymbol{M}_{kn} (s - s_k)^n \tag{2.8}$$

Here $\boldsymbol{M}_{kn}$ is the nth moment vector of the Taylor expansion about $s = s_k$ and is given by

$$\boldsymbol{M}_{kn} = \frac{1}{n!} \frac{\partial^n}{\partial s^n} \left[\boldsymbol{Y}^{-1}(s) \right]_{s=s_k} \boldsymbol{E} \tag{2.9}$$

Moment matching techniques employ a recursive relationship to compute the moment vectors. This relationship is given by

$$\boldsymbol{Y}(s_k) \boldsymbol{M}_{kn} = -\sum_{r=1}^{n} \frac{1}{n!} \left[\frac{\partial^r}{\partial s^r} \boldsymbol{Y}(s) \right]_{s=s_k} \boldsymbol{M}_{k,n-r} \tag{2.10}$$

with

$$\boldsymbol{Y}(s_k)\boldsymbol{M}_{k0} = \boldsymbol{E} \tag{2.11}$$

From (2.10) and (2.11), it can be seen that the generation of moment vectors about one expansion point $s = s_k$ requires only one LU factorization and each vector $\boldsymbol{M}_{kn}$ $(n \geq 1)$ can be obtained by performing only one forward-backward substitution. As a result, the CPU cost associated with this procedure is approximately equal to that for the solution of the network equation at one frequency point.

To generate the moments of the network, one needs to calculate the derivatives of $\boldsymbol{Y}(s)$ at the frequency expansion point $s = s_k$. Using a superscript (r) to represent the rth derivative at $s = s_k$, we have

$$[\boldsymbol{Y}]^{(1)} = \begin{bmatrix} \boldsymbol{C} & 0 & 0 & \cdots & 0 \\ \boldsymbol{A}_1^{(1)}\boldsymbol{D}_1^T & \boldsymbol{B}_1^{(1)} & 0 & \cdots & 0 \\ \boldsymbol{A}_2^{(2)}\boldsymbol{D}_2^T & 0 & \boldsymbol{B}_2^{(2)} & \cdots & 0 \\ \vdots & \vdots & \vdots & \cdots & 0 \\ & & & \cdots & 0 \\ \boldsymbol{A}_{N_s}^{(1)}\boldsymbol{D}_{N_s}^T & 0 & 0 & \cdots & \boldsymbol{B}_{N_s}^{(1)} \end{bmatrix} \tag{2.12}$$

and

$$[\boldsymbol{Y}]^{(r)} = \begin{bmatrix} 0 & 0 & 0 & \cdots & 0 \\ \boldsymbol{A}_1^{(r)}\boldsymbol{D}_1^T & \boldsymbol{B}_1^{(r)} & 0 & \cdots & 0 \\ \boldsymbol{A}_2^{(r)}\boldsymbol{D}_2^T & 0 & \boldsymbol{B}_2^{(r)} & \cdots & 0 \\ \vdots & \vdots & \vdots & \cdots & 0 \\ & & & \cdots & 0 \\ \boldsymbol{A}_{N_s}^{(r)}\boldsymbol{D}_{N_s}^T & 0 & 0 & \cdots & \boldsymbol{B}_{N_s}^{(r)} \end{bmatrix} \qquad (r \geq 2). \tag{2.13}$$

If the network contains lumped components only, it is readily seen that

$$[\boldsymbol{Y}]^{(r)} = 0 \qquad (r \geq 2) \tag{2.14}$$

and (2.10) can be reduced to

$$\boldsymbol{Y}(s_k)\boldsymbol{M}_{kn} = -\left[\frac{\partial}{\partial s}\boldsymbol{Y}(s)\right]_{s=s_k} \boldsymbol{M}_{k,n-1}. \tag{2.15}$$

In the case where the subnetwork κ contains distributed transmission lines, (2.14) does not hold, and this in turn requires the calculation of higher order moments of the transmission lines. Several approaches can be used to generate moments of distributed multiconductor transmission lines. They include the eigenvalue moment method [11], the matrix exponential moment method [20], as well as the modified matrix exponential moment method [52] introduced by the author of this thesis. Their performance in the generation of transmission line moments is discussed in chapter four in detail.

Moment matching describes a process where a set of coefficients of a low-order approximate rational transfer function is found such that the moments of the approximate function match a given number of initial moments of the original function. For the sake of illustration, moment matching techniques that use one single frequency expansion point are first considered. Let s_k be an arbitrary expansion point. The Taylor expansion of the transfer function for a selected output of the network is given by

$$H(s) = m_{k0} + m_{k1}(s - s_k) + m_{k2}(s - s_k)^2 + \cdots \tag{2.16}$$

where m_{kn}, $n = 0, 1, 2, \cdots$, are moments that are generated from (2.10)-(2.11) about the expansion point $s = s_k$. To determine the coefficients of an qth order rational function $\hat{H}(s)$ which approximates $H(s)$, we extract the first $2q$ moments m_{kn}, $0 \le n \le 2q-1$, and then match the moment set to the corresponding coefficients of the rational function $\hat{H}(s)$ as follows

$$\sum_{n=0}^{2q-1} m_{kn}(s-s_k)^n = \frac{a_0 + a_1 s + \cdots + a_{q-1}s^{q-1}}{1 + b_1 s + b_2 s^2 + \cdots + b_q s^q} \tag{2.17}$$

or

$$\sum_{n=0}^{2q-1} m_{kn}\hat{s}^n = \frac{\hat{a}_0 + \hat{a}_1\hat{s} + \cdots + \hat{a}_{q-1}\hat{s}^{q-1}}{1 + \hat{b}_1\hat{s} + \cdots + \hat{b}_q\hat{s}^q} \tag{2.18}$$

with $\hat{s} = s - s_k$.

The coefficients of the numerator and denominator polynomials in (2.18) are computed from the moments by using,

$$\begin{bmatrix} m_{k0} & m_{k1} & \cdots & m_{k,q-1} \\ m_{k1} & m_{k2} & \cdots & m_{kq} \\ \vdots & \vdots & & \vdots \\ m_{k,q-1} & m_{kq} & \cdots & m_{k,2q-1} \end{bmatrix} \begin{bmatrix} \hat{b}_q \\ \hat{b}_{q-1} \\ \vdots \\ \hat{b}_1 \end{bmatrix} = -\begin{bmatrix} m_{kq} \\ m_{k,q+1} \\ \vdots \\ m_{k,2q-1} \end{bmatrix} \tag{2.19}$$

$$\hat{a}_i = \sum_{j=0}^{i} m_{k,i-j}\hat{b}_j \; ; \qquad i = 0, 1, 2, \cdots, q-1 \tag{2.20}$$

where $\hat{b}_0 = 1$. The approximation transfer function $\hat{H}(s)$ in (2.17), which is known as a Padé approximation, is determined once the coefficients $\hat{a}_0, \hat{a}_1, \cdots, \hat{a}_{q-1}$, $\hat{b}_1, \cdots, \hat{b}_q$ are calculated. By using a partial fraction decomposition, we can write $\hat{H}(s)$ in the form of

$$\hat{H}(s) = \sum_{j=1}^{q} \frac{\hat{k}_j}{s - \hat{p}_j} \tag{2.21}$$

The poles $\hat{p}_j$ of $\hat{H}(s)$ in (2.21) can be obtained by applying a root-solving algorithm to the equation

$$b_q s^q + b_{q-1}s^{q-1} + \cdots + b_1 s + 1 = 0 . \tag{2.22}$$

The residues $\hat{k}_j$ are related to the poles and the moments by

$$\begin{bmatrix} \hat{p}_1^{-1} & \hat{p}_2^{-1} & \cdots & \hat{p}_q^{-1} \\ \hat{p}_1^{-2} & \hat{p}_2^{-2} & \cdots & \hat{p}_q^{-2} \\ \vdots & \vdots & & \vdots \\ \hat{p}_1^{-q} & \hat{p}_2^{-q} & \cdots & \hat{p}_q^{-q} \end{bmatrix} \begin{bmatrix} \hat{k}_1 \\ \hat{k}_2 \\ \vdots \\ \hat{k}_q \end{bmatrix} = -\begin{bmatrix} m_{k0} \\ m_{k1} \\ \vdots \\ m_{k,q-1} \end{bmatrix} \tag{2.23}$$

Finally, applying the Laplace transform to (2.21) yields the approximate impulse transient response of the output in the form

$$\hat{h}(t) = \sum_{j=1}^{q} \hat{k}_j e^{\hat{p}_j t} \tag{2.24}$$

More details on moment matching algorithms can be found in [7].

While moment matching techniques based on a single point expansion can be accurate in generating approximations for several types of linear circuits, inaccurate results were sometimes observed due to the inherent limitations of Padé approximations [10]. Padé approximations attempt to extract pole/residue information from the moments. It was noticed that Padé approximations are sensitive to the evaluation of the moments, any small deviation in the value of the moments causing large deviation in the value of the poles, which then result in errors in the simulated waveforms. Therefore, it is critical that one should perform Padé approximations on high precision machines and use numerically stable algorithms in computing moments. Moreover, numerical experiments showed that a single moment matching Padé approximations typically generate no more than eight accurate poles since the matrix in (2.19) can become increasingly ill-conditioned as its size increases [27]. In order to improve the accuracy of the

approximation, implementations of moment matching techniques that are based on multiple point expansions have to be considered.

2.4. PASSIVITY OF REDUCED-ORDER MODELS

The moment-matching based Padé approximation techniques can be used to construct macromodels of multiport linear networks. Macromodeling is useful in overcoming the difficulties encountered in solving mixed frequency/time domain problems since it allows large linear distributed systems, which are usually characterized in the frequency domain, to be represented by macromodels and then inserted into standard nonlinear solvers or general-purpose circuit simulators [2]. To ensure the accuracy of the simulation results, the macromodels generated are required to be not only stable but also passive. For a linear *N*-port network characterized by an admittance matrix $\mathbf{Y}(s)$, the network is passive if and only if [53]: 1) $\mathbf{Y}(s^*) = \mathbf{Y}^*(s)$ for all s, 2) $\mathbf{Y}(s)$ is analytic in Re(s)>0, and 3) $\mathbf{Y}(s)$ is a positive real matrix, i.e., $z^{*T}\left[\mathbf{Y}^T(s^*) + \mathbf{Y}(s)\right]z \geq 0$ for all complex values of s satisfying Re(s)>0 and for any arbitrary vector z. In the practical case of networks with symmetric admittance matrices, the condition 3) also implies that, $\mathrm{Re}(\mathbf{Y}(s)) = \left[\mathbf{Y}^T(s^*) + \mathbf{Y}(s)\right]/2$ must be a positive definite matrix for Re(s)>0.

Since the poles/residues generated by Padé approximation techniques are either real or in complex conjugate pairs, the resulting reduced-order model for an admittance matrix $\mathbf{Y}(s)$ can always satisfy the first condition. Since the entries of $\mathbf{Y}(s)$ are obtained in the form of rational functions with real coefficients, the second condition is also satisfied. However, the reduced-order model cannot ensure the condition 3), even though the stability is ensured by removing all the unstable poles. Thus, it is necessary to assess

the resulting reduced-order models for a possible passivity violation. In the case when passivity is violated, adequate compensation techniques, such as those presented in [37]-[40], can be implemented to enforce non-passive reduced-order models to be passive. In this way, any potential instability in the transient simulation can be eliminated.

2.5. SUMMARY

In this chapter, the concepts and fundamentals of single-point expansion based moment matching techniques are reviewed. The formulations used in the processes of moment generation and moment matching are presented. The limitations related to applications of moment-matching based Padé approximation techniques for interconnect analysis are discussed.

Chapter 3. Multipoint Padé Approximations

It has been observed that approximations relying on a single expansion point can only extract a small number of dominant poles due to ill-conditioning of the Padé approximation matrix and will be accurate only near the expansion point [20], [27]. In the analysis of networks containing transmission line models, high frequency effects can be significant and techniques that extract only a small number of poles may not provide accurate waveform estimation. In order to overcome the limitations associated with single-point expansion based moment matching techniques, multiple point expansion based techniques have been considered in the literature [20], [21], [26]. In this chapter, an improved method that is based on multiple point expansions and Padé approximations is presented for efficiently computing the frequency and transient responses of large interconnect networks.

3.1. FORMULATION FOR MULTIPOINT PADÉ APPROXIMATION

Suppose we expand $X(s)$ at K expansion points s_k, $k = 1, 2, \cdots, K$, and truncate the expansion (2.8) at each expansion point to the first $2N$ vector moment terms. For a specified output $X_l(s)$, K moment sets are generated, comprising $2NK$ moments, $m_{kn} = [\boldsymbol{M}_{kn}]_l$, $n = 0, 1, 2, \cdots, 2N-1$. We then match the K moment sets to a rational network transfer function of order $q = NK$ in the form

$$\frac{a_0 + a_1 s + \cdots + a_{q-1} s^{q-1}}{1 + b_1 s + \cdots + b_q s^q} = m_{k0} + m_{k1}(s - s_k) + \cdots + m_{k,2N-1}(s - s_k)^{2N-1},$$

$$k = 1, 2, \cdots, K \qquad (3.1)$$

Using the variable substitution $\hat{s} = s - s_k$, we then obtain the following equation for each of the expansion points

$$\frac{\hat{a}_0 + \hat{a}_1 \hat{s} + \cdots \hat{a}_{q-1} \hat{s}^{q-1}}{\hat{b}_0 + \hat{b}_1 \hat{s} + \cdots + \hat{b}_q \hat{s}^q} = m_{k0} + m_{k1} \hat{s} + \cdots + m_{k,2N-1} \hat{s}^{2N-1}, \qquad (3.2)$$

$$k = 1, 2, \cdots, K$$

where

$$\hat{b}_0 = 1 + \sum_{j=1}^{q} b_j s_k^j \qquad (3.3)$$

$$\hat{b}_i = \sum_{j=i}^{q} b_j \binom{j}{i} s_k^{j-i}, \qquad i = 1, 2, \cdots, q \qquad (3.4)$$

$$\hat{a}_i = \sum_{j=i}^{q-1} a_j \binom{j}{i} s_k^{j-i}, \qquad i = 0, 1, \cdots, q-1 \qquad (3.5)$$

with $\binom{\ }{\ }$ denoting the binomial coefficient. Now, multiplying both sides by the denominator of the rational function in (3.2) and, then, equating terms with like powers of $\hat{s}$ up to $\hat{s}^{2N-1}$ yields for each k

$$\hat{a}_0 = m_{k0} \hat{b}_0$$

$$\hat{a}_1 = m_{k0} \hat{b}_1 + m_{k1} \hat{b}_0$$

$$\vdots$$

$$\hat{a}_{2N-1} = m_{k0} \hat{b}_{2N-1} + \cdots + m_{k,2N-1} \hat{b}_0 \ . \qquad (3.6)$$

Equations in (3.3) can be written in a compact matrix form as

$$\boldsymbol{Q}_k \boldsymbol{c} = \boldsymbol{m}_k \ , \tag{3.7}$$

where $\boldsymbol{c} = \begin{bmatrix} a_0 & \cdots & a_{q-1} & b_1 & \cdots & b_q \end{bmatrix}^T$ is a vector that contains the coefficients of the rational transfer function to be solved, $\boldsymbol{m}_k = \begin{bmatrix} m_{k0} & \cdots & m_{k,2N-1} \end{bmatrix}^T$ is a moment vector, and $\boldsymbol{Q}_k$ is a $2N \times 2q$ matrix and is expressed as

$$\boldsymbol{Q}_k = \begin{bmatrix} \boldsymbol{C}_1 & \boldsymbol{C}_{2_k} & -\boldsymbol{B}_k \boldsymbol{C}_{2_k} & -\boldsymbol{B}_k \boldsymbol{C}_{3_k} \end{bmatrix} \tag{3.8}$$

where $\boldsymbol{C}_1$ and $\boldsymbol{C}_{3_k}$ are two vectors of dimension $2N$, i.e.,

$$\boldsymbol{C}_1 = \begin{bmatrix} 1 & 0 & \cdots & 0 \end{bmatrix}^T \tag{3.9}$$

$$\boldsymbol{C}_{3_k} = \begin{bmatrix} s_k^q & \binom{q}{1} s_k^{q-1} & \cdots & \binom{q}{2N-1} s_k^{q-2N+1} \end{bmatrix}^T . \tag{3.10}$$

$\boldsymbol{C}_{2_k}$ is a $2N \times (q-1)$ matrix which is defined as

$$\boldsymbol{C}_{2_k} = \begin{bmatrix} s_k & s_k^2 & \cdots & s_k^{q-1} \\ 1 & \binom{2}{1} s_k & \cdots & \binom{q-1}{1} s_k^{q-2} \\ 0 & 1 & \cdots & \\ 0 & 0 & & \\ \vdots & \vdots & & \vdots \\ 0 & 0 & \cdots & \binom{q-1}{2N-1} s_k^{q-2N} \end{bmatrix} \tag{3.11}$$

and $\boldsymbol{B}_k$ is a matrix of size $2N \times 2N$ and is given by

$$\boldsymbol{B}_k = \begin{bmatrix} m_{k0} & 0 & \cdots & 0 \\ m_{k1} & m_{k0} & & 0 \\ \vdots & \vdots & \ddots & \vdots \\ m_{k,2N-1} & m_{k,2N-2} & \cdots & m_{k0} \end{bmatrix} \tag{3.12}$$

The combination of the matrix equations for all expansion points results in a $2q \times 2q$ matrix equation in the form

$$\begin{bmatrix} \boldsymbol{Q}_1 \\ \boldsymbol{Q}_2 \\ \vdots \\ \boldsymbol{Q}_K \end{bmatrix} \boldsymbol{c} = \begin{bmatrix} \boldsymbol{m}_1 \\ \boldsymbol{m}_2 \\ \vdots \\ \boldsymbol{m}_K \end{bmatrix} \tag{3.13}$$

The solution of equation (3.13) yields the coefficients of the rational transfer function

$$\hat{H}(s) = \frac{a_0 + a_1 s + \cdots + a_{q-1} s^{q-1}}{1 + b_1 s + \cdots + b_q s^q}. \tag{3.14}$$

It is to be noted that the values of some of the entries in the matrix (3.13) are expected to be large as the number of expansion points K increases. This is because the order of the rational network transfer function in (3.1) will increase as K increases. As a result, the matrix may become ill-conditioned in some cases. In view of this, it is important to use double precision arithmetic, and employ an adequate frequency scaling such that the absolute values of frequency expansion points are reduced to about unity.

3.2. ALGORITHM FOR SELECTION OF FREQUENCY EXPANSION POINTS

In implementing the multipoint moment matching for simulating large circuits, the computational cost is dominated by the moment-generation stage, which requires the solutions of the network matrix equation (2.4) at different frequency-expansion points. To minimize the number of frequency-expansion points, a new, more efficient algorithm for the expansion point selection is developed in this section by combining a bisection search technique with a multipoint Padé approximation for all the moment sets available

from all updated expansion points. As a result, the number of expansion points required can be reduced as compared with that in the previous techniques [21], [26].

To illustrate the algorithm, assume that there are currently K expansion points within the frequency range [0, f_{max}]. Let $H_{all}(s)$ denote the rational Padé transfer function generated by the moments of all K expansion points. If we specify a middle frequency point f between two consecutive expansion points, let $H_{mid}(s)$ denote the rational Padé transfer function generated from the moments of K-1 expansion points that are the closest to that mid-frequency point (see Fig. 3.1). The search algorithm is described below, starting with two expansion points:

Step 1: Set $f_L = 0$ and $f_H = f_{max}$.

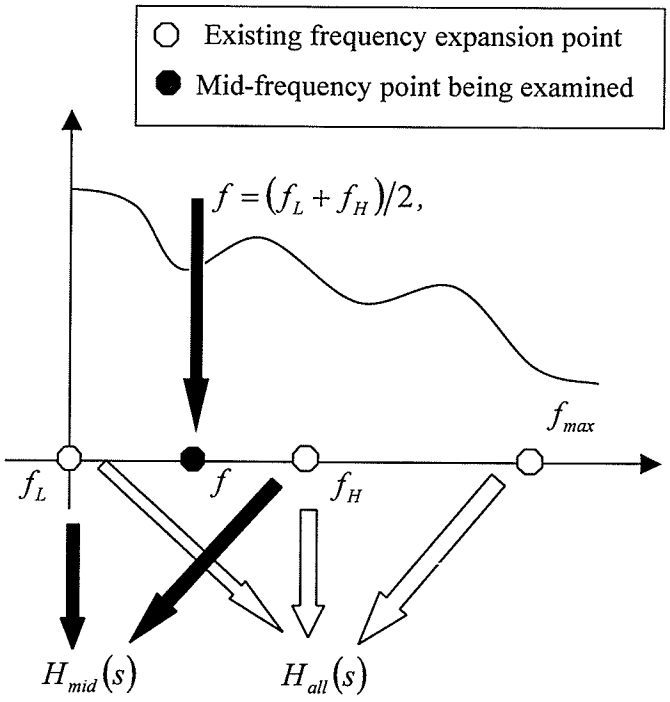

Fig. 3.1. An illustration of the search algorithm in the case of 3 existing expansion points

Step 2: Expand the network impulse response at f_L and f_H using equation (2.8).

Step 3: Construct $H_{all}(s)$ from moments in the expansions at f_L and f_H using equation (3.14).

Step 4: Construct $H_{mid}(s)$ corresponding to the mid-point $f = (f_L + f_H)/2$.

Step 5: If $|H_{all}(j2\pi f) - H_{mid}(j2\pi f)| < \varepsilon$, where ε is a specified error tolerance, proceed to step 6. Otherwise, expand at the mid-point and update $H_{all}(s)$ to include the moment information from all existing expansion points.

Step 6: If no mid-point expansion is needed between any two consecutive expansion points, end the algorithm. Otherwise, repeat step 4-5 using the new subintervals, with f_L and f_H corresponding to each new subinterval.

Once the search process is completed, a network transfer function in the form of the rational function (equation 3.14) is automatically generated which is accurate over $[0, f_{max}]$. The poles of the network transfer function for the interval $[-f_{max}, f_{max}]$ can be obtained by first finding the roots of the denominator polynomial and then duplicating them for the conjugate quadrant. As in the AWE or PVL implementation, the multipoint Padé approximation approach may also produce a few unstable poles. If poles with positive real part occur, we simply discard them at this stage. The residues $\hat{k}_j$ corresponding to the q' remaining stable poles $\hat{p}_j$ can be obtained by a least squares approximation solution of the following system of linear equation

$$\sum_{j=1}^{q'} \frac{\hat{k}_j}{s_i - \hat{p}_j} = \hat{H}(s_i), \qquad i = -m, \cdots, 0, \cdots, m \tag{3.15}$$

Here s_i are $2m+1$ frequency fitting points within $[-f_{max}, f_{max}]$, with $s_{-\alpha} \equiv s_\alpha^*$ and with $\hat{H}(s_\alpha) \equiv H_{all}(s_\alpha)$ for $\alpha \geq 0$, such that $\hat{H}(s_{-\alpha}) \equiv H_{all}^*(s_\alpha)$. The number m is usually chosen to be larger than $(q'-1)/2$. Instead of solving this complex linear system of equations, we transform it into a real linear system and solve it to determine the approximate residues. This finally yields a single network transfer function which has a frequency domain form and a corresponding impulse transient response in the form

$$\hat{H}(s) = \sum_{j=1}^{q'} \frac{\hat{k}_j}{s - \hat{p}_j}, \tag{3.16}$$

$$\hat{h}(t) = \sum_{j=1}^{q'} \hat{k}_j e^{\hat{p}_j t}. \tag{3.17}$$

3.3. NUMERICAL RESULTS

3.3.1. Interconnect Circuits with Lossy Multiconductor Transmission Lines

The multipoint Padé approximation method was applied to the interconnect circuit example [21] shown in Fig.3.2. The circuit contains two lossy coupled transmission lines and is excited by a 1 V pulse with 0.4 ns rise/fall time and 5 ns duration. Both lines have the same length of 0.1 m while line 1 is characterized by following parameters:

$$\boldsymbol{L} = \begin{bmatrix} 494.6 & 63.3 \\ 63.3 & 494.6 \end{bmatrix} \text{nH/m} \qquad \boldsymbol{C} = \begin{bmatrix} 62.8 & -4.9 \\ -4.9 & 62.8 \end{bmatrix} \text{pF/m}$$

$$\boldsymbol{R} = \begin{bmatrix} 75 & 15 \\ 15 & 75 \end{bmatrix} \Omega\text{/m} \qquad \boldsymbol{G} = \begin{bmatrix} 0.1 & -0.01 \\ -0.01 & 0.1 \end{bmatrix} \text{S/m}$$

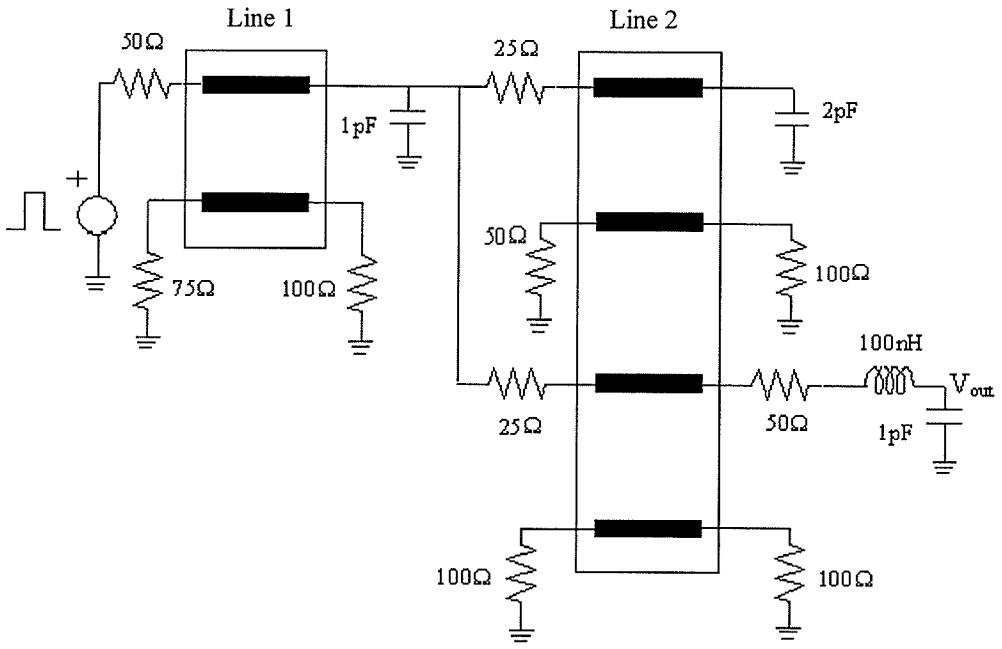

Fig. 3.2. Interconnect circuit with lossy multiconductor transmission lines.

and the parameters for line 2 are:

$$\boldsymbol{L} = \begin{bmatrix} 494.6 & 63.3 & 7.8 & 0.0 \\ 63.3 & 494.6 & 63.3 & 7.8 \\ 7.8 & 63.3 & 494.6 & 63.3 \\ 0.0 & 7.8 & 63.3 & 494.6 \end{bmatrix} \text{nH/m} \qquad \boldsymbol{C} = \begin{bmatrix} 62.8 & -4.9 & -0.3 & 0.0 \\ -4.9 & 62.8 & -4.9 & -0.3 \\ -0.3 & -4.9 & 62.8 & -4.9 \\ 0.0 & -0.3 & -4.9 & 62.8 \end{bmatrix} \text{pF/m}$$

$$\boldsymbol{R} = \begin{bmatrix} 50 & 10 & 1 & 0.0 \\ 10 & 50 & 10 & 1 \\ 1 & 10 & 50 & 10 \\ 0.0 & 1 & 10 & 50 \end{bmatrix} \Omega\text{/m} \qquad \boldsymbol{G} = \begin{bmatrix} 0.1 & -0.01 & -0.001 & 0.0 \\ -0.01 & 0.1 & -0.01 & -0.001 \\ -0.001 & -0.01 & 0.1 & -0.01 \\ 0.0 & -0.001 & -0.01 & 0.1 \end{bmatrix} \text{S/m}$$

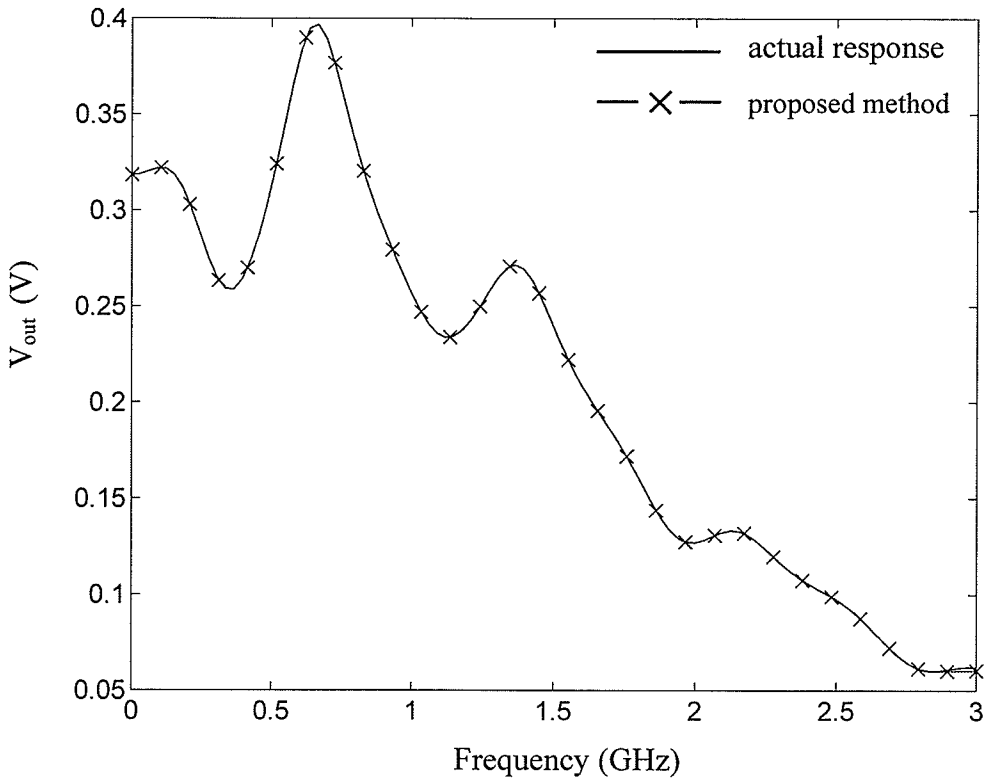

Fig. 3.3. Frequency response at the load end of the circuit in Fig. 3.2 for an impulse excitation.

The frequency response at the load capacitor has been calculated using the proposed method with $f_{max} = 2.5$ GHz. Using ten moments at each expansion point, it was found that four frequency expansion points were required at 0, 0.625, 1.25 and 2.5 GHz. Fig. 3.3 shows the comparison of the approximate frequency response with the actual response obtained by solving equation (2.4) at 1024 frequency points. The resulting transient waveform is shown in Fig. 3.4 and compared with the result obtained by applying an inverse fast Fourier transform (IFFT) to the actual response. The CFH multipoint moment-matching technique [21] has also been applied to simulate the circuit.

With ten moments employed at each expansion point, the CFH required seven frequency expansion points to achieve the same accuracy.

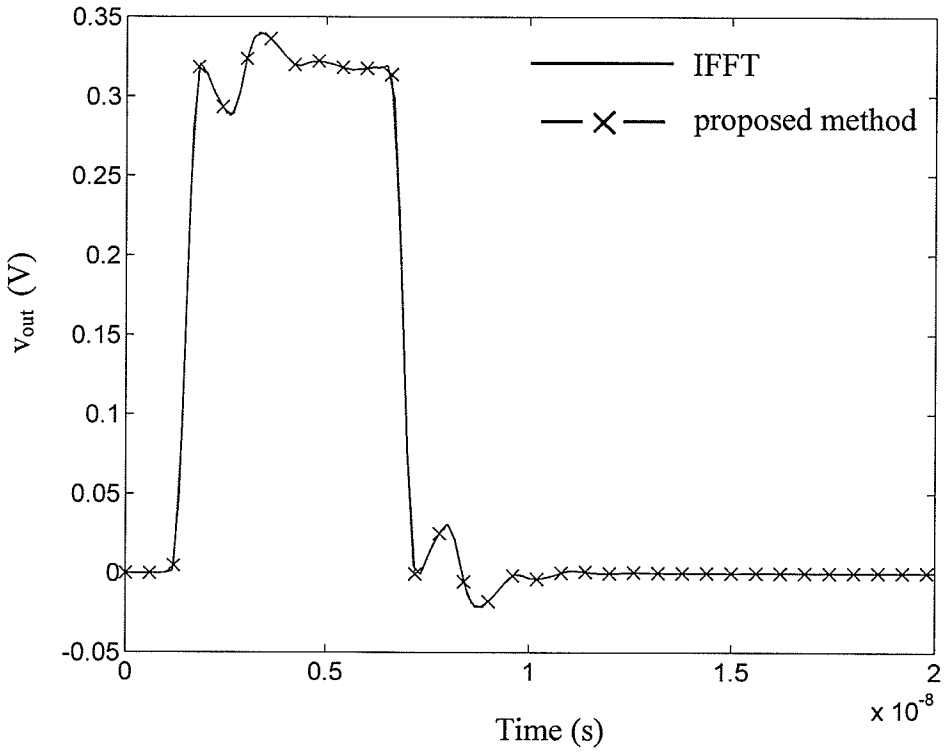

Fig. 3.4. Transient response at the load end of the circuit in Fig. 3.2 for a 1V pulse excitation with 0.4 ns rise/fall time and 5 ns duration.

The second example circuit [54] is shown in Fig. 3.5 and was examined to further demonstrate the performance of the proposed method. The circuit contains two lossy coupled transmission lines. Both lines have a length of 5 cm and identical parameters given by

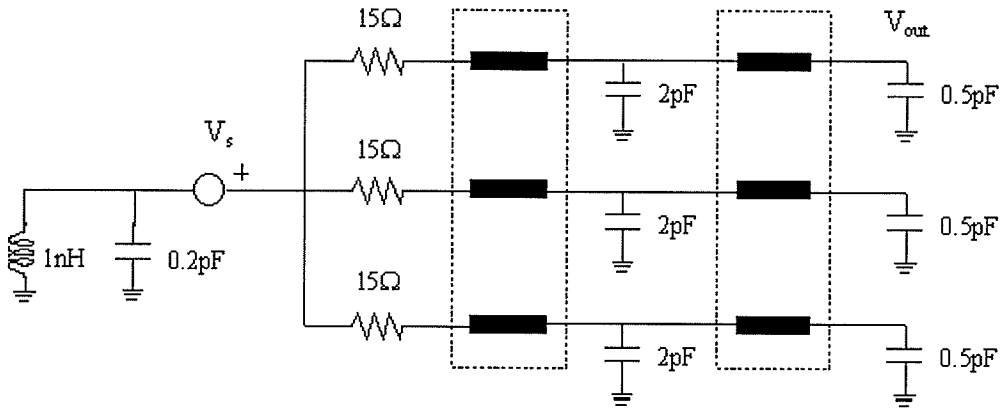

Fig. 3.5. Interconnect network with lossy multiconductor transmission lines.

$$\boldsymbol{R} = \begin{bmatrix} 344.8 & 0 & 0 \\ 0 & 344.8 & 0 \\ 0 & 0 & 344.8 \end{bmatrix} \Omega/\text{m}, \qquad \boldsymbol{L} = \begin{bmatrix} 497.6 & 76.5 & 15.2 \\ 76.5 & 497.6 & 76.5 \\ 15.2 & 76.5 & 497.6 \end{bmatrix} \text{nH/m},$$

$$\boldsymbol{C} = \begin{bmatrix} 108.2 & -19.7 & -0.6 \\ -19.7 & 112.4 & -19.7 \\ -0.6 & -19.7 & 108.2 \end{bmatrix} \text{pF/m}, \qquad \boldsymbol{G} = 0$$

Fig. 3.6 shows the impulse frequency response of the network obtained by using the proposed method with the maximum frequency chosen to be 5 GHz. Using 10 moments for each expansion point, it was noticed that five expansion points were required, with their locations at 0, 1.25, 2.5, 3.75 and 5 GHz, resulting in 44 stable poles. The exact frequency response obtained by solving the equation (2.4) at 1024 frequency points is

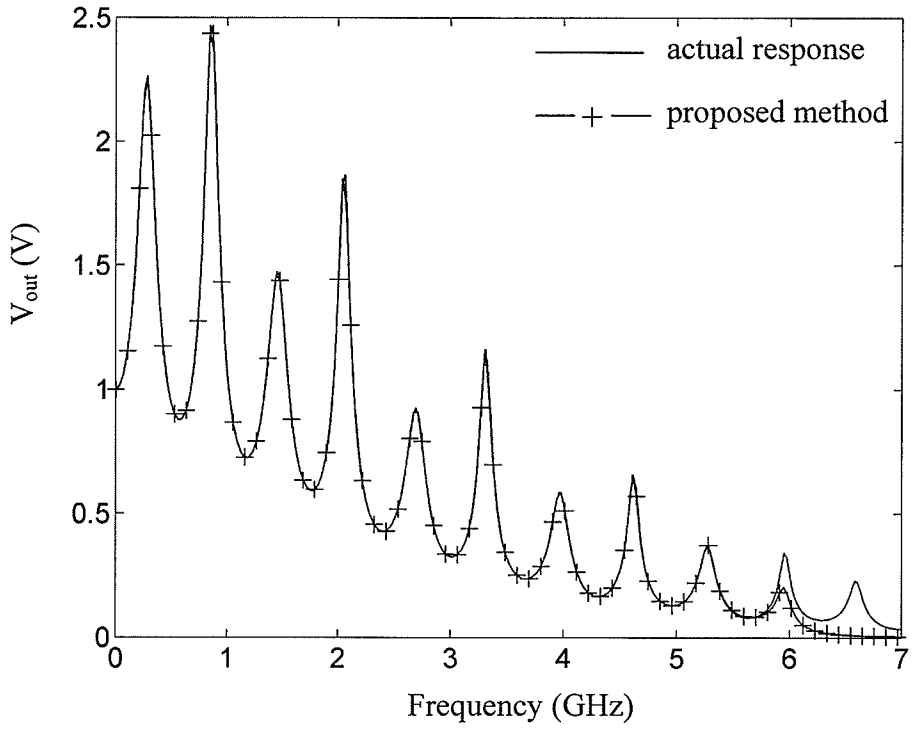

Fig. 3.6. Frequency response of the interconnect network in Fig.3.5 calculated at the output node V_{out}.

also shown in Fig. 3.6 for comparison. The transient response, corresponding to a 1V pulse with 0.1 ns rise and fall times and 1 ns duration, as determined by the proposed method, is shown in Fig. 3.7. The result obtained by using the exact frequency response and then applying the IFFT is also shown. The CFH technique [21] was also applied to the same problem. Using 10 moments as above, the CFH technique required 17 expansion points to achieve the same accuracy. When the number of moments was increased to 14, it was found that 9 expansion points were required for CFH while the proposed method still required only 5 expansion points. In other words, to achieve a solution with the same accuracy as in the proposed method with the same number of

expansion points, CFH requires higher-order moments at each expansion point. This also results in an increased computation error since high-order moments contain more truncation error due to the recursive generation of the moments. Similar observations were also reported in reference [55]. It is worth to note that the expansion points used in [55], which are identical to the ones as shown above, were selected in a heuristic manner. However, the proposed search algorithm can automatically generate these expansion points in the multipoint Padé approximation.

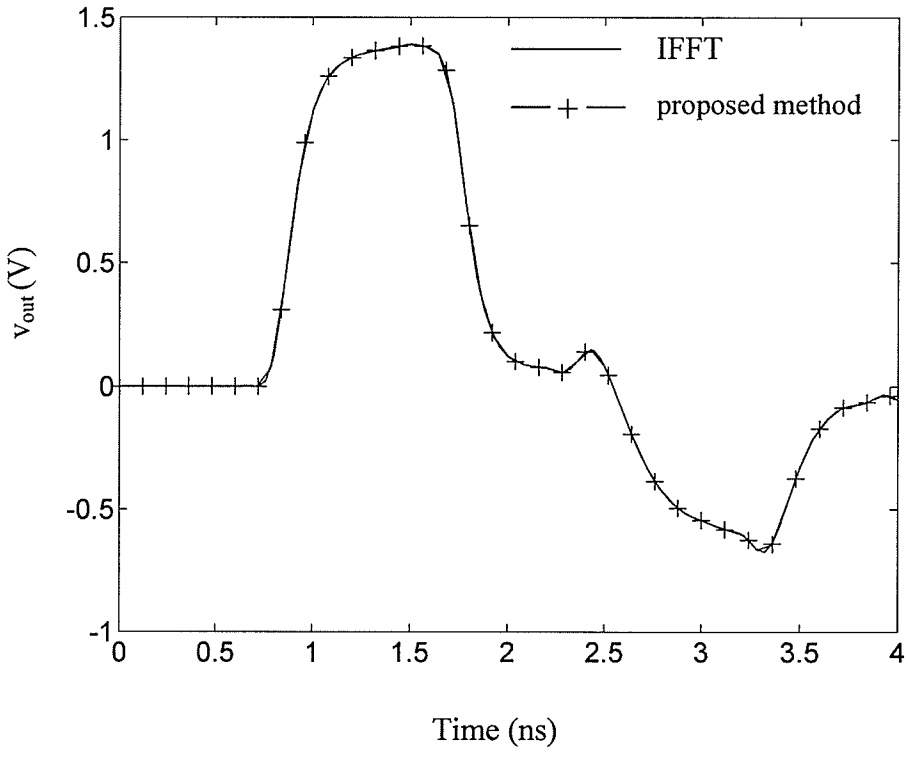

Fig. 3.7. Transient response of the interconnect network in Fig. 3.5 for a 1V pulse excitation with 0.1 ns rise and fall times and 1 ns duration.

3.3.2. Solution Accuracy and Convergence Analysis

To verify the accuracy and efficiency of the proposed algorithm, a simple circuit which contains a lossless transmission line as shown in Fig. 3.8 was simulated. The exact frequency response at the load resistor is given by [56]

$$H(s) = \frac{1}{2.25e^{s} - 0.25e^{-s}} \ .$$

With the maximum frequency of interest at 5 GHz and 8 moments at each expansion point, the multipoint Padé approximation method required 5 expansion points (located at 0, 1.25, 2.5, 3.75 and 5 GHz) to obtain an approximate frequency response at the load resistor. Comparison of the approximate frequency response with the exact response is shown in Fig. 3.9. The network was simulated using the CFH technique [21] taking 8 moments at each expansion point and the result is also plotted in Fig. 3.9. It is noticed that the CFH simulation result is obtained with 17 expansion points, this being more than 3 times the number of expansion points required in the proposed method. Also shown in Fig. 3.9 for comparison is the sixth order AWE result, which demonstrates that numerical instabilities degrade higher frequency solutions in this method. In order to compare the accuracy of the proposed method with that of the above mentioned techniques, relative errors in the frequency response with respect to the exact response was computed. The results plotted in Fig. 3.10 show clearly that the accuracy of the proposed method over the entire frequency range of interest is much higher than that of AWE or CFH. Fig. 3.11 presents the dynamic change in relative error of the approximate response in the process of implementing the proposed search algorithm. As it can be seen, the accuracy of

successive approximations is constantly improved by using all the moment sets available from all updated expansion points.

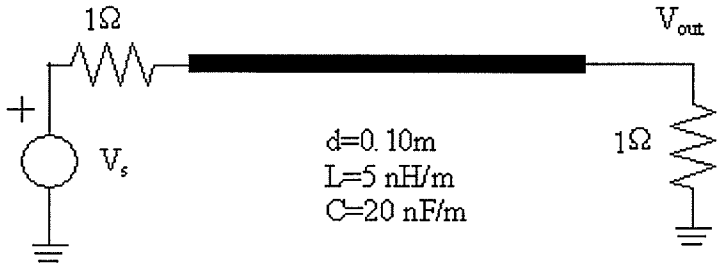

Fig. 3.8. An interconnect circuit with one lossless transmission line.

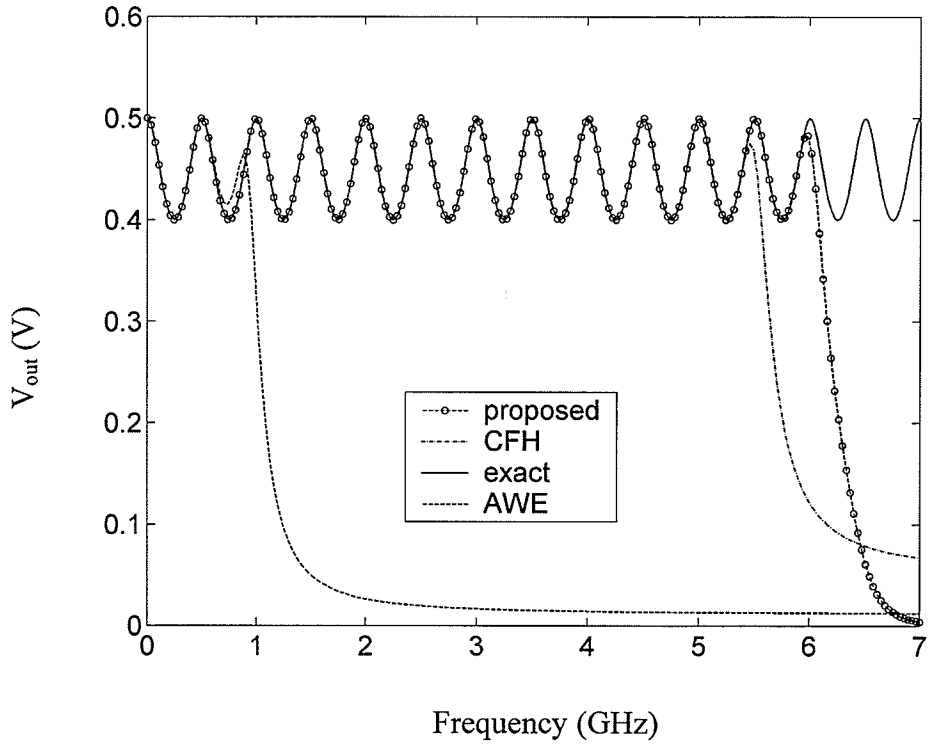

Fig. 3.9. Frequency response at the load end of the example circuit in Fig. 3.8.

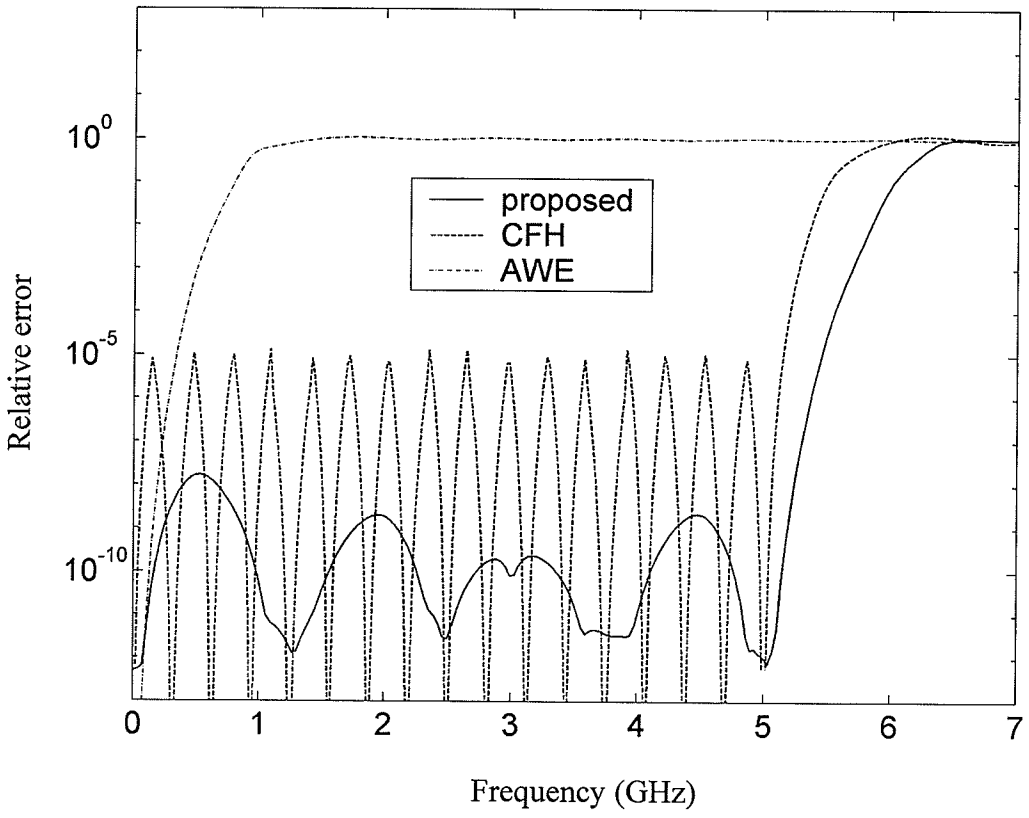

Fig. 3.10. Relative errors in the frequency response of the example circuit shown in Fig. 3.8.

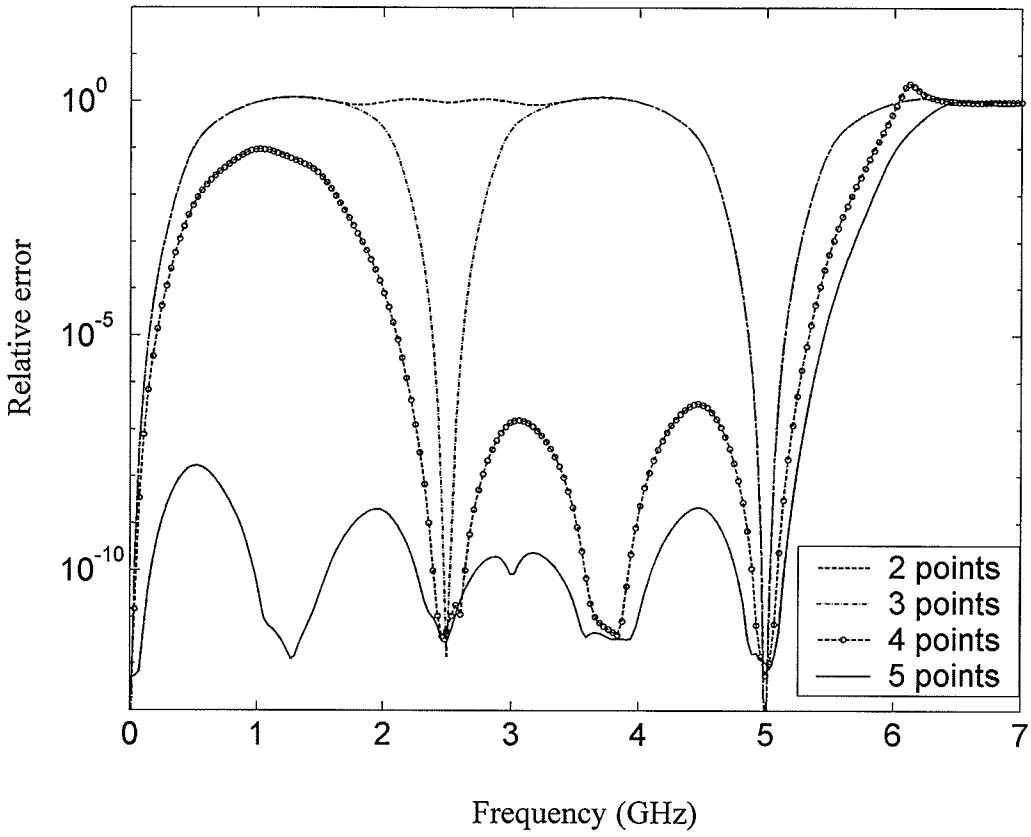

Fig. 3.11. Relative errors in the frequency response of the example circuit shown in Fig. 3.8. The circuit was simulated by the proposed method for various number of expansion points: 2 points [0, 5GHz], 3 points [0, 2.5, 5GHz], 4 points [0, 2.5, 3.75, 5GHz], and 5 points [0, 1.25, 2.5, 3.75, 5GHz]. The number of moments used at each expansion point is 8.

The convergence of solutions obtained by applying the proposed multipoint Padé algorithm to interconnect problems can be evaluated by the standard deviation parameter σ, which is defined as in [57].

$$\sigma = \sqrt{\frac{1}{\mathcal{N}} \sum_{i=1}^{N} \left(X_i - \hat{X}_i \right)^2}$$

where $\mathcal{N}$ is the number of frequency points used for evaluation, X_i is the actual solution for the i^{th} point and $\hat{X}_i$ is the multipoint Padé approximation solution for the same point.

Consider an interconnect circuit example taken from [7]. The interconnect circuit contains three sets of lossy coupled transmission lines, as shown in Fig. 3.12, and the lengths of the lines 1, 2 and 3 are 0.05m, 0.04m and 0.03m, respectively. The electrical parameter matrices for the three transmission lines are identical and are given as

$$\boldsymbol{L} = \begin{bmatrix} 494.6 & 63.3 \\ 63.3 & 494.6 \end{bmatrix} \text{nH/m} \qquad \boldsymbol{C} = \begin{bmatrix} 62.8 & -4.9 \\ -4.9 & 62.8 \end{bmatrix} \text{pF/m}$$

$$\boldsymbol{R} = \begin{bmatrix} 75 & 15 \\ 15 & 75 \end{bmatrix} \Omega\text{/m} \qquad \boldsymbol{G} = \begin{bmatrix} 0.1 & -0.01 \\ -0.01 & 0.1 \end{bmatrix} \text{S/m.}$$

First, the circuit was analyzed at the output node V_{out} by using an increasing number of expansion points. The approximate frequency response produced by using one expansion point at the origin with 8 moments, as compared with the actual frequency response at the output, is shown in Fig. 3.13. Increasing the number of expansion points to three yields the frequency response shown in Fig. 3.14. The converged solution was obtained by implementing the proposed multipoint Padé approximation algorithm with five expansion points and with an error tolerance $\varepsilon = 10^{-3}$, as displayed in Fig. 3.15.

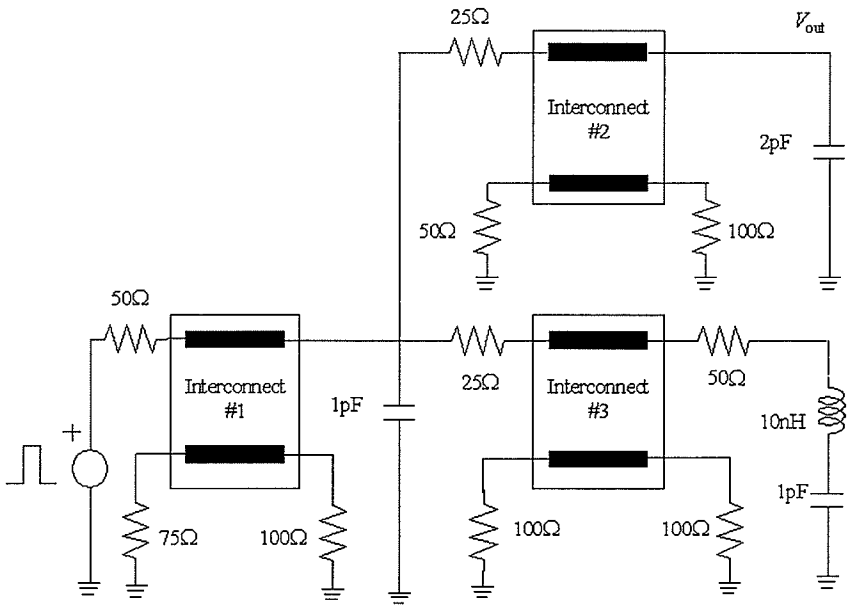

Fig. 3.12. A lossy coupled transmission line network.

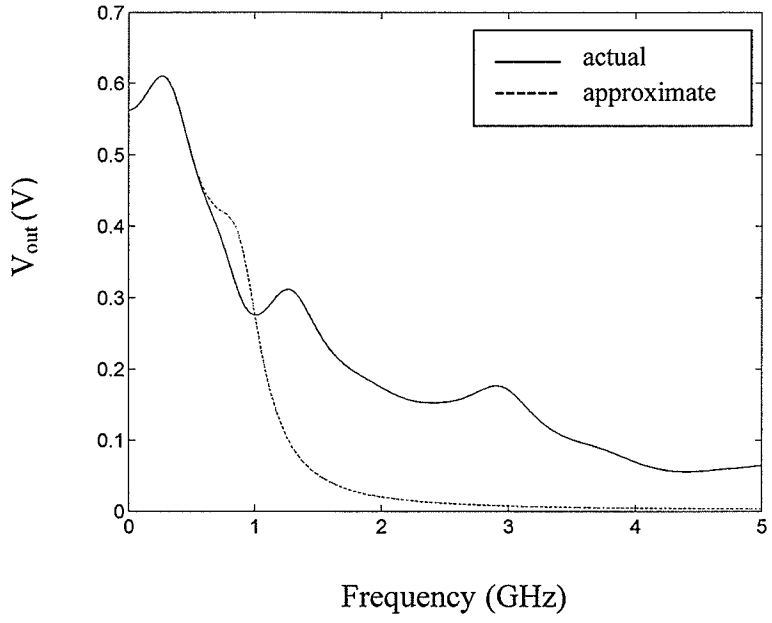

Fig. 3.13. Frequency response at the output node of the example circuit in Fig.3.12 obtained by using one expansion point at the origin. The number of moments used at the expansion point is 8.

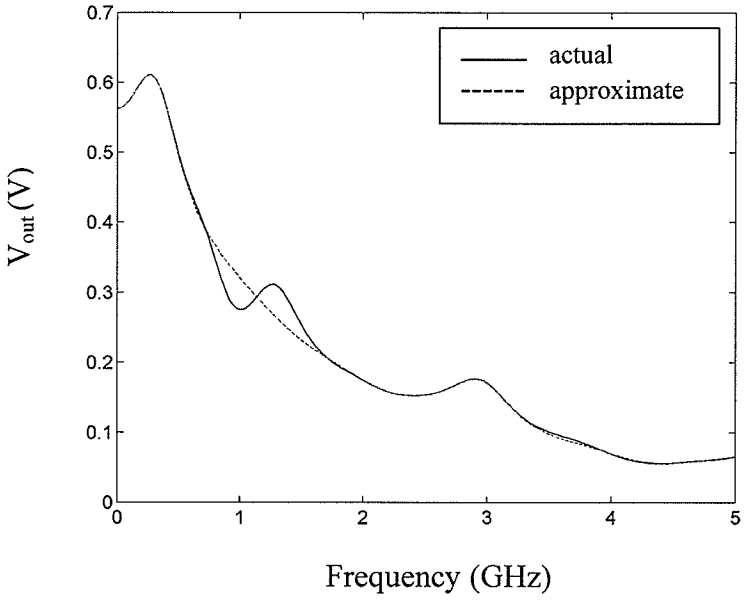

Fig. 3.14. Frequency response at the output node of the example circuit in Fig. 3.12 obtained by using three expansion points [0, 2.5, 5GHz]. The number of moments used at each expansion point is 8.

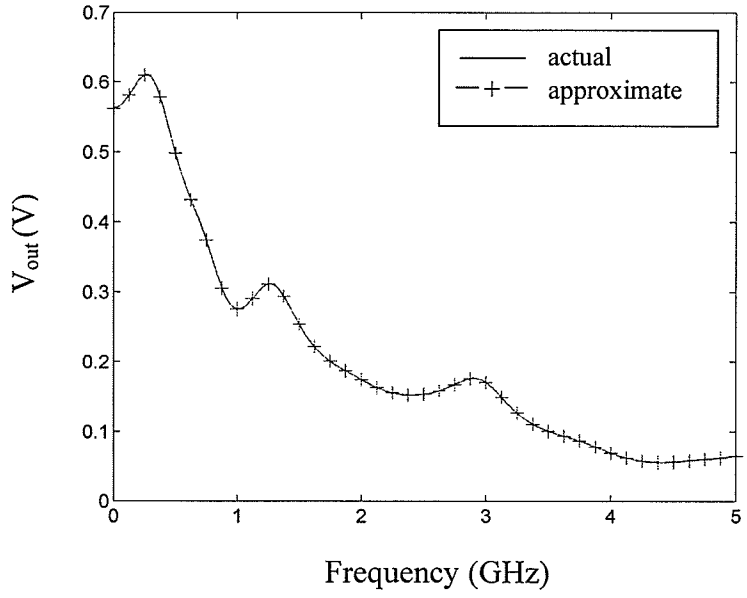

Fig. 3.15. Frequency response at the output node of the example circuit in Fig. 3.12 obtained by applying the proposed algorithm with five expansion points [0, 1.25, 2.5, 3.75, 5GHz]. The number of moments used at each expansion point is 8.

Next, the convergence behavior of the multipoint Padé approximation solutions was analyzed with respect to the number of moments chosen at each expansion point. With a pre-specified and the highest frequency of interest GHz, In Fig. 3.16, the solution accuracy, measured by the standard deviation parameter σ as related to the indicated number of moments taken at each expansion point and the corresponding number of expansion points, is shown for a range of frequency up to $f_{max} = 5$ GHz, and for a pre-specified error tolerance $\varepsilon = 10^{-3}$ and for $\mathcal{N}$=201. It can be seen that choosing a smaller number of moments at each expansion point requires the same or a larger number of expansion points to achieve convergence and *vice versa.* In other words, there is a trade-off between the number of moments and the number of expansion points required to achieve a desired accuracy. Also, it is observed that the proposed multipoint Padé approximation method converges to a solution (within the specified error tolerance) for any number of moments chosen at each expansion point, as long as the number of moments is not more than 16. As mentioned in chapter one, the necessity to not use more than 16 moments at each expansion point is solely due to the limitations associated with direct moment-matching Padé approximations [27]. The example circuit was again analyzed using the proposed multipoint Padé algorithm when the pre-specified error tolerance is reduced to 10^{-5} and the results for solution accuracy are plotted in Fig. 3.17. The same observations regarding the solution convergence with respect to the number of moments and the number of expansion points are made in this case, except that the multipoint Padé approximation algorithm may require a larger number of expansion points to achieve a higher accuracy requirement, e.g., 4 expansion points in the case

$\varepsilon = 10^{-5}$ vs. 3 expansion points in the case $\varepsilon = 10^{-3}$, when the number of moments chosen at each point is 12.

Finally, the convergence rates of the solutions obtained by applying the proposed multipoint Padé approximation algorithm and the CFH technique to the example circuit are compared and the results are presented in Fig. 3.18. It can be seen that, when the same number of moments is chosen at each expansion point, the CFH technique requires a larger number of expansion points to produce a solution of same accuracy, as compared with the proposed multipoint Padé approximation algorithm.

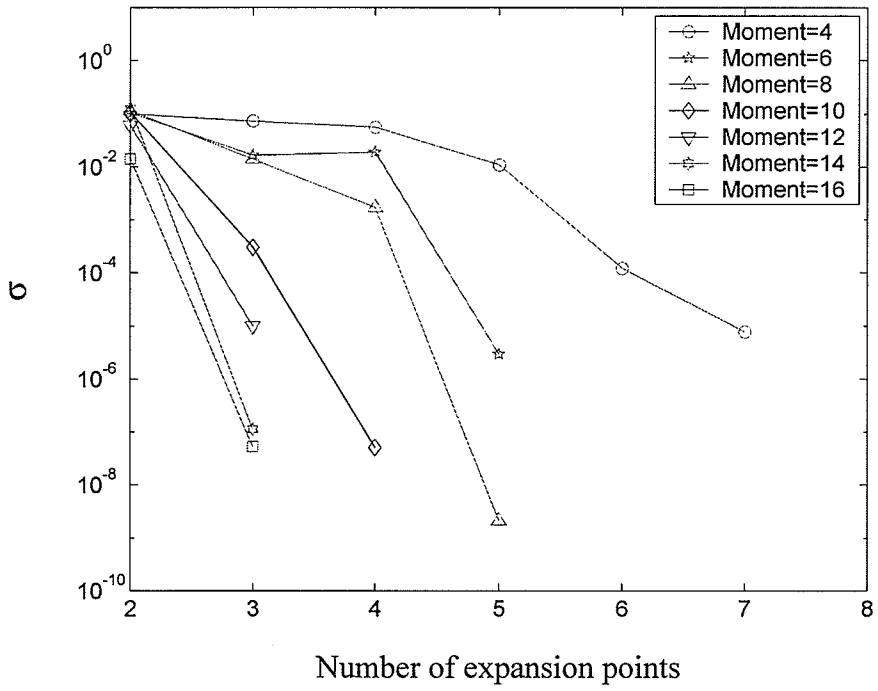

Fig. 3.16. Analysis of solution convergence ($\varepsilon = 10^{-3}$).

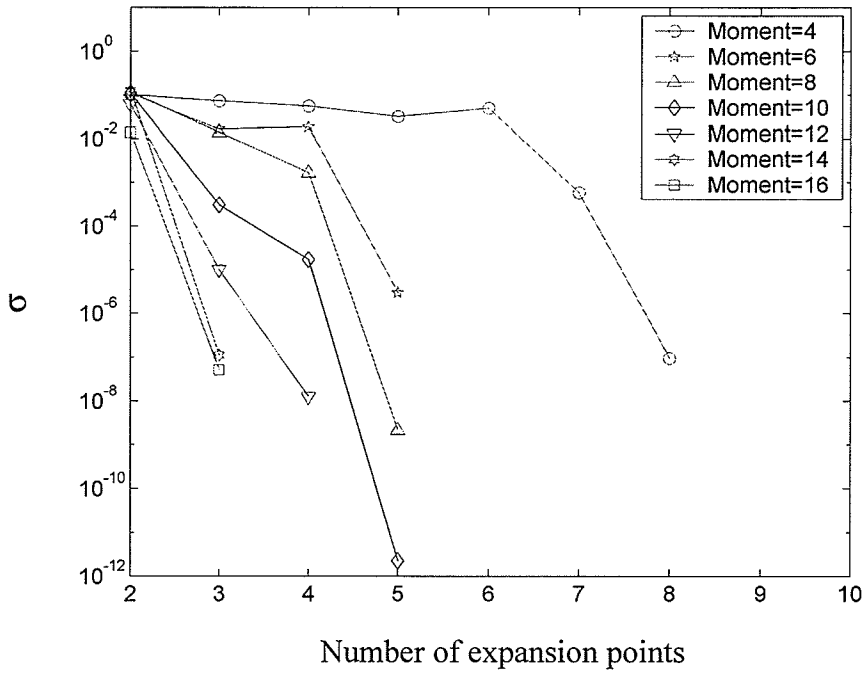

Fig. 3.17. Analysis of solution convergence ($\varepsilon = 10^{-5}$).

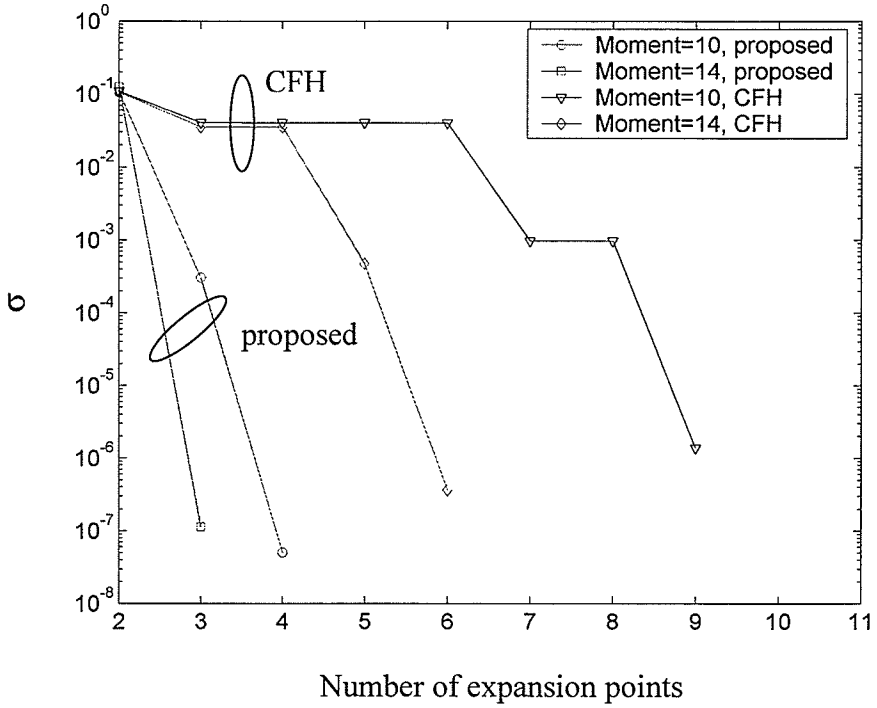

Fig. 3.18. Analysis of solution convergence ($\varepsilon = 10^{-4}$).

The convergence analysis of the multipoint Padé approximation solutions was again conducted using the example network shown in Fig. 3.5. This network was first simulated with an increasing number of expansion points and the results were compared with the actual solution. Fig. 3.19 shows the approximate frequency response at the output node obtained by using ten moments generated at the origin, while Fig. 3.20 displays the frequency response produced by using moments generated at three expansion points. The frequency response produced by using only one or three expansion points, as shown in Figs. 3.19 and 3.20, is obvious inadequate to model the response of the circuit. The frequency response which agrees well with the actual one was obtained by implementing the proposed multipoint Padé approximation algorithm with $\varepsilon = 10^{-3}$, resulting in five expansion points being required, and is plotted in Fig. 3.21.

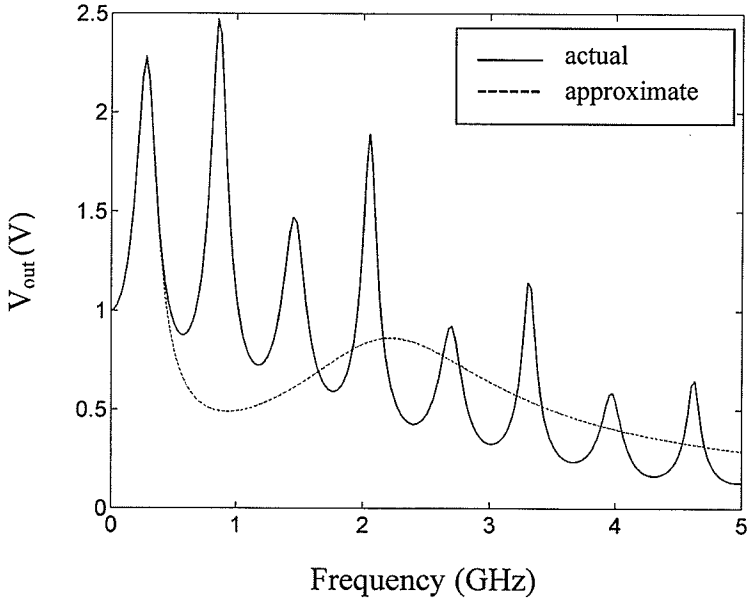

Fig. 3.19. Frequency response at the output node of the example circuit in Fig. 3.5 obtained by using one expansion point at the origin. The number of moments used at the expansion point is 10.

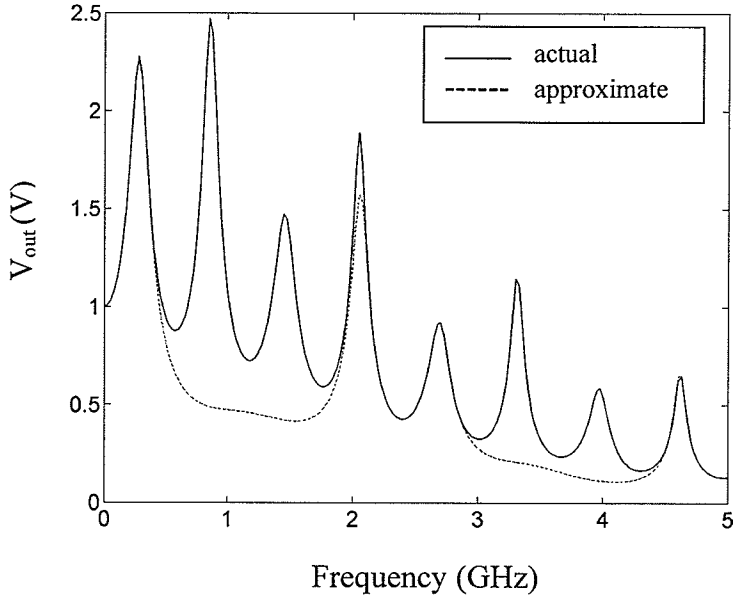

Fig. 3.20. Frequency response at the output node of the example circuit in Fig. 3.5 obtained by using three expansion points [0, 2.5, 5GHz]. The number of moments used at each expansion point is 10.

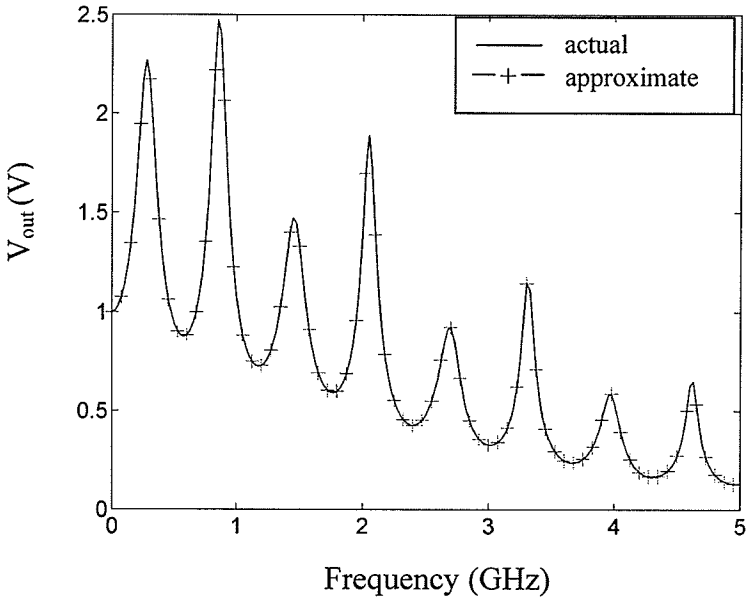

Fig. 3.21. Frequency response at the output node of the example circuit in Fig. 3.5 obtained by using the proposed algorithm with five expansion points [0, 1.25, 2.5, 3.75, 5GHz]. The number of moments used at each expansion point is 10.

The example circuit was then simulated using the multipoint Padé approximation method to study the solution convergence behavior with respect to the number of moments chosen at each expansion point. Figs. 3.22 and 3.23 show the standard deviation σ with $\mathcal{N}$=201 evaluation points of the approximate solutions obtained by using the proposed algorithm when the error tolerance is specified to be 10^{-2} and 10^{-4}, respectively. It is again observed that, when the number of moments chosen at each expansion point is not more than 16, the resultant multipoint Padé approximation solutions are convergent in both cases and that, solutions obtained by using an increasing number of moments at each expansion point can, in general, achieve convergence with a smaller number of expansion points being required.

Based on numerous simulation experiments for example circuits similar to that presented in this study, it has been found that, in the application of the proposed multipoint Padé approximation method to analyze typical interconnect circuits: (1) using no more than 16 moments at each expansion point guarantees solution convergence; (2) a choice of the number of moments between 8 and 16 at each expansion point produces convergent solutions with an optimum computational efficiency determined in relation with the number of expansion points.

In order to compare the solution convergence of the proposed multipoint Padé approximation algorithm, the CFH technique was also applied to analyze the example network considered. In Fig. 3.24, a comparison of the standard deviation of solutions obtained by applying the CFH technique and the proposed multipoint Padé approximation algorithm is presented. It can be seen that, using the same number of moments at each expansion point as in the proposed algorithm, the CFH technique

requires a larger number of expansion points to obtain a solution with same accuracy as that in the proposed algorithm.

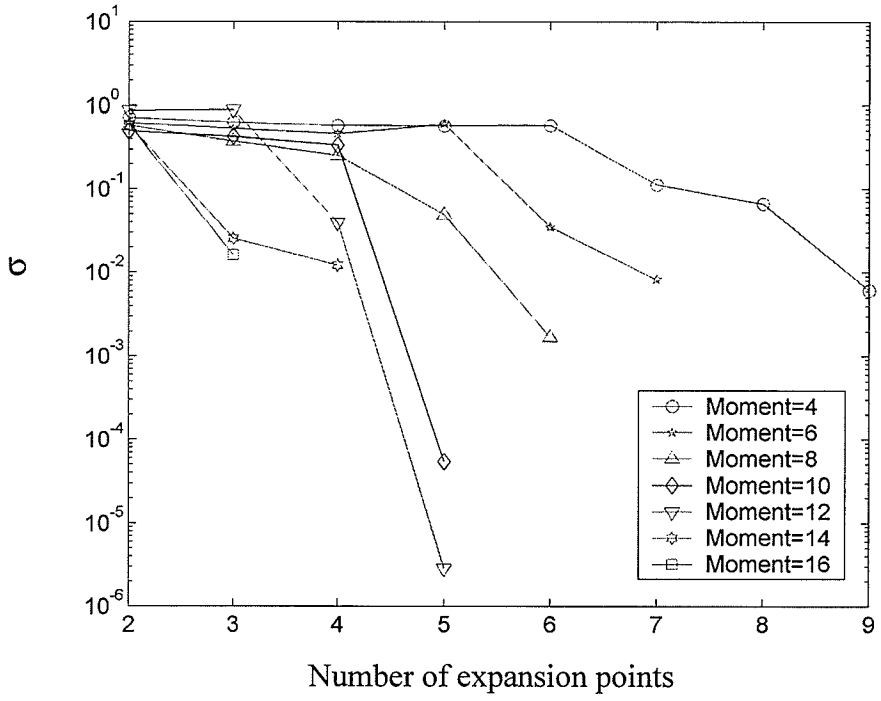

Fig. 3.22. Analysis of solution convergence ($\varepsilon = 10^{-2}$).

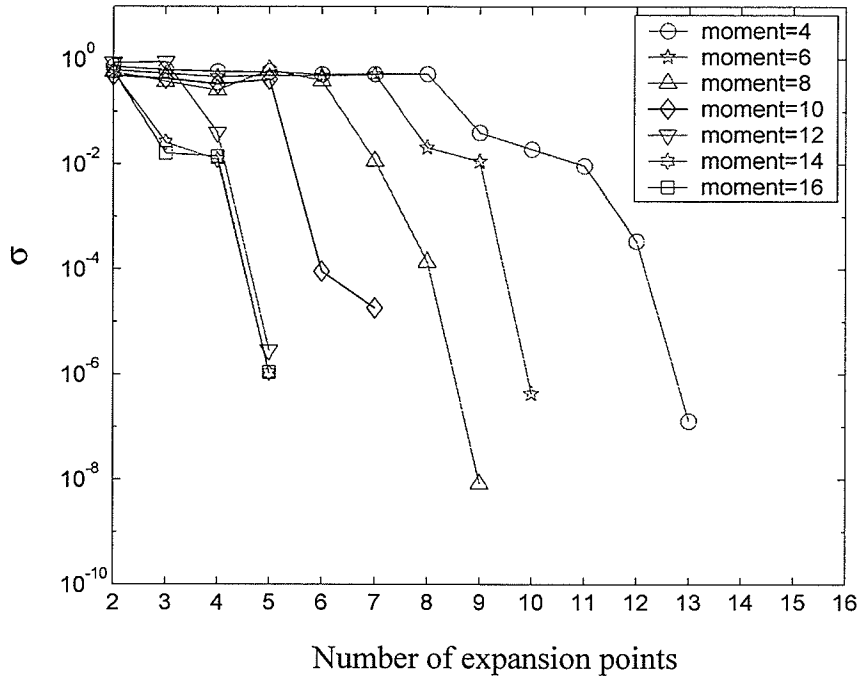

Fig. 3.23. Analysis of solution convergence ($\varepsilon = 10^{-4}$).

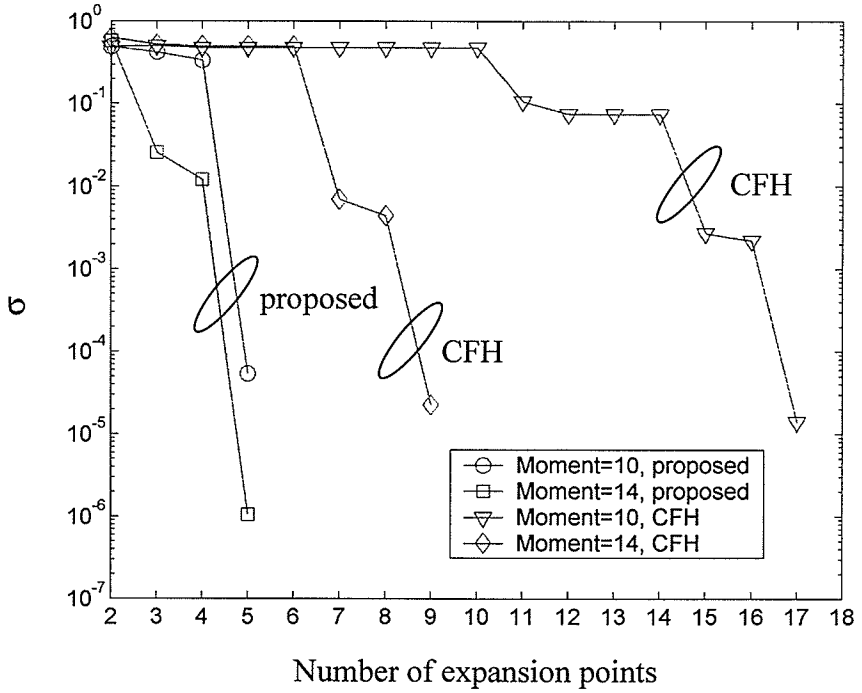

Fig. 3.24. Analysis of solution convergence ($\varepsilon = 10^{-3}$).

3.3.3. CPU Cost Comparisons

To demonstrate the efficiency of the proposed multipoint Padé approximation algorithm, two relatively large interconnect circuits containing lossy transmission lines were investigated. The first example circuit is obtained by cascading the circuit block [55] shown at the top of Fig. 3.25 five times such that the resulting circuit has a total of 35 transmission lines. The second example is a circuit which contains a total of 70 transmission lines, constructed from cascading the circuit block ten times. All lines in the circuit block are assumed to have zero conductance while their resistance is taken to be the same value of 10 Ω/m. For each type of line, the capacitance C, the inductance L, and the length of l are given as follows: line T1, C=100 pF/m, L=60 nH/m, l=0.03 m; line T2, C=100 pF/m, L=100 nH/m, l=0.05 cm; line T3, C=120 pF/m, L=60 nH/m, l=0.03 m; line T4, C=100 pF/m, L=60 nH/m, l=0.04 m; line T5, C=150 pF/m, L=100 nH/m, l=0.02 m. The excitation source applied is a 1V pulse with 100 ps rise/fall time and a 5 ns duration. In using the multipoint Padé approximation algorithm to simulate both example circuits, the maximum frequency of interest was chosen at 4 GHz and the required number of frequency expansion points for each case was five. As an example, the transient waveform at the output node of the second example circuit, containing 70 transmission lines, is plotted in Fig. 3.26. Also shown in the Fig. 3.26 is the result obtained by using a direct solution of the equation (2.4) at 1024 frequency points and then applying the IFFT technique to the resultant frequency response. A comparison of CPU costs from simulating the two example circuits using the proposed multipoint Padé approximation algorithm, the CFH technique, and the direct solution is given in Table I. In the

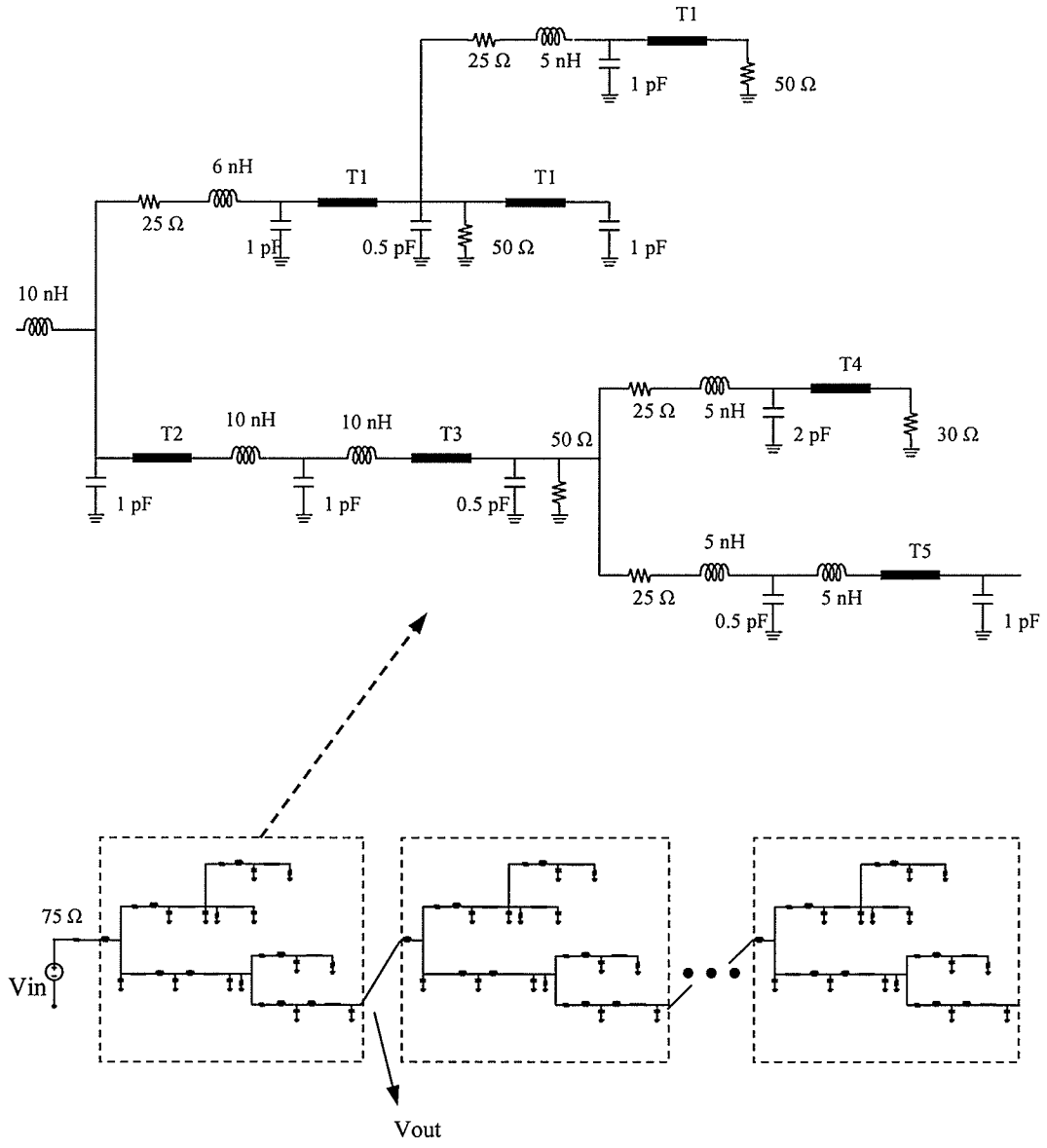

Fig. 3.25. Interconnect circuits used for CPU cost comparisons consisting of multiple cascaded subcircuits.

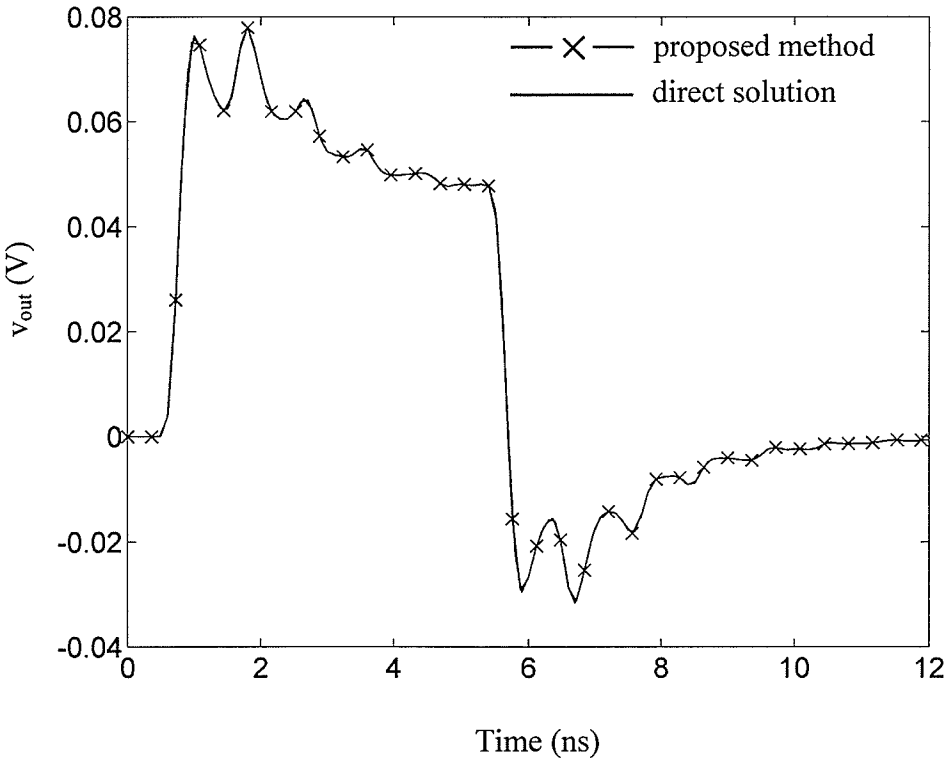

Fig. 3.26. Transient response at the output node of the interconnect circuit containing a total of 70 lossy transmission lines [55].

TABLE I

COMPARISON OF CPU COSTS (10 MOMENTS USED AT ALL EXPANSION POINTS)

	Number of Transmission Lines	Number of lumped elements	CPU Time in second		
			Proposed method	CFH algorithm	Direct solution
Circuit 1	35	131	4.07	8.18	251.82
Circuit 2	70	261	17.35	39.7	1432.5

examples presented, the same number of moments at each expansion point was used in both the CFH technique and the proposed multipoint Padé approximation method. However, it is possible that the performance of the CFH technique, as well as the proposed technique, can be optimized by using a different number of moments at each expansion point.

3.4. SUMMARY

To efficiently analyze interconnect networks containing distributed transmission lines, a new method which is based on multipoint Padé approximations has been introduced. The proposed method differs from existing moment matching techniques in that it utilizes all the moment sets at all updated expansion points in the process of yielding approximations and can be used to efficiently obtain a closed-form solution of the interconnect network response. Meanwhile, an improved search algorithm for the selection of frequency expansion points has been presented, resulting in a smaller number of expansion points being required for the same accuracy and yielding a reduction in CPU cost. Several examples were studied in order to demonstrate the performance of the proposed method. In the first two examples, interconnect circuits with lossy multiconductor transmission lines were simulated using the conventional approach and the proposed method. The numerical results obtained in frequency domain and time domain for both cases are in excellent agreement. Next, an interconnect modeled with a lossless transmission line was analyzed and was used to further investigate the accuracy of the proposed method. The frequency responses of the interconnect circuit were obtained by using the proposed method and the existing moment matching techniques, and their relative errors with respect to the exact frequency response are computed. It was

shown that the proposed method exhibited higher accuracy over the entire frequency range of interest. In addition, the convergence rates of solutions obtained by using the proposed method were studied. The comparison of CPU costs was conducted by simulating two relatively large interconnect circuits for the case of equal moments at all expansion points. It was shown that, compared with conventional methods, the proposed multipoint Padé approximation method is more efficient in simulating large interconnect networks.

Chapter 4. Moments for Frequency Dependent Transmission Lines

When applying moment matching techniques to simulation of interconnect networks containing lossy coupled transmission lines, the transmission line moments are usually generated by using either the eigenvalue moment method [11] or the matrix exponential method [20]. In the eigenvalue moment method, moment generation is performed by using the eigenvalues and eigenvectors of the transmission line propagation matrix. The truncation error in the computation of the eigenvalues and eigenvectors increases for higher order moments, resulting in a degradation of accuracy for waveform evaluation. The matrix exponential method was introduced to improve the computation accuracy of the moments. The method generates moments by expanding the transmission line parameter matrix as a Taylor series. In [54], the matrix exponential method was extended to handle transmission lines with frequency-dependent parameters. Although the matrix exponential method yields more accurate moments, it is computationally more costly than the eigenvalue method due to the slow convergence of the matrix exponential series. In this chapter, a modified matrix exponential method [52] for generating the moments of frequency-dependent lossy transmission lines is introduced. The proposed method yields the same accuracy as the original matrix exponential method, but also has a computational efficiency which is comparable to that of the eigenvalue moment method.

4.1. MODIFIED MATRIX EXPONENTIAL METHOD

Consider a linear interconnect network containing distributed transmission lines and its model using a modified nodal admittance formulation [51]. When employing the moment matching approach, the generation of frequency derivatives (moments) of the modified nodal admittance matrix is required, which in turn requires computation of the transmission line moments.

Fig. 4.1 shows a lossy coupled transmission line that contains N conductors. The multiconductor transmission line can be characterized by the line length and the per-unit length (p.u.l.) transmission line parameter matrices, i.e., series resistance matrix, $\boldsymbol{R}$, the

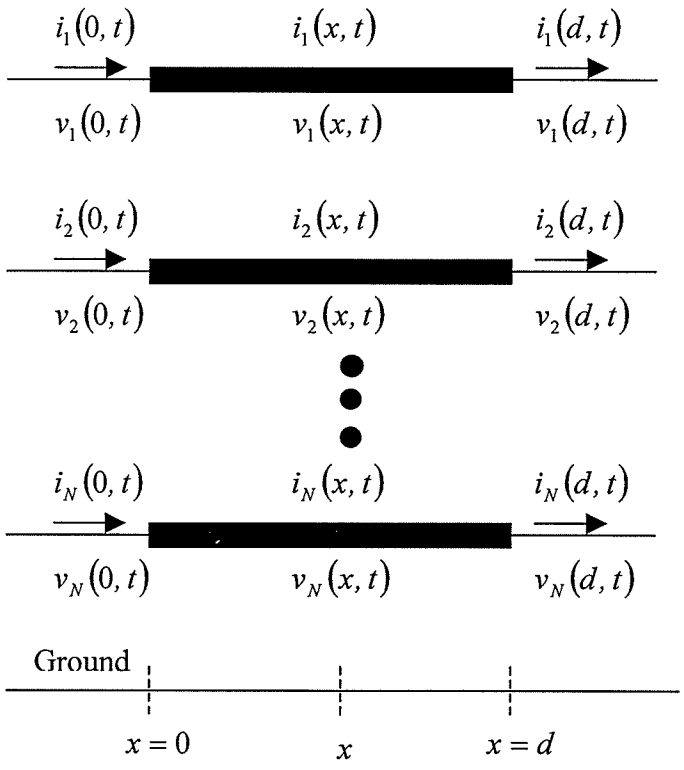

Fig. 4.1. Multiconductor transmission line of length d.

shunt conductance matrix, $\boldsymbol{G}$, the series inductance matrix, $\boldsymbol{L}$, and the shunt capacitance matrix $\boldsymbol{C}$. The line voltages $\boldsymbol{v}(x,t)$ and line currents $\boldsymbol{i}(x,t)$ at points along the transmission line are described by the Telegrapher's partial differential equations, i.e.,

$$\frac{\partial}{\partial x}\boldsymbol{v}(x,t) = -\boldsymbol{R} * \boldsymbol{i}(x,t) - \boldsymbol{L} * \frac{\partial}{\partial t}\boldsymbol{i}(x,t) \tag{4.1}$$

$$\frac{\partial}{\partial x}\boldsymbol{i}(x,t) = -\boldsymbol{G} * \boldsymbol{v}(x,t) - \boldsymbol{C} * \frac{\partial}{\partial t}\boldsymbol{v}(x,t) \tag{4.2}$$

with

$$\boldsymbol{v}(x,t) = \begin{bmatrix} v_1(x,t) \\ v_2(x,t) \\ \vdots \\ v_N(x,t) \end{bmatrix} \qquad \boldsymbol{i}(x,t) = \begin{bmatrix} i_1(x,t) \\ i_2(x,t) \\ \vdots \\ i_N(x,t) \end{bmatrix} \tag{4.3}$$

Taking Laplace transform of (4.1) and (4.2), the multiconductor transmission line is described by the following equations:

$$\frac{\partial}{\partial x}\boldsymbol{V}(x,s) = -(\boldsymbol{R} + s\boldsymbol{L})\boldsymbol{I}(x,s) \tag{4.4}$$

$$\frac{\partial}{\partial x}\boldsymbol{I}(x,s) = -(\boldsymbol{G} + s\boldsymbol{C})\boldsymbol{V}(x,s) \tag{4.5}$$

In the case of coupled lossy transmission lines with frequency-dependent parameters, the transmission line moments can be derived from the Laplace-domain partial differential equations

$$\frac{\partial}{\partial x}\begin{bmatrix} \boldsymbol{V}(x,s) \\ \boldsymbol{I}(x,s) \end{bmatrix} = \begin{bmatrix} \boldsymbol{0} & -\boldsymbol{Z}(s) \\ -\boldsymbol{Y}(s) & \boldsymbol{0} \end{bmatrix} \begin{bmatrix} \boldsymbol{V}(x,s) \\ \boldsymbol{I}(x,s) \end{bmatrix} \tag{4.6}$$

with

$$\boldsymbol{Z}(s) = \boldsymbol{R}(s) + s\boldsymbol{L}(s) \tag{4.7}$$

$$\boldsymbol{Y}(s) = \boldsymbol{G}(s) + s\boldsymbol{C}(s) \tag{4.8}$$

where $\boldsymbol{Z}(s)$ and $\boldsymbol{Y}(s)$ are the p.u.l. impedance and admittance matrices, and $\boldsymbol{R}(s)$, $\boldsymbol{G}(s)$, $\boldsymbol{L}(s)$, and $\boldsymbol{C}(s)$ are the p.u.l. *frequency-dependent* series resistance, shunt conductance, series inductance, and shunt capacitance transmission line parameter matrices, respectively.

From (4.6)-(4.8), the relationship between the voltages and currents at the far end of a transmission line of length d, $\boldsymbol{V}(d,s)$, and $\boldsymbol{I}(d,s)$ and those at the near end, $\boldsymbol{V}(0,s)$ and $\boldsymbol{I}(0,s)$, can be described in terms of the transmission line parameter matrix $\boldsymbol{T}$ as

$$\begin{bmatrix} \boldsymbol{V}(d,s) \\ \boldsymbol{I}(d,s) \end{bmatrix} = \boldsymbol{T}(s) \begin{bmatrix} \boldsymbol{V}(0,s) \\ \boldsymbol{I}(0,s) \end{bmatrix} \tag{4.9}$$

where

$$\boldsymbol{T}(s) = e^{\boldsymbol{F}(s)d} \tag{4.10}$$

$$\boldsymbol{F}(s) = \begin{bmatrix} \boldsymbol{0} & -\boldsymbol{Z}(s) \\ -\boldsymbol{Y}(s) & \boldsymbol{0} \end{bmatrix} \tag{4.11}$$

The p.u.l. impedance and admittance $\boldsymbol{Z}(s)$ and $\boldsymbol{Y}(s)$ matrices can be expanded as a Taylor series in the form

$$\boldsymbol{Z}(s) = \sum_{n=0}^{\infty} \boldsymbol{Z}_n s^n \tag{4.12}$$

$$\boldsymbol{Y}(s) = \sum_{n=0}^{\infty} \boldsymbol{Y}_n s^n \tag{4.13}$$

and thus

$$\boldsymbol{F}(s) = \sum_{n=0}^{\infty} \boldsymbol{F}_n s^n \tag{4.14}$$

with

$$\boldsymbol{F}_n = \begin{bmatrix} \boldsymbol{0} & -\boldsymbol{Z}_n \\ -\boldsymbol{Y}_n & \boldsymbol{0} \end{bmatrix} \tag{4.15}$$

For the special case when the line parameters $\boldsymbol{R}$, $\boldsymbol{G}$, $\boldsymbol{L}$ and $\boldsymbol{C}$ are frequency independent, we have $\boldsymbol{Z}_0 = \boldsymbol{R}$, $\boldsymbol{Z}_1 = \boldsymbol{L}$, $\boldsymbol{Y}_0 = \boldsymbol{G}$, $\boldsymbol{Y}_1 = \boldsymbol{C}$, and $\boldsymbol{Z}_n = \boldsymbol{Y}_n = \boldsymbol{0}$ for $n > 1$.

In the implementation of moment matching techniques, the coefficients of the Taylor series expansion of the transmission matrix $\boldsymbol{T}(s)$ are required

$$\boldsymbol{T}(s) = [\boldsymbol{I}] + \frac{\boldsymbol{F}(s)}{1!} + \frac{\boldsymbol{F}^2(s)d^2}{2!} + \cdots + \frac{\boldsymbol{F}^n(s)d^n}{n!} + \cdots. \tag{4.16}$$

In the matrix exponential method presented in [20], [54], the expansion coefficients are obtained by substituting (4.14) into (4.16) and collecting terms with same power of s. The computation of the coefficients in this manner usually requires summation of a large number of terms due to the slow convergence of a series of the exponential type.

In order to more efficiently generate the moments of transmission line systems, a modified matrix exponential method is presented in this chapter [52]. Starting from (4.12) and (4.13), the product $\boldsymbol{Z}(s)\boldsymbol{Y}(s)$ can be written as a Taylor series expansion in the form

$$\boldsymbol{Z}(s)\boldsymbol{Y}(s) = \sum_{n=0}^{\infty} \boldsymbol{W}_n s^n \tag{4.17}$$

with

$$\boldsymbol{W}_n = \sum_{i=0}^{n} \boldsymbol{Z}_{n-i}\boldsymbol{Y}_i \tag{4.18}$$

Let the matrix $\boldsymbol{T}(s)$ be expanded in the form

$$\boldsymbol{T}(s) = \begin{bmatrix} \boldsymbol{A}(s) & \boldsymbol{B}(s) \\ \boldsymbol{C}(s) & \boldsymbol{D}(s) \end{bmatrix} = \sum_{n=0}^{\infty} \begin{bmatrix} \boldsymbol{A}_n & \boldsymbol{B}_n \\ \boldsymbol{C}_n & \boldsymbol{D}_n \end{bmatrix} s^n \tag{4.19}$$

By expanding (4.10) in an exponential series as in (4.16), we have

$$\boldsymbol{T}(s)=\begin{bmatrix}\boldsymbol{1} & \boldsymbol{0}\\ \boldsymbol{0} & \boldsymbol{1}\end{bmatrix}+\frac{d}{1!}\begin{bmatrix}\boldsymbol{0} & -\boldsymbol{Z}(s)\\ -\boldsymbol{Y}(s) & \boldsymbol{0}\end{bmatrix}+\frac{d^2}{2!}\begin{bmatrix}\boldsymbol{Z}(s)\boldsymbol{Y}(s) & \boldsymbol{0}\\ \boldsymbol{0} & \boldsymbol{Y}(s)\boldsymbol{Z}(s)\end{bmatrix}$$

$$+\frac{d^3}{3!}\begin{bmatrix}\boldsymbol{0} & -\boldsymbol{Z}(s)\boldsymbol{Y}(s)\boldsymbol{Z}(s)\\ -\boldsymbol{Y}(s)\boldsymbol{Z}(s)\boldsymbol{Y}(s) & \boldsymbol{0}\end{bmatrix}$$

$$+\frac{d^4}{4!}\begin{bmatrix}\boldsymbol{Z}(s)\boldsymbol{Y}(s)\boldsymbol{Z}(s)\boldsymbol{Y}(s) & \boldsymbol{0}\\ \boldsymbol{0} & \boldsymbol{Y}(s)\boldsymbol{Z}(s)\boldsymbol{Y}(s)\boldsymbol{Z}(s)\end{bmatrix}+\cdots \tag{4.20}$$

Equating (4.19) and (4.20) gives

$$\boldsymbol{A}(s)=\sum_{n=0}^{\infty}\boldsymbol{A}_n s^n=[\boldsymbol{I}]+\frac{d^2}{2!}\boldsymbol{Z}(s)\boldsymbol{Y}(s)+\frac{d^4}{4!}\boldsymbol{Z}(s)\boldsymbol{Y}(s)\boldsymbol{Z}(s)\boldsymbol{Y}(s)+\cdots \tag{4.21}$$

Now, using (4.17) and matching powers of s yields the recursive formulas

$$\boldsymbol{A}_0=[\boldsymbol{I}]+\sum_{j=1}^{\infty}\boldsymbol{A}_{1,j}\,, \tag{4.22}$$

$$\boldsymbol{A}_i=\sum_{j=1}^{\infty}\boldsymbol{A}_{i+1,j}\,; \qquad i=1,2,\cdots \tag{4.23}$$

where

$$\boldsymbol{A}_{i,1}=\frac{d^2\boldsymbol{W}_{i-1}}{2} \tag{4.24}$$

$$\boldsymbol{A}_{i,j}=d^2\sum_{k=0}^{i-1}\frac{\boldsymbol{W}_k\boldsymbol{A}_{i-k,j-1}}{2j(2j-1)} \qquad j=2,3,\cdots. \tag{4.25}$$

It can be easily shown that $\boldsymbol{B}_n$, $\boldsymbol{C}_n$, and $\boldsymbol{D}_n$, for $n\geq 0$, are also calculated as

$$\boldsymbol{D}_n=\boldsymbol{A}_n^t \tag{4.26}$$

$$\boldsymbol{C}_n=-d\left[\boldsymbol{Y}_n-\sum_{k=0}^{n}\boldsymbol{Y}_k\boldsymbol{U}_{n-k}\right] \tag{4.27}$$

$$\boldsymbol{B}_n=-d\left[\boldsymbol{Z}_n-\sum_{k=0}^{n}\boldsymbol{Z}_k\boldsymbol{U}_{n-k}^t\right] \tag{4.28}$$

where the superscript t denotes the transpose of a matrix and

$$\boldsymbol{U}_i = \sum_{j=1}^{\infty} \frac{\boldsymbol{A}_{i+1,j}}{2j+1}, \qquad i = 0, 1, \cdots. \tag{4.29}$$

It can be seen that the number of terms in $\boldsymbol{U}_i$ required for a desired accuracy is the same as in $\boldsymbol{A}_i$ [see (4.22) and (4.23)]. Compared to the original matrix exponential method, it has been found that the proposed approach is more efficient, the series in (4.22) and (4.23) requiring a relatively smaller number of terms for convergence. The faster convergence is due to two factors. First, in contrast to (4.16), the terms in the series (4.21) will decay more quickly due to the faster increase in the values of the denominators. Secondly, the size of the matrices in (4.21) is only half of that of the matrices in (4.16). This results in less computational effort for calculating the line moments by the proposed recursive procedure.

4.2. NUMERICAL RESULTS

Three examples are given to demonstrate the performance of the method described in section 4.1. As a first example, the interconnect circuit from [20] as shown in Fig. 4.2 is considered, which consists of two cascaded lossy transmission lines with identical length d. Line 1 is characterized by the parameters $Rd = 25\Omega$, $Gd = 0.005$ S, $Ld = 0.1\,\mu$H, and $Cd = 40$ pF. Line 2 has the same parameters except $Rd = 3.125\Omega$. Fig. 4.3 displays the magnitude of the moments of the voltage V_{out} at a frequency expansion point at the origin as generated by the presented method and by the matrix exponential method in [20]. Identical results are obtained, but with less computational effort. For example, using the smallest machine precision as the truncation criterion, the matrix exponential method

(4.16) typically required twice as many terms for convergence as compared to the presented method (4.21) (28 versus 14 for moment number 15 in Fig. 4.3). Fig. 4.3 also shows that the moments generated by the eigenvalue moment method exhibit an increase in numerical truncation error for higher order moments.

In order to demonstrate the computational efficiency of the proposed modified matrix exponential method in generating moments of transmission lines, two lossy multiconductor transmission line cases are considered as a second example. The first case considered is a transmission line consisting of two-conductors with a length of 0.1m and characterized by the following line parameters:

$$\boldsymbol{L}=\begin{bmatrix}403.043 & 76.96\\ 76.96 & 403.043\end{bmatrix}\text{nH/m} \qquad \boldsymbol{C}=\begin{bmatrix}45.65 & -12.319\\ -12.319 & 45.65\end{bmatrix}\text{pF/m}$$

$$\boldsymbol{R}=\begin{bmatrix}10 & 0\\ 0 & 10\end{bmatrix}\Omega\text{/m} \qquad \boldsymbol{G}=0.$$

The second case is a four-conductor transmission line which has a length of 0.1m. The line parameters are given by

$$\boldsymbol{L}=\begin{bmatrix}494.6 & 63.3 & 7.8 & 0.0\\ 63.3 & 494.6 & 63.3 & 7.8\\ 7.8 & 63.3 & 494.6 & 63.3\\ 0.0 & 7.8 & 63.3 & 494.6\end{bmatrix}\text{nH/m} \quad \boldsymbol{C}=\begin{bmatrix}62.8 & -4.9 & -0.3 & 0.0\\ -4.9 & 62.8 & -4.9 & -0.3\\ -0.3 & -4.9 & 62.8 & -4.9\\ 0.0 & -0.3 & -4.9 & 62.8\end{bmatrix}\text{pF/m}$$

$$\boldsymbol{R}=\begin{bmatrix}50 & 10 & 1 & 0.0\\ 10 & 50 & 10 & 1\\ 1 & 10 & 50 & 10\\ 0.0 & 1 & 10 & 50\end{bmatrix}\Omega\text{/m} \quad \boldsymbol{G}=\begin{bmatrix}0.1 & -0.01 & -0.001 & 0.0\\ -0.01 & 0.1 & -0.01 & -0.001\\ -0.001 & -0.01 & 0.1 & -0.01\\ 0.0 & -0.001 & -0.01 & 0.1\end{bmatrix}\text{S/m.}$$

The proposed modified matrix exponential method was applied to generate line moments at a frequency expansion point, $f=0$, for each of transmission line cases. The number

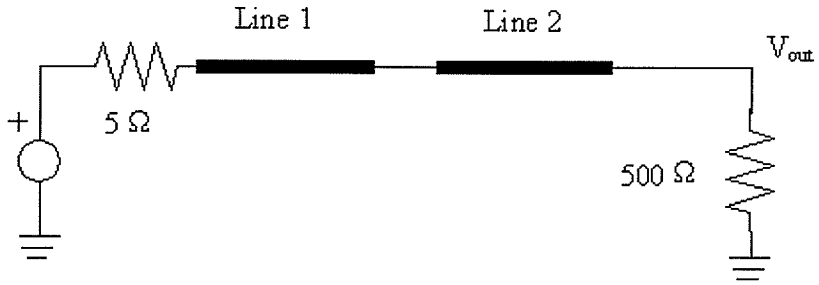

Fig. 4.2. Circuit containing two cascaded lossy transmission lines (from [20]).

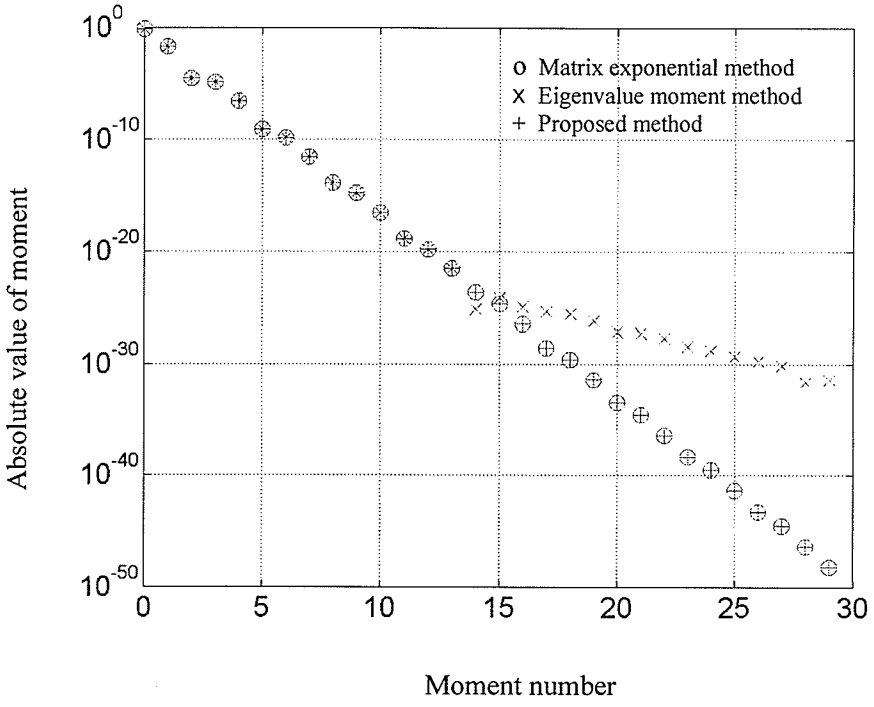

Fig. 4.3. Comparison of moments generated by the proposed technique, the matrix exponential method in [20], and the eigenvalue moment method.

of terms required for convergence with respect to moment number are displayed in Figs. 4.4 and 4.5. Also shown in the Figs. 4.4 and 4.5 are the corresponding results obtained by using the original matrix exponential method. Table II shows the number of terms required for convergence when computing the 12th transmission line moment at several frequency points for the proposed method and the original matrix exponential method. It can be seen that the proposed modified matrix exponential method typically requires half the number of terms for convergence as compared with the original matrix exponential method. Numerous other numerical experiments have also verified the above observation. This enables the proposed method to be more efficient in computing the moments of coupled transmission lines as compared with the original matrix exponential method.

As a third example, a printed circuit coplanar strip transmission line is considered, with the skin effect loss taken into account [58]. The circuit and its geometry are shown in Fig. 4.6 and Fig. 4.7, respectively, and the transmission line has a p.u.l. inductance $L = 0.805969\,\mu\text{H/m}$ and capacitance $C = 88.2488\,\text{pF/m}$. A frequency dependent conductor impedance Z_i, due to the skin effect, is accounted for as [58]

$$Z_i = \begin{cases} R_{dc}\left(1+\dfrac{jf}{f_o}\right), & f \le f_o \\ R_{dc}\sqrt{\dfrac{f}{f_o}}(1+j), & f \ge f_o \end{cases} \tag{4.30}$$

where $R_{dc} = 86.207\,\Omega/\text{m}$ is the p.u.l. dc resistance and $f_o = 393.06\,\text{MHz}$. The source voltage is a ramp function rising to 1V in 50 ps. The transient response at the load resistor is shown in Fig. 4.8, as computed using the multipoint moment matching technique described in chapter two, with the line divided into four identical sections. The moments for 9 frequency expansion points, with $f_{max} = 6.5$ GHz, were generated using both the

matrix exponential method [20], [54] and the presented method [52]. Fig. 4.8 shows that results are in good agreement. The number of terms required to achieve convergence using the presented method was again half of that required by the matrix exponential method in [20].

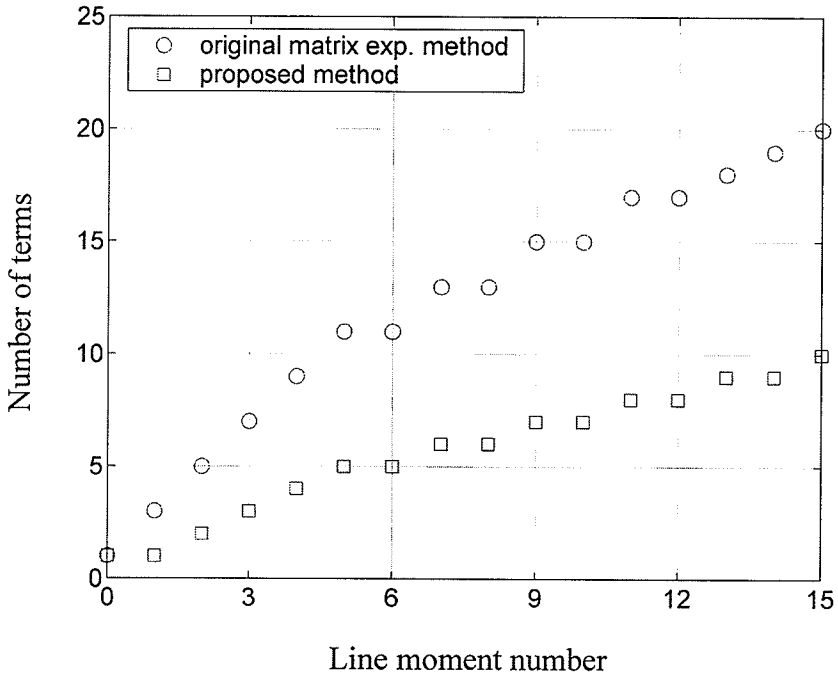

Fig. 4.4. Comparison of the number of terms required for convergence in generating the moments of a 2-conductor transmission line using the proposed method and the original matrix exponential method.

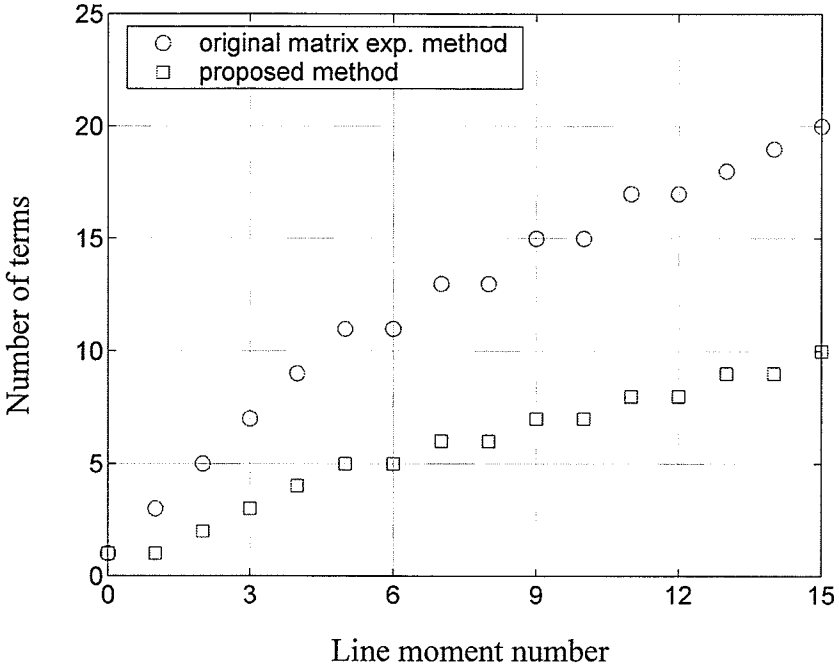

Fig. 4.5. Comparison of the number of terms required for convergence in generating the moments of a 4-conductor transmission line using the proposed method and the original matrix exponential method.

TABLE II

NUMBER OF TERMS REQUIRED FOR CONVERGENCE IN GENERATING THE 12th MOMENT OF TRANSMISSION LINES

Transmission line example	Transmission line with 2 coupled conductors			Transmission line with 4 coupled conductors		
Freq (GHz)	0	2.5	5	0	2.5	5
Proposed method	*8*	*27*	*38*	*12*	*31*	*44*
Original matrix exponential method	*17*	*55*	*77*	*25*	*63*	*89*

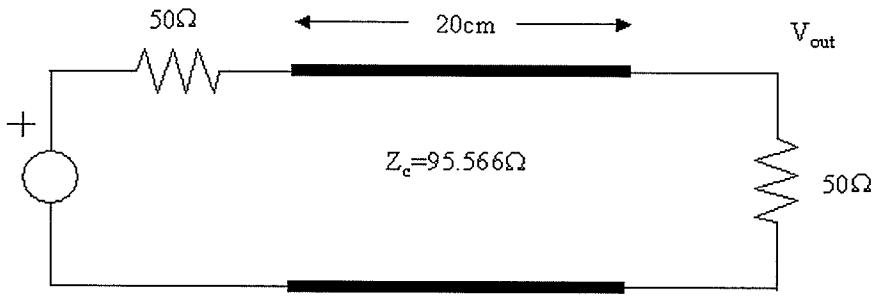

Fig. 4.6. Lossy printed circuit transmission line (from [58]).

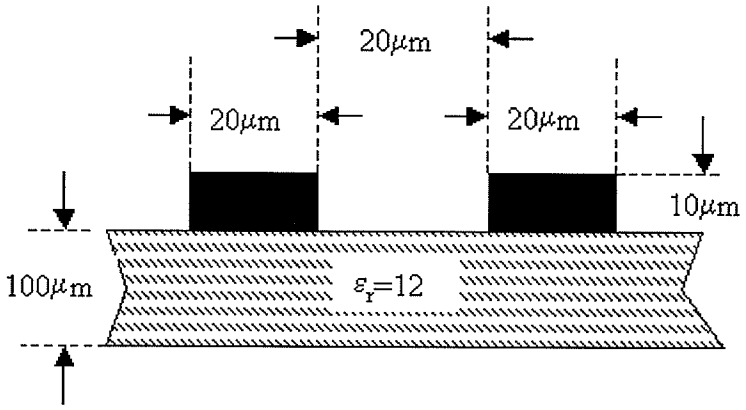

Fig. 4.7. Cross-sectional dimensions of the two-conductor circuit in Fig. 4.6.

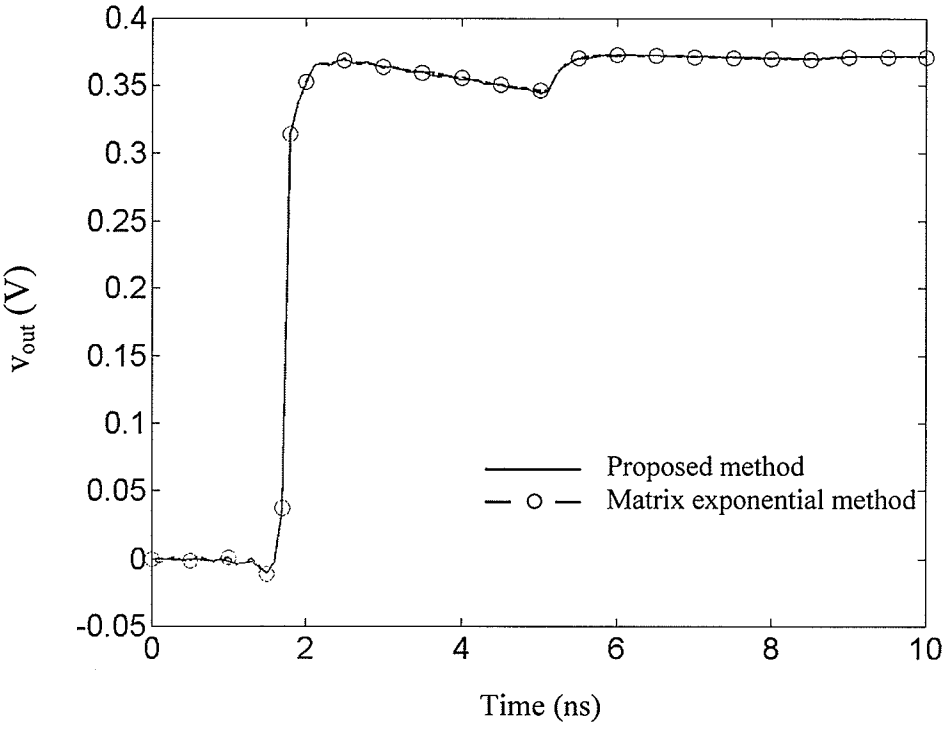

Fig. 4.8. Transient response at the load end of the circuit in Fig. 4.6.

4.3. SUMMARY

In this chapter, a modified matrix exponential method has been proposed for efficiently generating the moments of interconnects modeled as lossy coupled transmission lines with frequency dependent parameters. The proposed method can generate transmission line moments that are identical to the original matrix exponential method, but with less computational effort. Under the same truncation criterion, the original matrix exponential method typically requires twice as many terms for convergence when compared with the proposed method. A recursive procedure for

calculating the moments for multiconductor transmission lines with frequency-dependent parameters has been derived. Numerical experimentation showed that the modified matrix exponential method can be used for accurate and efficient generation of moments of frequency-dependent multiconductor transmission lines and can be readily incorporated in existing moment matching techniques for an efficient interconnect analysis.

Chapter 5. Frequency Dependent Transmission Lines with Sampled Data

In this chapter, the techniques presented in chapter three and chapter four are extended to handle multiconductor transmission lines with frequency dependent parameters characterized by sampled data. Unlike the assumption that transmission line parameters are constants with respect to frequency, these parameters are functions of frequency, such as that due to inhomogeneous dielectric and ohmic loss-induced dispersion. The frequency dependence typically becomes more noticeable as the operating frequency increases. Therefore, it is necessary to take into account its effects for accurate and reliable high-speed interconnect simulations.

Some approaches have been presented in order to incorporate frequency dependent transmission line parameters, which are usually obtained in the form of sampled or measured data, into model order reduction algorithms. In [59], the least squares method was used to curve-fit sampled transmission line parameters to piecewise polynomials as functions of frequency. The curve fitting technique was then integrated with the CFH algorithm to obtain transfer functions of interconnect networks. The curve fitting of line parameters using polynomial representations has a disadvantage in that multiple polynomials are often required in order to accurately model lines parameters that show strong frequency dependence over a wide spectrum. Also, in implementation of moment matching techniques based on multiple point expansions, it is necessary to take care of

any cross over between expansion points and polynomial break points. The authors of [54], [60] used a weighted least squares method to approximate measured data as rational functions of frequency. To avoid ill-conditioned problem arising from the approximations of transmission line parameters over a wide frequency range, local approximations about expansion points were performed and the derivatives extracted from the local approximations were used to calculate moments of transmission lines. The main drawback of this method is that it requires knowledge of the frequency expansion points so that the line parameters can be approximated over partitioned frequency ranges, which may prevent the method from being used in practical applications as it is difficult to determine *a-priori* information on the expansion points necessary for obtaining accurate system responses. In [61] and [62], the vector fitting algorithm [63], [64] was applied to approximate frequency dependent p.u.l. transmission line impedance and admittance matrices. The equivalent lumped circuit element representations of multiconductor transmission line are then obtained by using a segmentation approach. The reduced-order model of the transmission line can then be generated using a proper model order reduction algorithm. To ensure accuracy of simulation over a wideband, however, the segmentation method requires a large number of equivalent circuit elements, which leads to a large circuit matrix. In [43], the frequency dependent line parameters are first approximated using rational functions of frequency. The rational functions are then represented with a number of circuit elements with which time-domain macromodels of the transmission line can be realized. However, to accurately account for line delay, this method requires high-order Padé approximations or a large number of line segments [49]. Techniques to incorporate sampled/measured network parameters, such as through

admittance and scattering parameters, into model order reduction algorithms have also presented in the literature [38]-[40], [65]-[69].

The applications of multipoint Padé approximations to transient simulation of frequency dependent power transmission lines are also highlighted in this chapter. Transmission line structures are commonly found in electrical power delivery systems. Efficient simulation of transients on power transmission line networks is important for characterization of power system performance. Conventionally, transients on power transmission lines can be computed using time domain techniques such as PSCAD/EMTDC simulation program [70], [71], but the associated computation effort is generally high. Furthermore, even though the multipoint Padé approximation method has been successfully implemented in solving interconnect circuit problems, its applications to transient simulation of power transmission lines is not always straightforward task. Due to the conductor skin effect and the ground return frequency dependency, power transmission lines parameters show strong frequency dependence over a wide spectrum which is different from that typically found in electronic circuit cases. As a result, the application of the multipoint Padé approximation method to solving power transient problems may bring about solution instability. More specifically, the matrix that is used to yield the coefficients of Padé rational transfer function is prone to be ill-conditioned when a multipoint Padé approximation method is used to simulate frequency dependent power transmission lines. To deal with this issue, an improved multipoint Padé approximation method is proposed in this chapter for the analysis of transients on frequency dependent power transmission lines.

5.1. APPROXIMATION OF FREQUENCY-DEPENDENT LINE PARAMETERS

Frequency-dependent transmission line parameters can be obtained from various electromagnetic simulation software or directly from measurements at a set of discrete frequency points. Since the computation of transmission line moments requires information on the frequency derivatives of the line parameters at the expansion point(s), it is difficult to incorporate such tabulated line parameters (or measured data/sampled data) directly into existing moment matching algorithms. Pre-processing in order to approximate the line parameters by differentiable functions is needed.

In this section, techniques that can be used for curve-fitting the measured frequency-dependent transmission line parameters over a desired frequency range will be described. They include the classic polynomial approximation method and recently developed vector fitting technique [63], [64]. Examples of their application in approximating frequency dependent line parameters will be provided with individual simulation cases presented in this chapter.

Polynomial approximation

Let $r(\omega)$ be one of the parameters to be approximated in the form

$$r(\omega) = r_0 + r_1\omega^2 + r_2\omega^4 + \cdots \tag{5.1}$$

In (5.1), we use even functions of $\omega = 2\pi f$ to ensure the result is real when converted to the s domain, i.e.,

$$r(s) = r_0 + r_1\left(\frac{1}{j}\right)^2 (j\omega)^2 + r_2\left(\frac{1}{j}\right)^4 (j\omega)^4 + \cdots = r_0' + r_1's^2 + r_2's^4 + \cdots \tag{5.2}$$

The coefficients of the polynomial in (5.1) are obtained by using a least squares approximation method to fit the values of the polynomial to the given line parameter data at a set of discrete frequency points, $\bar{r}(\omega_i)$, $i = 1, 2, \cdots$,

$$r_0 + r_1\omega_i^2 + r_2\omega_i^4 + \cdots = \bar{r}(\omega_i) \qquad i = 1, 2, \cdots \tag{5.3}$$

When using polynomial representations to approximate frequency dependent line parameters, a single polynomial is often not be suitable to adequately curve-fit the line parameters over a wide frequency range. In these cases, it is necessary to use multiple polynomials to describe the complex dependence of the line parameters on frequency.

Once the coefficients of the polynomials have been found, the derivatives of frequency-dependent line parameters can be readily obtained. The modified matrix exponential method described in chapter four can then be used to generate moments efficiently.

Vector Fitting Technique

For the case that the measured or calculated transmission line parameters exhibit a strong frequency dependency over the frequency band of interest, a more advanced curve fitting technique, such as Vector Fitting algorithm [63] [64], is often used. Vector fitting is a methodology for accurate fitting of frequency domain data with rational function approximations. For brief illustration of the method, consider a measured line parameter $r(s)$ obtained at a set of discrete frequency points. Vector fitting approximates $r(s)$ using a rational function representation in the form of

$$r(s) \approx \sum_{n=1}^{N} \frac{k_n}{s - p_n} + d + se \tag{5.4}$$

where residues k_n and poles p_n can be either real or in complex conjugate pairs, while d and e are real constant terms. Vector fitting estimates the unknown coefficients in (5.4) in two stages. First, it assumes a set of starting poles distributed over the frequency range of interest and then yields an improved set of poles via a scaling procedure. Next, the new set of poles is used to replace the starting poles and the residues k_n, and the constant terms d and e are obtained by solving an overdetermined linear problem. Compared with curve fitting using polynomial approximations, the vector fitting technique is more robust in accurately approximating sampled frequency dependent line parameter data. The trade-off is higher computational cost. Details on implementation of vector fitting algorithm can be found in reference [63], [64].

5.2. INTERCONNECT CIRCUITS WITH FREQUENCY DEPENDENT TRANSMISSION LINES

Fig. 5.1 shows an interconnect circuit containing two lossy frequency-dependent coupled transmission lines [54]. Both lines have a length of 5 cm and are characterized by the same line parameters. The p.u.l. capacitance and conductance parameters are:

$$\mathbf{C} = \begin{bmatrix} 1.082 & -0.197 & -0.006 \\ -0.197 & 1.124 & -0.197 \\ -0.006 & -0.197 & 1.082 \end{bmatrix} \text{pF/cm}, \quad \mathbf{G} = \mathbf{0} \ .$$

The frequency-dependent p.u.l. resistance and inductance parameters of the transmission lines are given at a set of discrete frequency points as shown in Table III and Table IV, respectively. To compute the transmission line moments, each element of the p.u.l. frequency-dependent resistance $\boldsymbol{R}$ and inductance $\boldsymbol{L}$ matrices is first represented as a polynomial in s such that

$$R(s) = R_0 + R_1 s^2 + R_2 s^4 + \cdots. \tag{5.5}$$

$$L(s) = L_0 + L_1 s^2 + L_2 s^4 + \cdots. \tag{5.6}$$

The coefficients of the polynomials are then found by fitting the values of the polynomials to the given line parameter data at the set of discrete frequency points using a least squares approximation method. The approximated and the original R_{22} and L_{22} are shown in Figs. 5.2 and 5.3, respectively. The impulse frequency response at the output node of the network was computed by using the multipoint moment matching algorithm proposed in chapter three [72]-[75]. With the maximum frequency of interest chosen at 5 GHz and using 10 moments in each expansion, it was found that only 5 frequency expansion points were required, with their location at 0, 1.25, 2.5, 3.75 and 5 GHz. Both the matrix exponential method [20], [54] and the modified matrix exponential method described in chapter four [52] were used to generate the transmission line moments at the expansion points and the frequency response results are in excellent agreement as shown in Fig. 5.4. Using the smallest machine precision as the truncation criterion, it was found, as previously observed in chapter four, that the modified matrix exponential method typically required half the number of terms for convergence when compared with the original matrix exponential method. The transient response at the output node, corresponding to a 1V pulse with 0.1 ns rise/fall time and 1ns duration, was simulated as shown in Fig. 5.5. The results obtained by using the proposed method in both frequency domain and time-domain are in good agreement with those in literature.

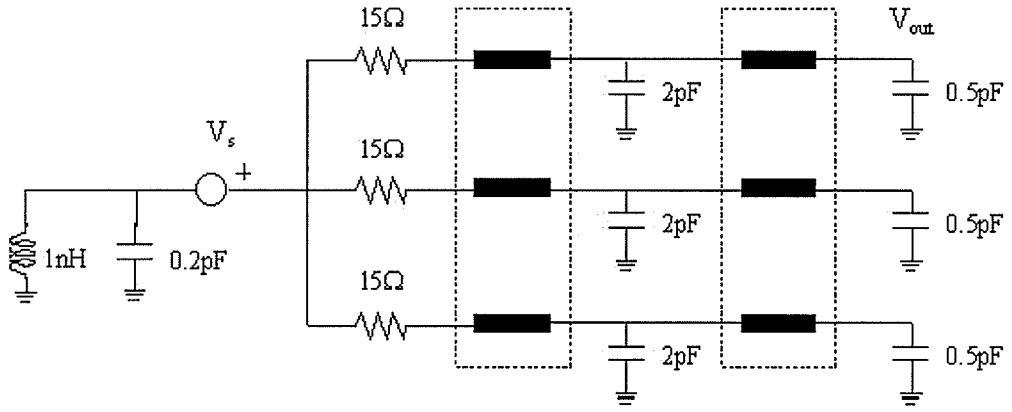

Fig. 5.1. Interconnect network containing lossy frequency-dependent coupled transmission lines [54].

5.3. SIMULATION OF TRANSIENTS ON POWER TRANSMISSION LINE USING IMPROVED MULTIPOINT PADÉ APPROXIMATION

In the case of power transmission line simulation, it is observed that the matrix equation obtained from multipoint moment matching using (3.1) is prone to be ill-conditioned due to the very wideband frequency dependence of power transmission line parameters. The parameters can vary by several orders of magnitude and differ from the frequency dependence of the line parameters typically found in electronic circuit cases. Further investigations reveal that the strong frequency dependence of the line parameters can lead to a significant difference in the values of moments generated in the low frequency range from those generated in the high frequency range. This in turn results in the matrix equation being ill-conditioned if the whole frequency bandwidth of

TABLE III

RESISTANCE AS FUNCTION OF FREQUENCY

Freq (GHz)	R_{11} (Ω/cm)	R_{22} (Ω/cm)
0.0001	3.4480	3.4480
0.0010	3.4480	3.4480
0.0100	3.4480	3.4480
0.1000	3.4480	3.4480
0.2000	3.4480	3.4480
0.4000	3.6140	3.6140
0.8000	4.0110	4.0110
1.0000	4.2440	4.2440
1.5000	4.8300	4.8300
2.0000	5.4210	5.4210
2.5000	5.9430	5.9430
3.0000	6.4400	6.5350
3.5000	6.8890	6.9920
4.0000	7.3030	7.4130
4.5000	7.6850	7.8020
5.0000	8.0510	8.1740
5.5000	8.3820	8.5110
6.0000	8.6800	8.8150
6.5000	8.9810	9.1200
7.0000	9.2550	9.4020

TABLE IV

INDUCTANCE AS FUNCTION OF FREQUENCY

Freq (GHz)	L_{11} (nH/cm)	L_{12} (nH/cm)	L_{13} (nH/cm)	L_{22} (nH/cm)
0.0001	4.9760	0.7650	0.1520	4.9760
0.0010	4.9760	0.7650	0.1520	4.9760
0.0100	4.9760	0.7650	0.1520	4.9760
0.1000	4.8470	0.7630	0.1520	4.8460
0.2000	4.8460	0.7630	0.1530	4.8440
0.4000	4.7630	0.7630	0.1560	4.7580
0.8000	4.7400	0.7640	0.1620	4.7300
1.0000	4.7280	0.7640	0.1620	4.7200
1.5000	4.6420	0.7660	0.1620	4.6300
2.0000	4.6130	0.7670	0.1620	4.5990
2.5000	4.5910	0.7680	0.1620	4.5770
3.0000	4.5540	0.7700	0.1620	4.5360
3.5000	4.5210	0.7700	0.1620	4.5030
4.0000	4.4950	0.7700	0.1620	4.4760
4.5000	4.4730	0.7700	0.1620	4.4550
5.0000	4.4550	0.7700	0.1620	4.4370
5.5000	4.4400	0.7700	0.1620	4.4210
6.0000	4.4270	0.7700	0.1620	4.4080
6.5000	4.4150	0.7700	0.1620	4.3960
7.0000	4.4050	0.7700	0.1620	4.3850

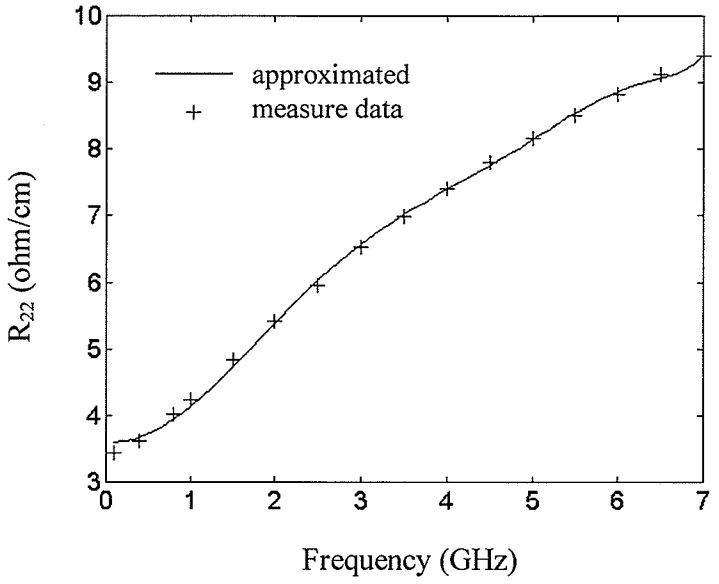

Fig. 5.2. R_{22} values for the frequency-dependent transmission lines in the example network in Fig. 5.1.

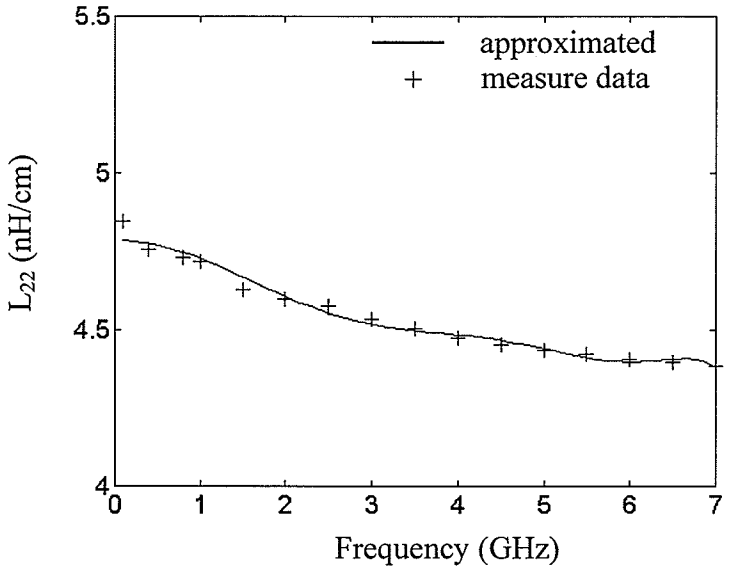

Fig. 5.3. L_{22} values for the frequency-dependent transmission lines in the example network in Fig. 5.1.

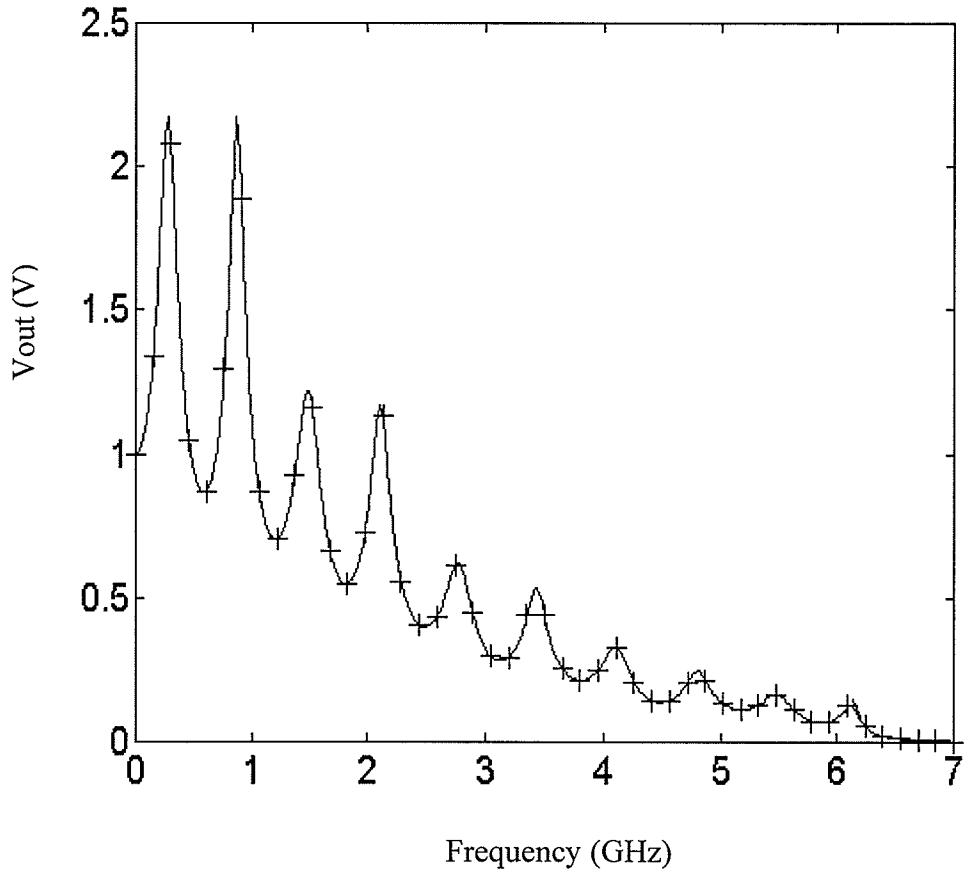

Fig. 5.4. Frequency response at the output node of the network in Fig. 5.1.

—— modified matrix exponential method

– + – matrix exponential method [20], [54]

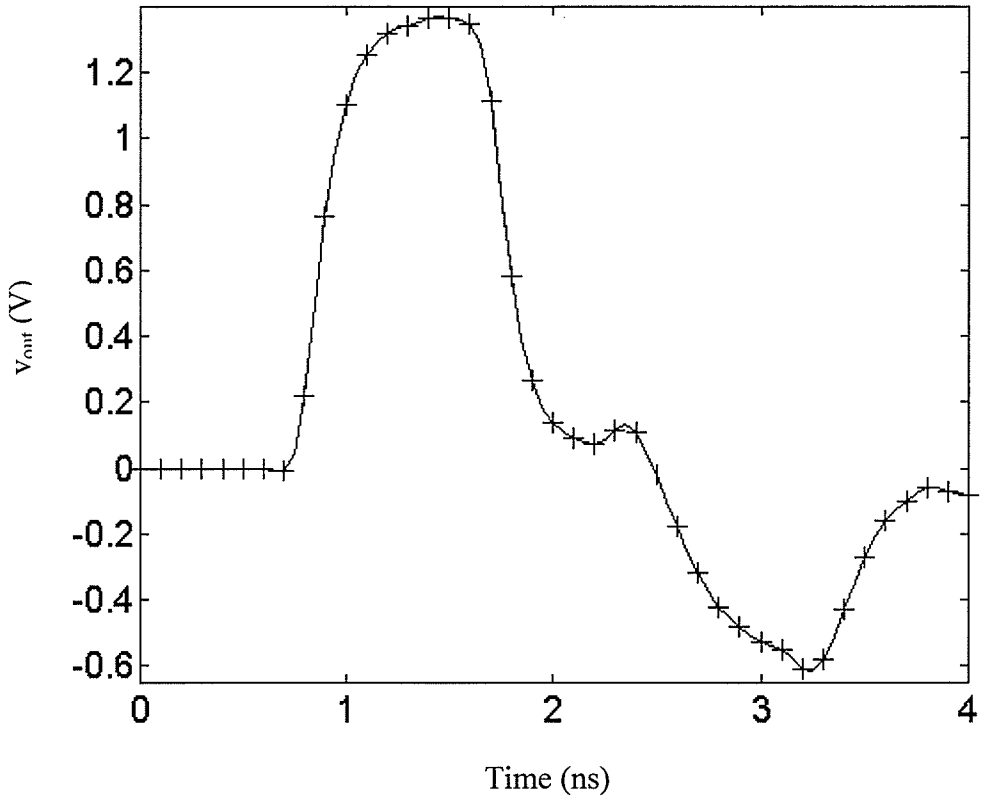

Fig. 5.5. Transient response at the output node of the network in Fig. 5.1.

—— modified matrix exponential method

–+– matrix exponential method [20], [54]

interest is considered. Consequently, direct applications of the multipoint Padé approximation method to power transmission line analysis can produce incorrect waveforms or even fail to obtain any solution.

To address this issue, an improved multipoint Padé approximation method that is based on a frequency band division strategy is proposed [76]. The principle behind the proposed method is to divide the original frequency band of interest into multiple sections and apply the multipoint Padé approximation over each subsection to ensure the solution stability, as illustrated in Fig. 5.6.

The key points of the improved multipoint Padé approximation method are summarized as follows:

Step 1: Apply the multipoint Padé approximation algorithm described in chapter three to a given frequency range of interest.

Step 2: Evaluate the condition number of the matrix equation resulting from the application of (3.1).

Step 3: If the matrix condition number is worse than a pre-defined criterion, divide the frequency range into subsections such that each matrix equation obtained is well-behaved over each frequency subsection.

Step 4: Collect poles from each transfer function that is accurate over a corresponding subsection (if any).

Step 5: Compute residues corresponding to stable poles using a least squares approximation method.

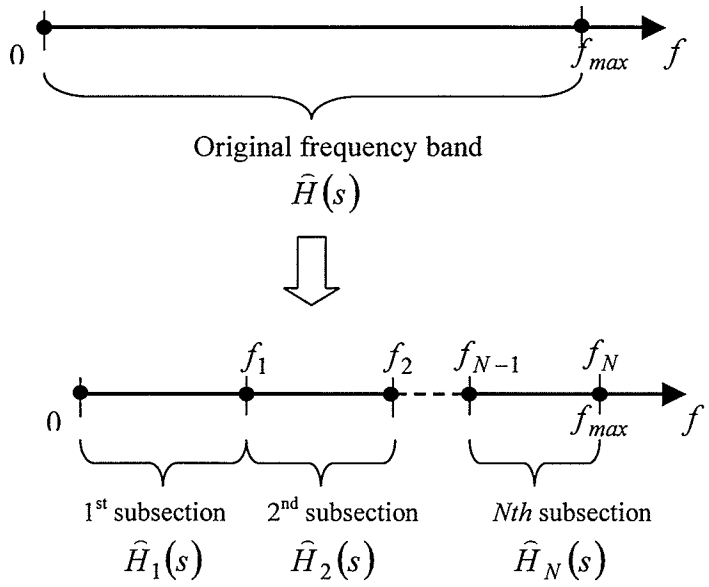

Fig. 5.6. Division of frequency band into frequency subsections.

Assuming the above algorithm results in q' poles $\hat{p}_j$ and residues $\hat{k}_j$, the approximate frequency domain and impulse transient response of power transmission lines can then be written, respectively, as

$$\hat{H}(s) = \sum_{j=1}^{q'} \frac{\hat{k}_j}{s - \hat{p}_j} \tag{5.6}$$

$$\hat{h}(t) = \sum_{j=1}^{q'} \hat{k}_j e^{\hat{p}_j t} \tag{5.7}$$

Assuming the frequency dependent line parameters are well approximated using adequate curve-fitting techniques and utilizing the search algorithm presented in chapter three for the selection of expansion points over each frequency subsection, the improved multipoint Padé approximation technique is described by the flowchart shown in Fig. 5.7.

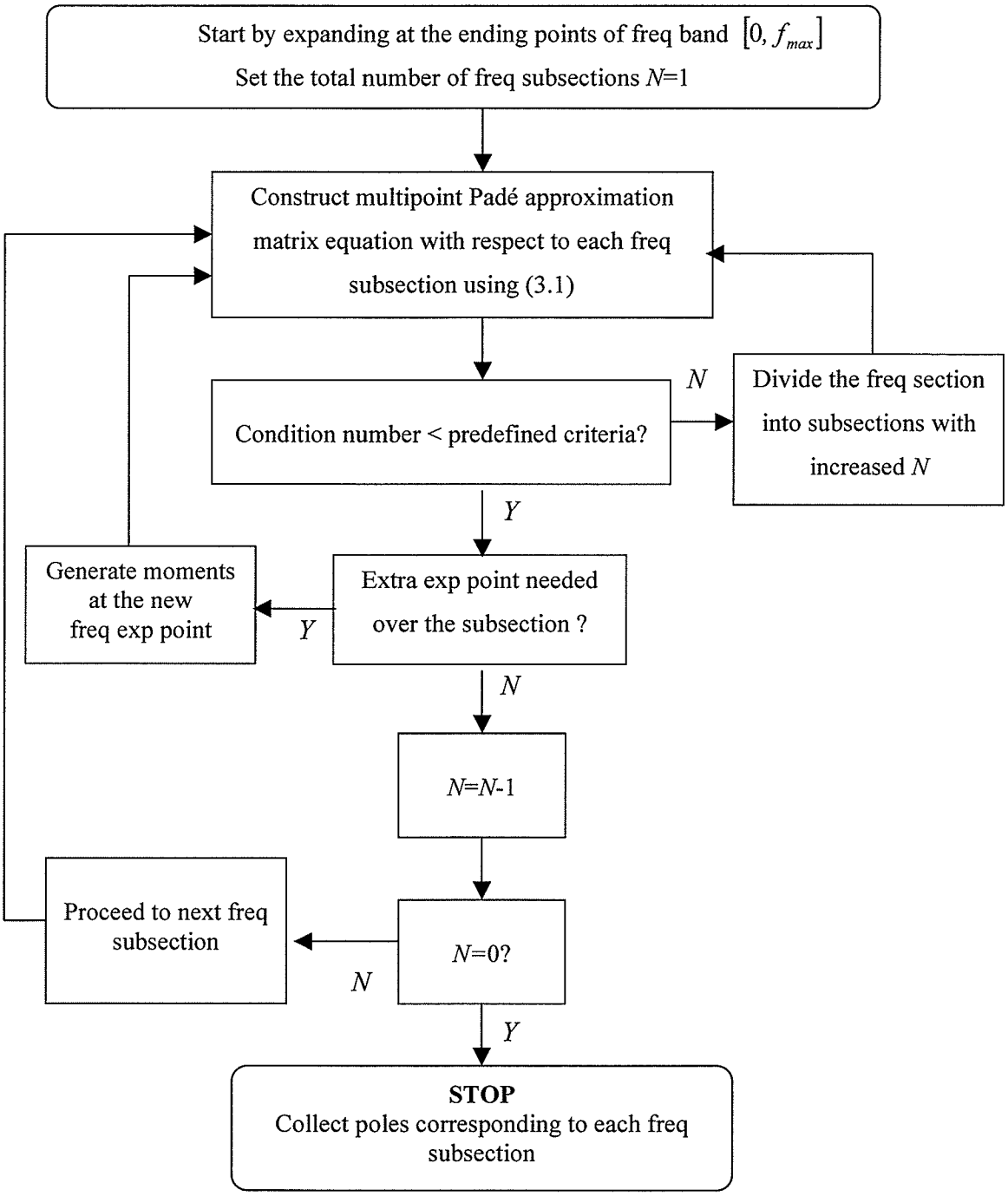

Fig. 5.7. Overview of the improved multipoint Padé approximation method.

5.4. NUMERICAL RESULTS

5.4.1. Single-phase Power Transmission Line

A power delivery system with a single-phase transmission line as shown is Fig. 5.8 is used to demonstrate the performance of the improved multipoint Padé approximation method. The power transmission line has a length of 10 km and a solid conductor of radius 2 cm. The height of the line over ground is 10 m. The conductivity for line conductor and ground is 2×10^{6} S/m and 10^{-2} S/m, respectively. Fig. 5.9 shows the circuit structure of the power system. The frequency dependent p.u.l. line parameters, shown in Table V are computed at a set of discrete frequency points using Carson's formulation [77]. The frequency dependent p.u.l. resistance and inductance parameters are then approximated using the vector fitting algorithm [63], [64] and are compared with corresponding original data as plotted in Fig. 5.10 and 5.19, respectively. It can be seen from the figures that the p.u.l. power line parameters display a strong frequency dependence from Hz to MHz due to the conductor skin effect and ground return loss. Since the network normally operates in the 100 Hz range but transients can exhibit MHz bandwidths, it is important to model the strong frequency dependency over a wide bandwidth. An attempt was made to simulate transients on the power transmission line using the original multipoint Padé approximation method described in chapter three. However, solution instability issues prevented the original multipoint Padé approximations from correctly capturing the large number of poles associated with the power line network. Fig. 5.12 shows the impulse frequency response at the output node of network obtained by using the improved multipoint Padé approximation method described in section 5.3. With the maximum frequency of interest chosen at 500 KHz, a

total of 6 frequency subsections is needed for obtaining the waveform, resulting in a total of 77 stable poles being generated. The exact frequency response obtained by solving MNA matrix equation of the network is also shown in Fig. 5.12 for comparison. The transient response at the output node, corresponding to a 1V pulse with 2 μs rise and fall times and 20 μs duration, was simulated and is shown in Fig. 5.13. The transient response obtained by using the exact frequency response and then applying the IFFT algorithm is also plotted in Fig. 5.13, which is in good agreement with that obtained by using the improved multipoint Padé approximation method.

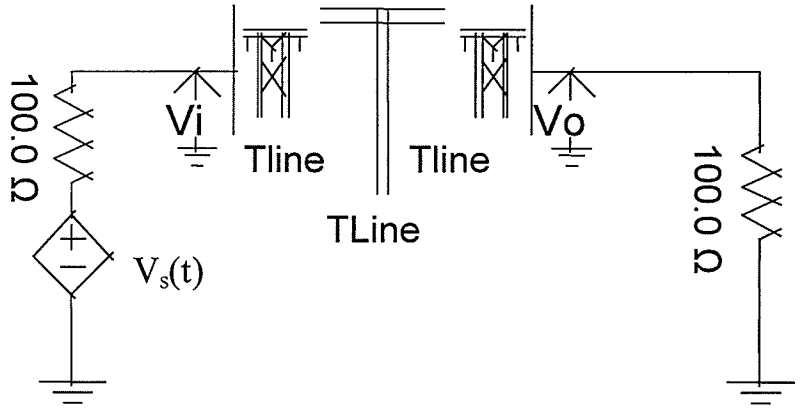

Fig. 5.8. Power delivery system containing a single-phase transmission line.

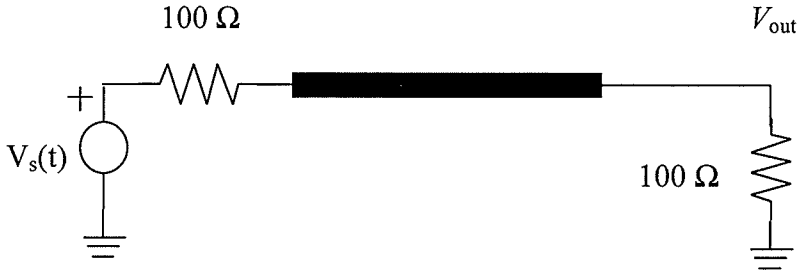

Fig. 5.9. Circuit structure of the power transmission line system in Fig. 5.8.

TABLE V

FREQUENCY DEPENDENT p.u.l. POWER LINE PARAMETERS

Frequency (KHz)	R (Ω/m)	L (μH/m)
0.000100	0.000398	2.8215
0.000251	0.000398	2.7294
0.000631	0.000399	2.6374
0.001000	0.000399	2.5915
0.002512	0.000400	2.4998
0.006309	0.000404	2.4081
0.010000	0.000408	2.3625
0.025119	0.000422	2.2713
0.063096	0.000459	2.1807
0.100000	0.000494	2.1357
0.251190	0.000639	2.0463
0.630960	0.001005	1.9573
1.000000	0.001366	1.9121
2.511900	0.002810	1.8177
6.309600	0.006005	1.7268
10.00000	0.008794	1.6853
25.11900	0.018685	1.6106
63.09600	0.038588	1.5477
100.0000	0.054619	1.5209
251..9000	0.105580	1.4767
630.9600	0.194340	1.4444
1000.000	0.259270	1.4321

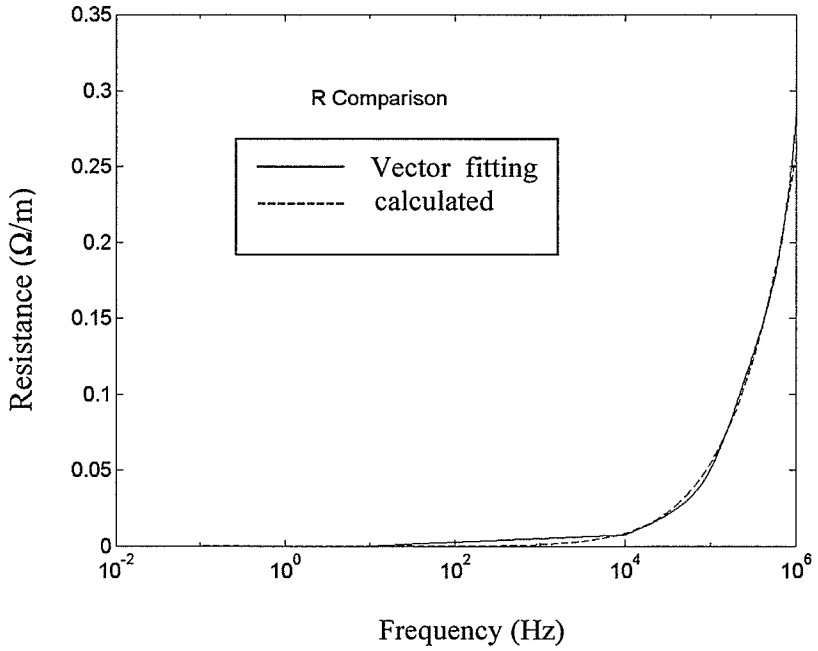

Fig. 5.10. Resistance of frequency dependent power transmission line.

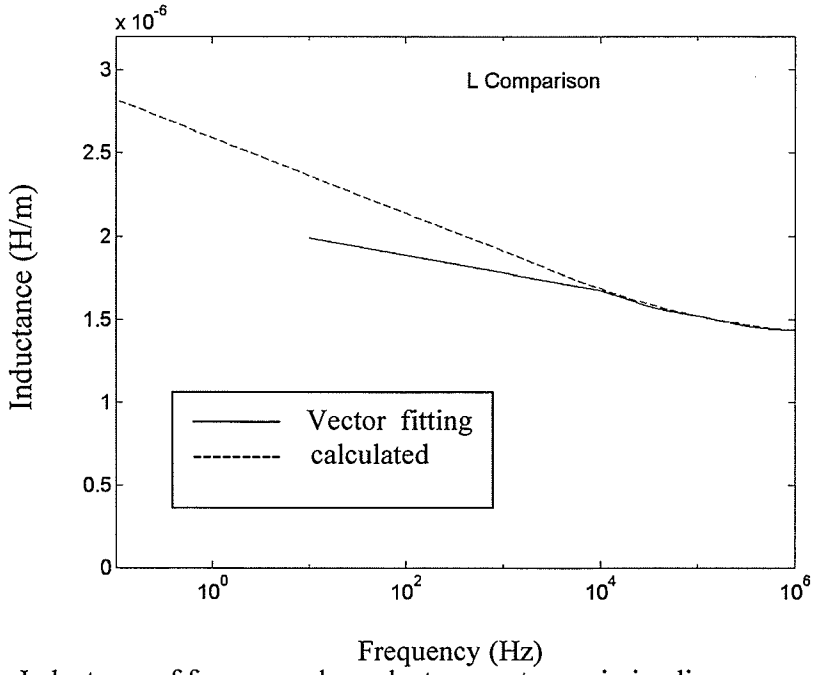

Fig. 5.11. Inductance of frequency dependent power transmission line.

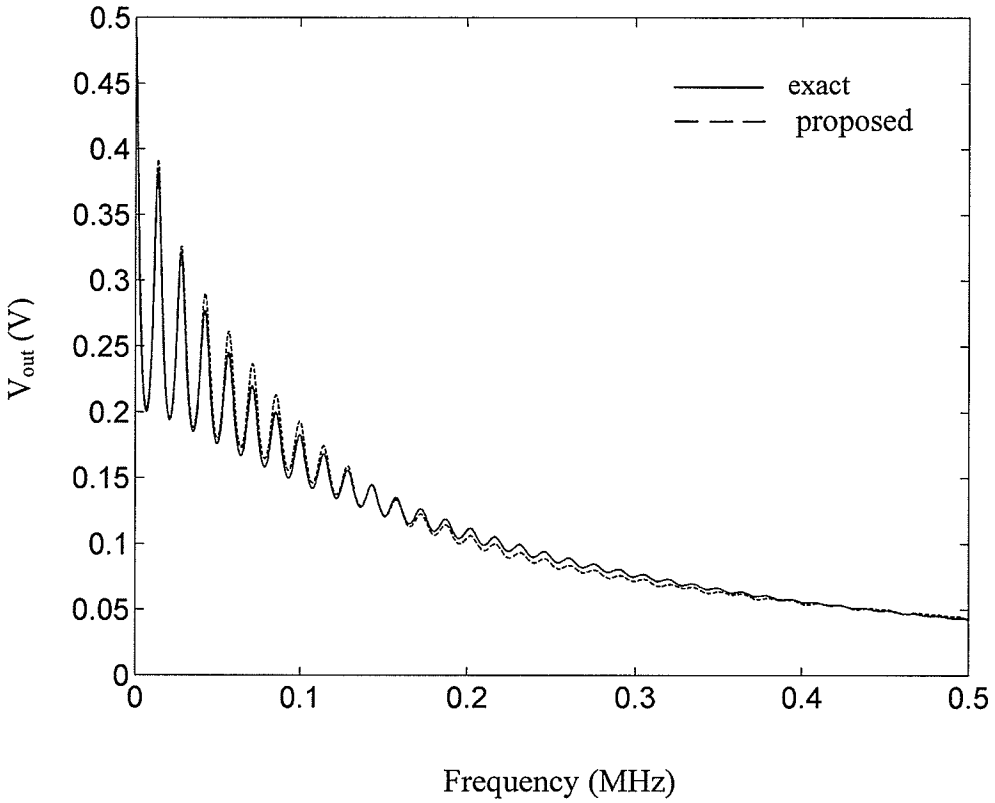

Fig. 5.12. Impulse frequency response at output node of the power transmission line shown in Fig. 5.8.

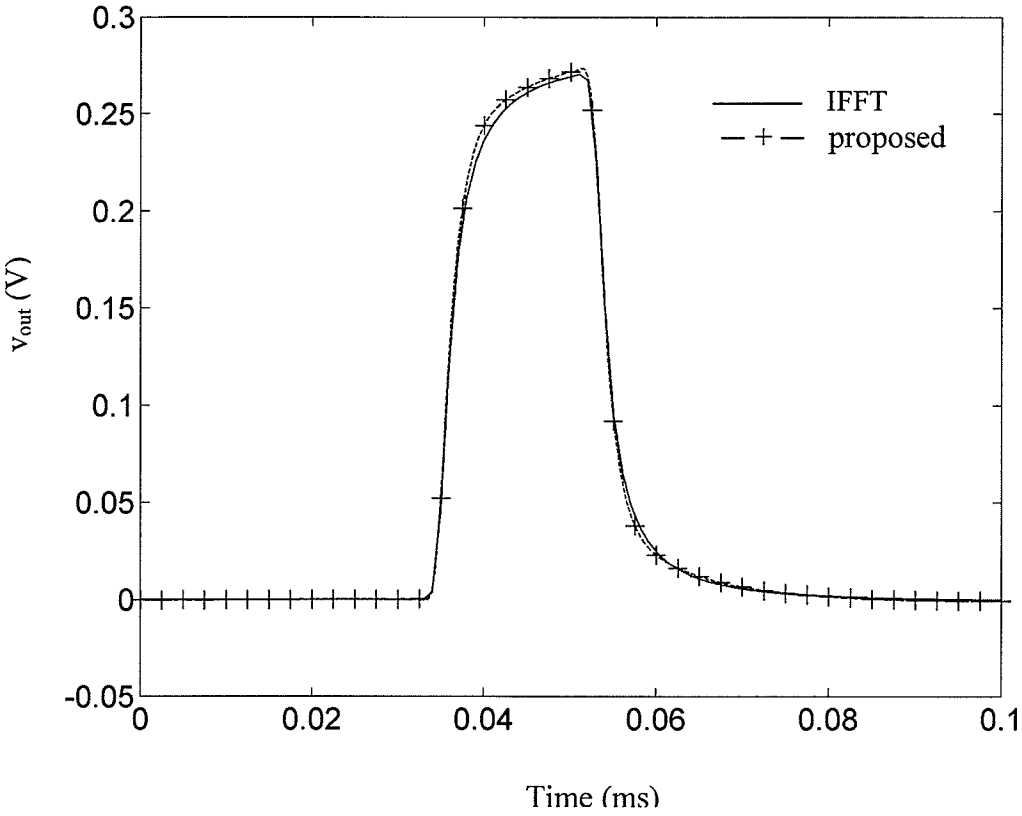

Fig.5.13. Transient response at output node of the power transmission network shown in Fig. 5.8.

5.4.2. Transient on 3-phase Power Transmission Lines

The proposed method presented in section 5.3 has been used to simulate transients on a 3-phase power transmission line system as shown in Fig. 5.14. The transmission line example is taken from [78] and its tower and conductor geometry is shown in Fig. 5.15. The length of the transmission line is 222.07 km. Each phase is connected to an inductor of 39.8 mH and a resistor of 10 MΩ. The excitation source for phase *A*, *B*, and *C* is $528.81\angle 0^\circ$ kV, $528.81\angle 240^\circ$ kV, and $528.81\angle 120^\circ$ kV, respectively, at a steady state frequency of 60 Hz. The frequency dependent p.u.l. line parameters were computed using Carson's formulation [77] at a discrete of frequency points and are shown in Tables VI and VII. The sampled line parameter data were then approximated by implementing the vector fitting algorithm [63], [64]. A comparison of the approximated line parameters with the corresponding original data is given in Fig. 5.16 and 5.17, respectively. It was noted that the power line network couldn't be analyzed using the original multipoint Padé approximate method. The improved multipoint Padé approximation algorithm was implemented to simulate transients on the 3-phase power line system. Fig. 5.18 and 5.20 show the transient responses at the load terminals of phase *A* and *B*, respectively. The 3-phase power transmission line system was also simulated using the commercial PSCAD/EMTDC simulator [70], [71] and the transient waveforms for phase *A* and *B* are provided for comparison in Fig. 5.19 and 5.21, respectively.

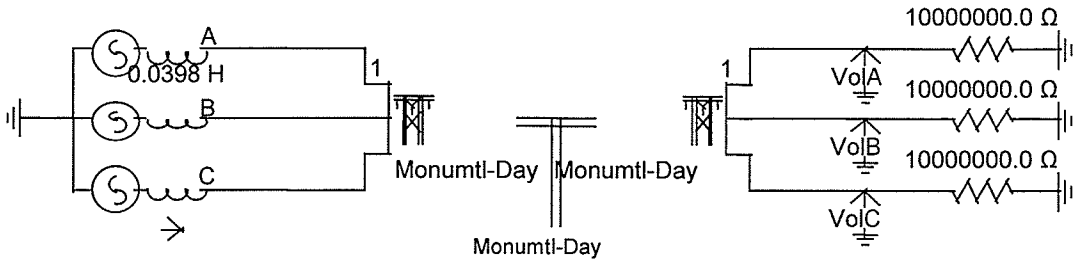

Fig. 5.14. Power delivery system containing a 3-phase transmission line [78].

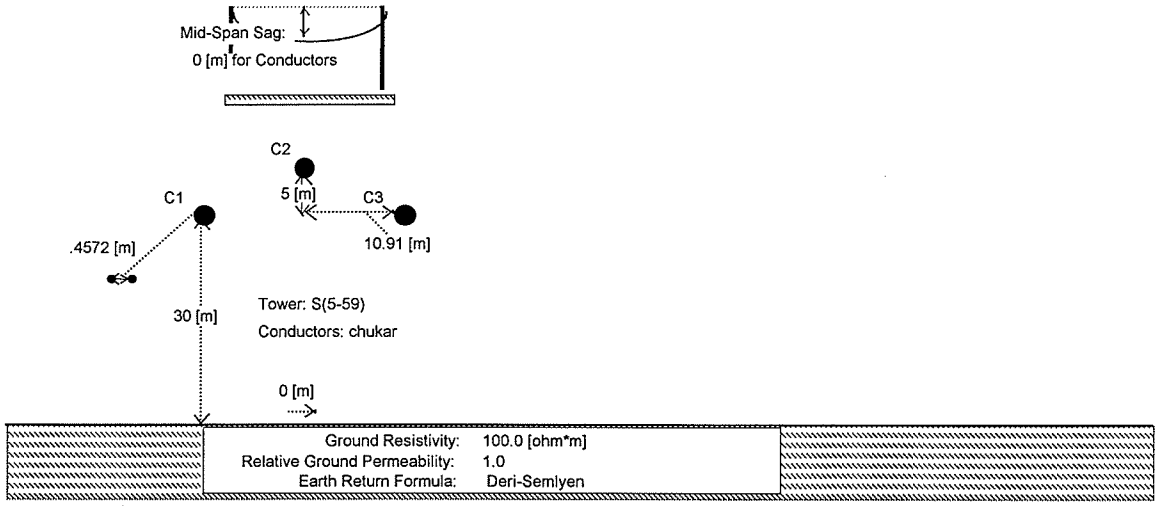

Fig. 5.15. Tower and conductor geometry for the 3-phase transmission line shown in Fig. 5.14 as generated using the PSCAD simulator [70], [71].

TABLEL VI

FREQUENCY DEPENDENT p.u.l. RESISTANCE PARAMETES OF THE 3-PHASE POWER TRANSMISSION LINE (FIG. 5.15)

Frequency (KHz)	R_{11} (Ω/m)	R_{12} (Ω/m)	R_{13} (Ω/m)	R_{22} (Ω/m)
0.000100	3.2125e-05	9.8420e-08	9.8427e-08	3.2125e-05
0.000237	3,2260e-05	2.3304e-07	2.3307e-07	3.2260e-05
0.000562	3.2579e-05	5.3137e-07	5.5145e-07	3.2578e-05
0.001000	33007e-05	9.7835e-07	9.7857e-07	3.3005e-05
0.002371	3.4345e-05	2.3094e-06	2.3101e-06	3.4339e-05
0.005623	3.7510e-05	5.4380e-06	5.4407e-06	3.7489e-05
0.010000	4.1765e-05	9.6070e-06	9.6131e-06	4.1718e-05
0.023714	5.5166e-05	2.2468e-05	2.2489e-05	5.5000e-05
0.056234	8.7575e-05	5.2187e-05	5.2261e-05	8.7000e-05
0.100000	1.3210e-04	9.1051e-05	9.1218e-05	1.3080e-04
0.237140	2.6773e-04	2.0758e-04	2.0814e-04	2.6341e-04
0.562340	5.5756e-04	4.6508e-04	4.6687e-04	5.4369e-04
1.000000	9.1345e-04	7.8626e-04	7.9006e-04	8.8393e-04
2.371400	1.9044e-03	1.6867e-03	1.6979e-03	1.8167e-03
5.623400	3.8900e-03	3.4900e-03	3.5212e-03	3.6457e-03
10.00000	6.1532e-03	5.5343e-03	5.5936e-03	5.6895e-03
23.71400	1.1839e-02	1.0623e-02	1.0767e-02	1.0711e-02
56.23400	2.1785e-02	1.9419e-02	1.9736e-02	1.9286e-02
100.0000	3.1905e-02	2.8289e-02	2.8800e-02	2.7872e-02
237.1400	5.4667e-02	4.8107e-02	4.9080e-02	4.6961e-02
562.3400	9.0633e-02	7.9291e-02	8.1033e-02	7.6892e-02
1000.000	1.2525e-01	1.0923e-01	1.1170e-01	1.0563e-01

TABLE VII

FREQUENCY DEPENDENT p.u.l. INDUCTANCE PARAMETERS OF THE 3-PHASE POWER TRANSMISSION LINE (FIG. 5.15)

Frequency (KHz)	L_{11} (H/m)	L_{12} (H/m)	L_{13} (H/m)	L_{22} (H/m)
0.000100	2.8181e-06	1.4923e-06	1.3727e-06	2.8183e-06
0.000237	2.7321e-06	1.4062e-06	1.2866e-06	2.7322e-06
0.000562	2.6460e-06	1.3202e-06	1.2006e-06	2.6462e-06
0.001000	2.5888e-06	1.2630e-06	1.1434e-06	2.5891e-06
0.002371	2.5031e-06	1.1774e-06	1.0578e-06	2.5035e-06
0.005623	2.4178e-06	1.0922e-06	9.7258e-07	2.4184e-06
0.010000	2.3611e-06	1.0357e-06	9.1607e-07	2.3619e-06
0.023714	2.2765e-06	9.5173e-07	8.3200e-07	2.2777e-06
0.056234	2.1914e-06	8.6892e-07	7.4912e-07	2.1933e-06
0.100000	2.1328e-06	8.1468e-07	6.9479e-07	2.1353e-06
0.237140	2.0410e-06	7.3574e-07	6.1530e-07	2.0447e-06
0.562340	1.9530e-06	6.5938e-07	5.3911e-07	1.9585e-06
1.000000	1.8987e-06	6.1128e-07	4.9081e-07	1.9058e-06
2.371400	1.8242e-06	5.4411e-07	4.2326e-07	1.8342e-06
5.623400	1.7586e-06	4.8445e-07	3.6313e-07	1.7723e-06
10.00000	1.7203e-06	4.4963e-07	3.2795e-07	1.7368e-06
23.71400	1.6717e-06	4.0564e-07	2.8337e-07	1.6927e-06
56.23400	1.6337e-06	3.7168e-07	2.4885e-07	1.6592e-06
100.0000	1.6141e-06	3.5432e-07	2.3108e-07	1.6422e-06
237.1400	1.5919e-06	3.3475e-07	2.1117e-07	1.6233e-06
562.3400	1.5767e-06	3.2152e-07	1.9763e-07	1.6105e-06
1000.000	1.5694e-06	3.1526e-07	1.9121e-07	1.6045e-06

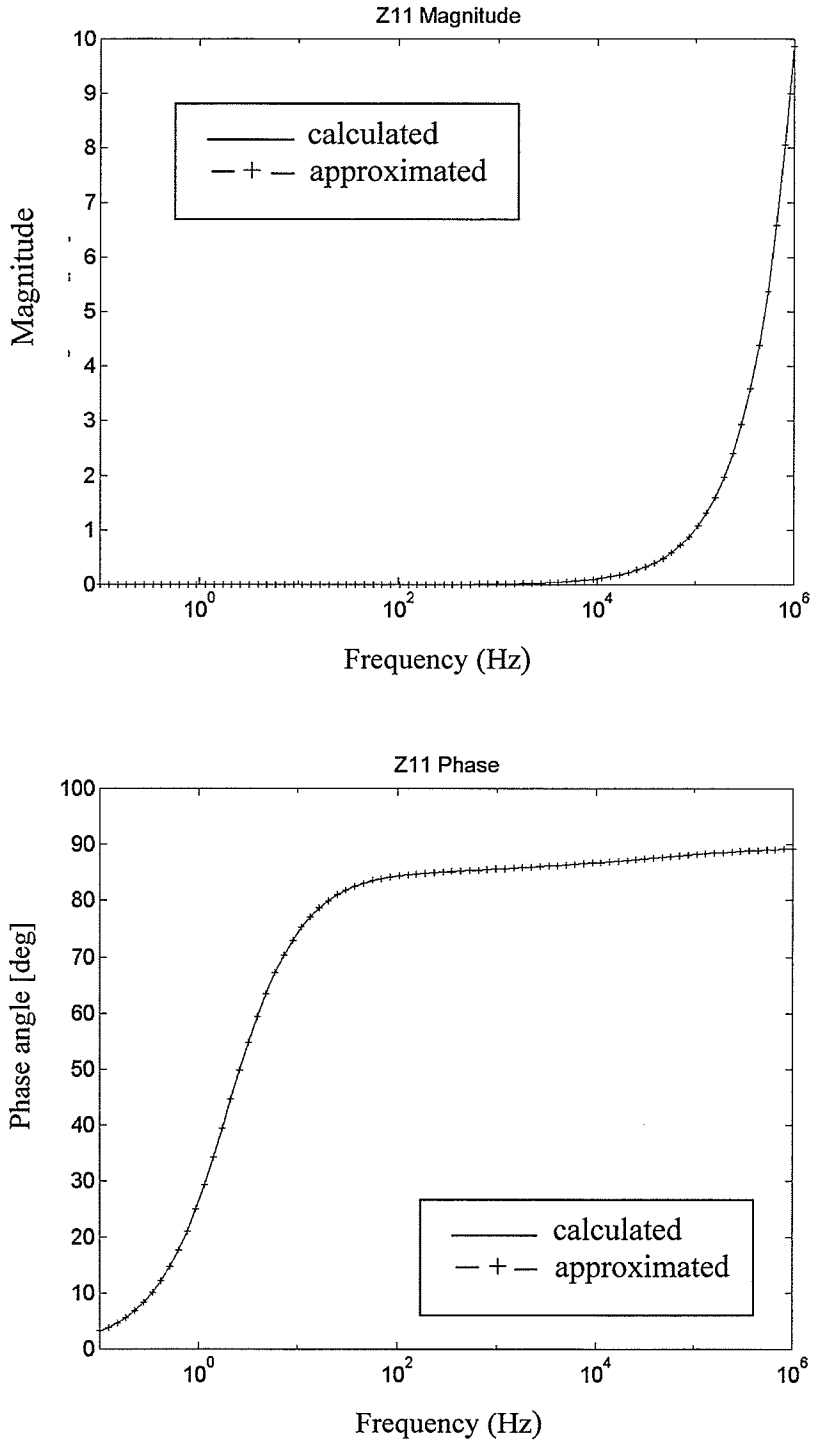

Fig. 5.16. Comparison of approximated line parameters with original data.

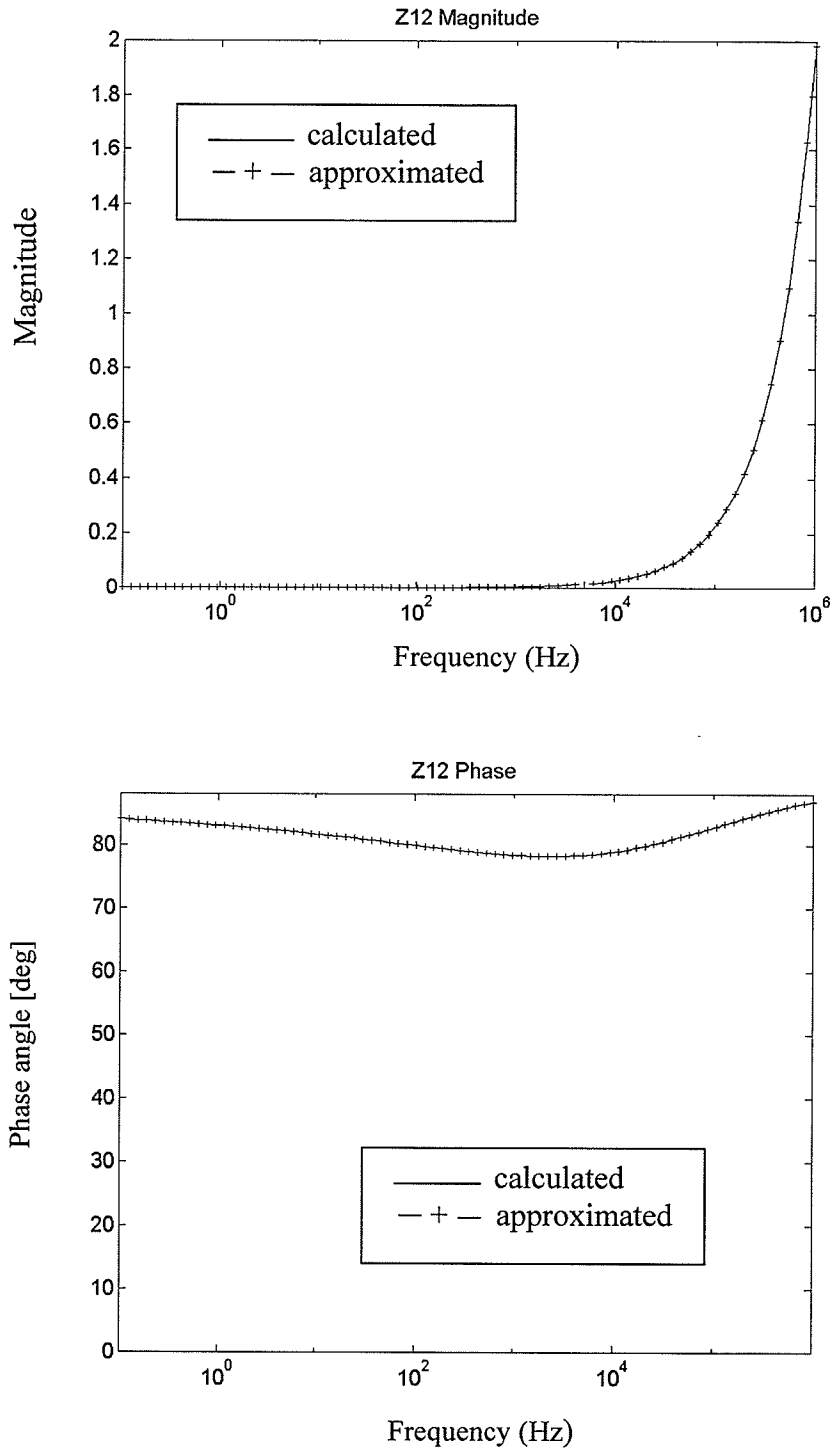

Fig. 5.17. Comparison of approximated line parameters with original data.

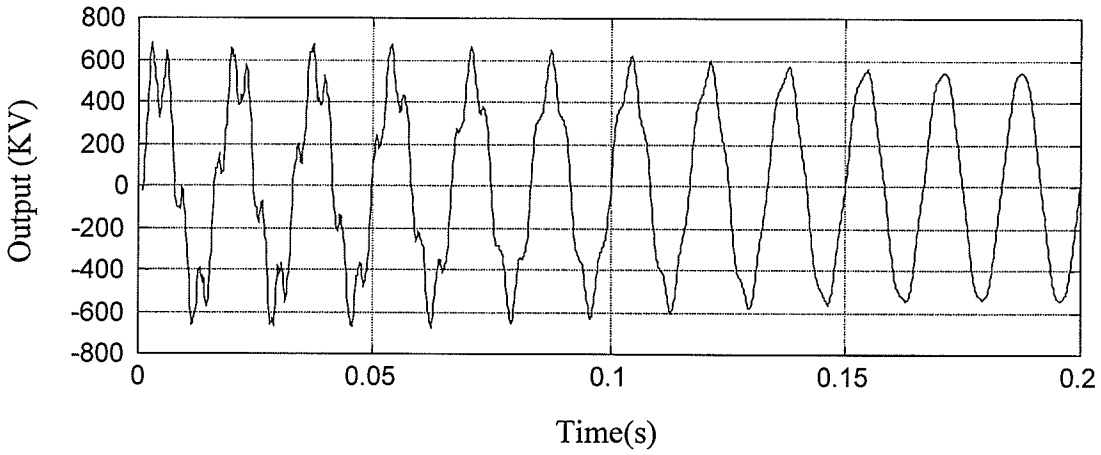

Fig. 5.18. Transient response at the load end of phase *A* of 3-phase transmission line obtained by using the improved multipoint Padé approximation method.

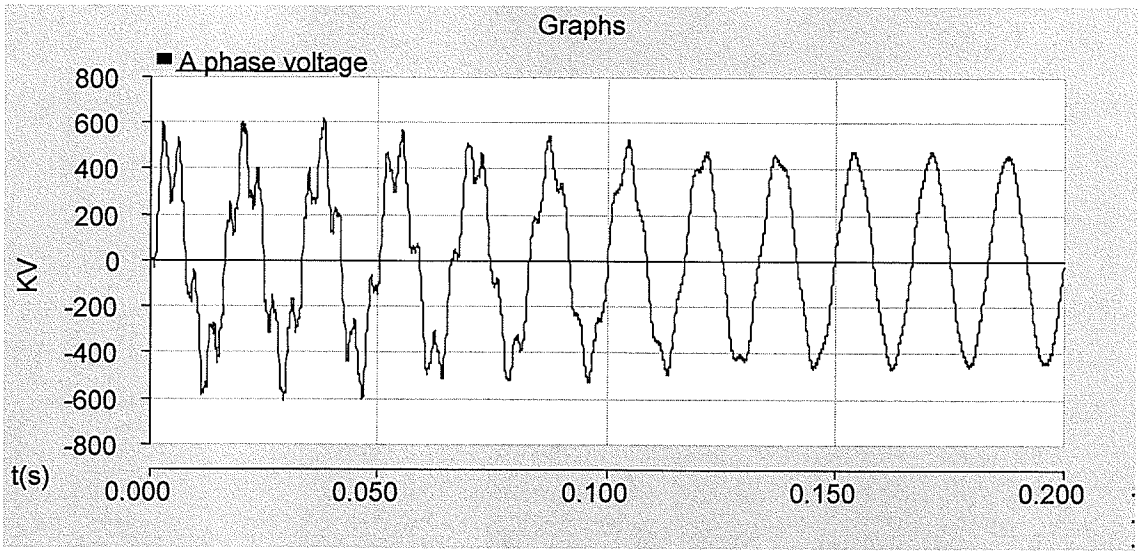

Fig. 5.19. Transient response at the load end of phase *A* of 3-phase transmission line obtained by using the PSCAD/EMTDC simulator [70], [71].

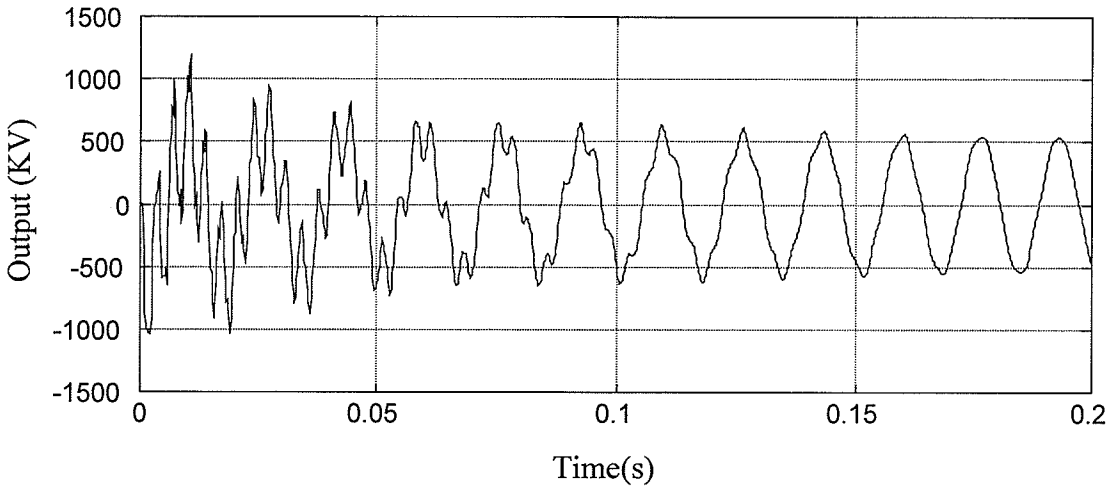

Fig. 5.20. Transient response at the load end of phase *B* of 3-phase transmission line obtained by using the improved multipoint Padé approximation method.

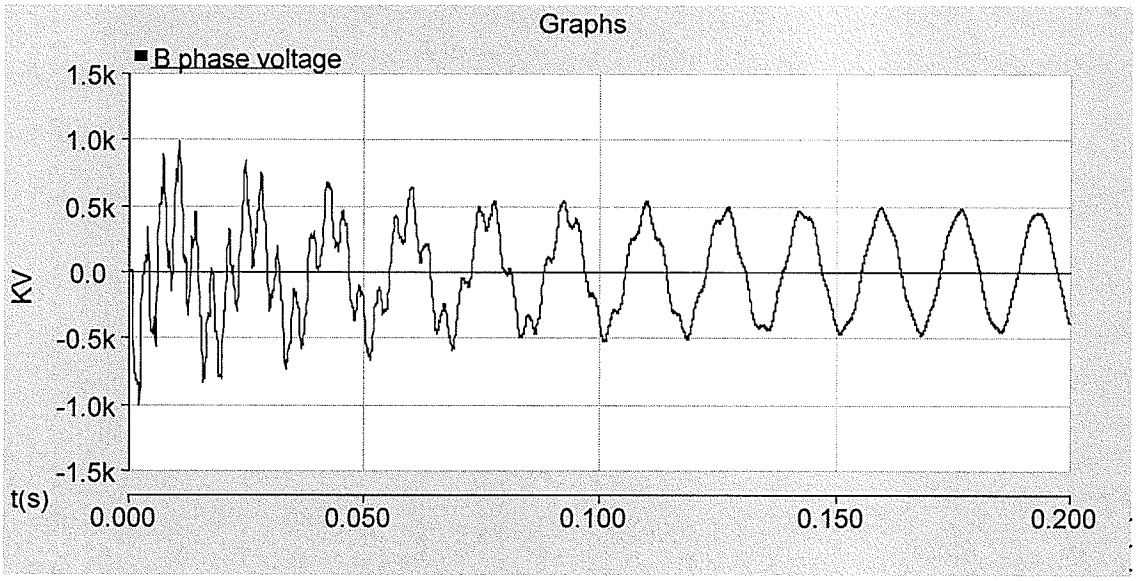

Fig. 5.21. Transient response at the load end of phase *B* of 3-phase transmission line obtained by using the PSCAD/EMTDC simulator [70], [71].

5.5. SUMMARY

Transients on frequency dependent transmission lines characterized with sampled or measured data have been studied using multipoint Padé approximations. In order to approximate the frequency dependent transmission line parameters that are obtained at a set of discrete frequency points, curve-fitting techniques, i.e. polynomial approximation and the vector fitting algorithm were briefly discussed. Combined with the polynomial approximation technique, the multipoint Padé approximation method presented in chapter three was successfully used to simulate an example circuit that contains multiconductor transmission lines with sampled frequency dependent parameters.

An improved multipoint Padé approximation method has been proposed for simulations of transients on power transmission lines. The new method is based on frequency band division technique and can eliminate the ill-conditioned problem associated with original multipoint Padé approximation when applied to analyze interconnect networks with frequency dependent parameters that vary over a very large bandwidth. Numerical examples of power transmission line systems, i.e., a single-phase power transmission line and a three-phase power transmission line, were simulated using the improved multipoint Padé approximation method.

Chapter 6. Conclusions and Suggestions

6.1. CONCLUSIONS

In this thesis interconnect networks consisting of linear lumped components and multiconductor transmission lines were analyzed using reduced–order model techniques. Specifically, an efficient method which is based on multipoint Padé approximations for all the moment sets available at all updated expansion points was proposed for solving interconnect problems. Since the computation effort associated with multipoint moment matching techniques is proportional to the number of frequency-expansion points, an improved algorithm for the selection of frequency expansion points was developed. As a result, the proposed method requires a smaller number of frequency expansion points when compared with existing multipoint moment matching techniques and considerable saving in CPU cost is achieved when compared with the conventional IFFT algorithm. In order to efficiently analyze interconnects with distributed transmission line models, a modified matrix exponential method was introduced for fast generation of the moments associated with frequency-dependent lossy transmission lines. Recursive formulas were derived for an efficient computation of the moments of frequency-dependent transmission lines and they can be readily incorporated into other moment matching techniques. It has been shown that the modified exponential method not only yields the same accuracy as the original matrix exponential method, but also has a computational efficiency which is comparable to that of the eigenvalue moment method. In addition, the proposed method

was successfully applied to analyze frequency dependent transmission lines characterized by sampled data. To simulate transients on interconnect networks having parameters that have a strong dependence over a very large bandwidth, such as power transmission lines, an improved multipoint Padé approximation method was presented. The improved multipoint Padé approximation method can eliminate the ill-conditioning problem that is observed when original multipoint Padé approximations are used to simulate transients on power transmission lines.

A variety of numerical examples were studied by using the proposed multipoint Padé approximation method and numerical results were given in chapters three, four and five of the thesis. In chapter three, two example circuits consisting of multiconductor transmission lines were first examined using the proposed multipoint Padé approximation method. Simulation results indicate that, with same number of moments employed at each expansion point, the proposed algorithm requires a smaller number of frequency expansion points when compared with existing multipoint moment-matching techniques. Also, the accuracy and convergence rates of solutions obtained by using the proposed method were investigated through the comparison of approximate frequency responses with the exact ones. A comparison of CPU cost was made through simulations of two relative large interconnect circuits using the proposed method, the CFH technique and the conventional method. In terms of the comparison, it is obvious that the proposed method exhibits a high computational efficiency, enabling it to be an efficient method for the analysis of large interconnect circuits containing distributed lossy transmission lines. The performance of the proposed modified matrix exponential method is demonstrated by numerical results given in chapter four. It was noticed that the proposed method can

generate transmission line moments that are identical to the original matrix exponential method, but with less computational effort. Under same the truncation criterion, the original matrix exponential method typically requires twice as many terms for convergence when compared with the proposed method. An extension of the proposed method to the case of interconnects modeled by coupled transmission lines with frequency-dependent parameters was presented in chapter five. The frequency dependency of line parameters is generally described in the form of sampled data. To calculate moments of frequency dependent transmission lines, adequate curve-fitting techniques are needed to approximate the measured/calculated frequency dependent line parameters. The vector fitting technique has an advantage over polynomial fitting in accurately approximating line parameters with strong frequency dependency over a wide frequency range. This is important for moment matching techniques as Padé approximations are sensitive to the accuracy of moments. In chapter five, applications of multipoint Padé approximations to simulate transients on frequency dependent power transmission lines are highlighted. From numerical experimentation, it is observed that power line parameters have strong frequency dependency over a wide frequency range, which is different from the cases typically found in high-speed interconnects or printed circuit boards. To compute transients on frequency dependent power transmission systems, it is necessary to accurately model line parameters over a wide frequency range. Also, the strong frequency dependency of the transmission line parameters can cause an ill-conditioning problem in the process of performing multipoint Padé approximations. Consequently, an improved multipoint Padé approximation method, which is based on frequency band division, should be used in simulation of interconnect networks with

wideband frequency dependence. It should be emphasized that although the improved multipoint Padé approximation method was developed to simulate transients on frequency dependent power transmission lines, it can also be used to analyze high-speed interconnect circuits where solutions over a wide frequency range are desired.

6.2. SUGGESTIONS FOR FURTHER STUDY

Even though the method/algorithm proposed in this thesis has been successfully applied to analyze a variety of interconnect and power transmission line examples, there are still several topics that may be interesting to explore in the future.

1. The multipoint Padé approximation technique can generate a stable reduced-order model, but the passivity of the reduced-order model is not necessarily ensured. The authors of [37]-[40] presented correction techniques that can be used in post-processing to enforce a non-passive reduced-order model to be passive. Combining these techniques with the multipoint Padé approximations and applying it to simulate interconnect networks would be a good practice.
2. For transient simulation of large power delivery networks, the development of reduced-order models from multiport power linear networks may be significant.
3. In chapter three, a bisection technique is coupled with the search algorithm for the selection of frequency expansion points. The frequency expansion point is always selected at the mid-point between two existing consecutive expansion points. An optimal selection of the location of the expansion points based on known moment information can further reduce the necessary number of expansion points.

4. By combining with other full-wave techniques, such as FEM, MoM or PEEC [79], the proposed method can be applied to solve general electromagnetic problems.

References

[1] H. B. Bakoglu, *Circuits, Interconnects and Packaging for VLSI*, Reading MA, Addison-Wesley, 1990.

[2] R. Achar and M. S. Nakhla, "Simulation of high-speed interconnects," *Proc. IEEE*, vol. 89, pp. 693-728, 2001.

[3] S. S. Gao, A. Y. Yang, and S. M. Kang, "Modeling and simulation of interconnection delays and crosstalks in high-speed integrated circuits, " *IEEE Trans. Circuits Syst.*, vol.37, pp. 1-9, Jan.1990.

[4] W. W. M. Dai, Guest Editor, "Special issue on simulation, modeling, and electrical design of high-speed and high-density interconnects," *IEEE Trans. Circuits Syst.*, vol. 39, pp. 857-982, Nov.1992.

[5] T. L. Quarles, " The SPICE3 implementation guide," Univ. California, Berkeley, Tech. Rep., ERL-M89/44, 1989.

[6] W. T. Weeks, A. J. Jimenez, G. W. Mahoney, D. Mehta, H. Quasemzadeh and T. R. Scott, " Algorithms for ASTAP – a network analysis program," *IEEE Trans. on Circuit Theory*, vol. 20, pp. 628-634, Nov. 1973.

[7] E. Chiprout and M. Nakhla, *Asymptotic Waveform Evaluation and Moment Matching for Interconnect Analysis*. Boston, MA: Kluwer, 1993.

[8] L. T. Pillage and R.A. Rohrer, "Asymptotic waveform evaluation for timing analysis," *IEEE Trans. Computer-Aided Design*, vol. 9, pp. 352-366, Apr.1990.

[9] J. E. Bracken, V. Raghavan, and R. A. Rohrer, "Interconnect simulation with asymptotic waveform evaluation (AWE)," *IEEE Trans. Circuits Syst.*, vol.39, pp. 869-878, Nov.1992.

[10] G. A. Baker Jr., *Essentials of* Padé *Approximants*. New York: Academic, 1975.

[11] T. Tang and M. S. Nakhla, "Analysis of high-speed VLSI interconnect using the asymptotic waveform evaluation technique," *IEEE Trans. Computer-Aided Design*, vol. 11, pp.341-352, Mar.1992.

[12] S. Lin and E. S. Kuh, "Transient simulation of lossy interconnects based on the recursive convolution formulation," *IEEE Trans. Circuits Syst.*, vol. 39, pp. 879-892, Nov.1992.

[13] E. Chiprout and M. S. Nakha, "Fast nonlinear waveform estimation of large distributed networks," in *Proc. IEEE MTT-S Int. Microwave Symp.* 1992, pp. 1341-1344.

[14] D. Xie and M. S. Nakhla, "Delay and crosstalk simulation of high speed VLSI interconnects with nonlinear terminations," *IEEE Trans. Computer-Aided Design*, vol. 12, pp. 1198-1811, Nov.1993.

[15] R. Achar, M. A. Kolbehdari, and M. Nakhla, "A unified approach for mixed EM and circuit simulation using model-reduction techniques," in *IEEE Int. Microwave Symp. Dig.*, June 1997, pp. 1017-1021.

[16] L. Y. Li and I. R. Ciric, "Application of a reduced-order model to transmission line analysis," in *Proc. ANTEM Symposium*, Ottawa, Ontario, Canada, 1998, pp. 409-412.

[17] J. E. Bracken, D. K. Sun, and Z. J. Cendes, "S-Domain methods for simultaneous time and frequency characterization of electromagnetic devices," *IEEE Trans. Microwave Theory Tech.*, vol. 46, pp. 1277-1290, Sep. 1998.

[18] X. M. Zhang and J. F. Lee, "Application of the AWE method with 3-D TVFEM to model spectral responses of passive microwave components," *IEEE Trans. Microwave Theory Tech.*, vol. 46, pp. 1735-1741, Nov. 1998.

[19] A. Cangellaris, M. Celik, S. Pasha, and L. Zhao, "Electromagnetic model order reduction for system-level modeling," *IEEE Trans. Microwave Theory Tech.*, vol. 47, pp. 840-849, June 1999.

[20] E. Chiprout and M. S. Nakhla, "Analysis of interconnect networks using complex frequency hopping," *IEEE Trans. Computer-Aided Design*, vol. 14 pp.186-200, Feb.1995.

[21] R. Sanaie, E. Chiprout, M. S. Nakhla, and Q. J. Zhang, "A fast method for frequency and time domain simulation of high-speed VLSI interconnects," *IEEE Trans. Microwave Theory Tech.*, vol. 42, pp. 2562-2571, Dec.1994.

[22] E. Chiprout, H. Heeb, M. S. Nakhla, and A. E. Ruehli, " Simulating 3D retarded interconnect models using complex frequency hopping (CFH)," in *Proc. IEEE Int. Conf. Computer-Aided Design(ICCAD)*, Nov. 1993, pp. 66-72.

[23] R. Achar, M. Nakhla, and Q. J. Zhang, "Full-wave analysis of high-speed interconnects using complex frequency hopping," *IEEE Trans. Compter-Aided Design, pp.* 997-1016, Oct. 1998.

[24] M. A. Kolbehdan, M. Srinivasan, M. Nakhla, Q. J. Zhang, and R. Achar, "Simultaneous time and frequency domain solution of EM problems using finite element and CFH techniques," *IEEE Trans. Microwave Theory Tech.*, vol. 44, pp. 1526-1534, Sept. 1996.

[25] L. Y. Li and I. R. Ciric, "Reduced-order models for field analysis of hybrid systems," *1999 IEEE Antennas and Propag. Society International Symp.*, July 1999, pp. 1712-1715.

[26] M. Celik, O. Ocali, M. A. Tan, and A. Atalar, "Pole-zero computation in microwave circuits using multipoint Padé approximation," *IEEE Trans. Circuis Syst.* I, vol. 42, pp. 6-13, 1995.

[27] P. Feldmann and R. W. Freund, "Efficient linear circuit analysis by Padé via Lanczos process," *IEEE Trans. Computer-Aided Design*, vol. 14, pp. 639-649, May 1995.

[28] I. M. Elfadel and D. D. Ling, "A block rational Arnoldi algorithm for multiport passive model-order reduction of multiport RLC networks," in *Proc. ICCAD-97*, Nov. 1997, pp. 66-71.

[29] L. M. Silviera, M. Kamen, I. Elfadel, and J. White, "A coordinate transformed Arnoldi algorithm for generating guaranteed stable reduced-order models for RLC circuits," in *Tech. Dig. ICCAD*, Nov. 1999, pp. 2288-2294.

[30] J. R. Phillips, L. Daniel, and L. M. Silveira, "Guaranteed passive balancing transformations for model order reduction," *IEEE Trans. Computer-Aided Design*, vol. 22, pp. 1027-1041, Aug. 2003.

[31] A. Odabasioglu, M. Celik, and L. T. Pillage, "PRIMA: Passive reduced-order interconnect macromodeling algorithm," *IEEE Trans. Computer-Aided Design*, vol. 17, pp. 645-654, Aug. 1998.

[32] K. J. Kerns and A. T. Yang, "Preservation of passivity during RLC network reduction via split congruence transformations," *IEEE Trans. Computer-Aided Design*, vol. 17, pp. 582-591, July 1998.

[33] Q. Yu, J. M. L. Wang and E. S. Kuh, "Passive Multipoint moment-matching model order reduction algorithm on multiport distributed interconnect networks," *IEEE Trans. Circuits Syst. I*, pp. 140-160, Jan. 1999.

[34] A. Dounavis, E. Gad, R. Achar, and M. Nakhla, "Passive model-reduction of multiport distributed networks," *IEEE Trans. Microwave Theory Tech.* pp. 2325-2334. Dec. 2000.

[35] P. Gunupudi, M. Nakhla, and R. Achar, "Simulation of high-speed distributed interconnects using Krylov-subspace techniques," *IEEE Trans. Computer-Aided Design*, vol. 19, pp. 799-808, July 2000.

[36] A. C. Cangellaris, S. Pasha, J. L. Prince, and M. Celik, "A new discrete time-domain model for passive model order reduction and macromodeling of high-speed interconnections," *IEEE Trans. Comp., Packag., Manufact. Technol.*, pp. 356-364, Aug. 1999.

[37] B. Gustavsen and A. Semlyen, "Enforcing passivity for admittance matrices approximated by rational functions," *IEEE Trans. Power Systems*, vol. 16, pp. 97-104, Feb. 2001.

[38] R. Achar, P. K. Gunupudi, M. Nakhla, and E. Chiprout, "Passive interconnect reduction algorithm for distributed/measured networks," *IEEE Trans. Circuits Syst. II*, pp. 287-301, Apr. 2000.

[39] D. Saraswat, R. Achar, and M. Nakhla, "Passive macromodels of microwave subnetworks characterized by measured/simulated data'" in *Int. Microwave Symp. Dig.*, Philadelphia, PA, June 2003, pp. 999-1002

[40] D. Saraswat, R. Achar, and M. Nakhla, "A fast algorithm and practical considerations for passive macromodeling of measured/simulated Data," *IEEE Trans. Adv. Packag.*, vol. 27, pp. 57-70, Feb. 2004.

[41] S. Pasha, M. Celik, A. C. Cangellaris, and J. L. Prince, "Passive spice-compatible models of dispersive interconnects," in *Proc. 49th Electron. Comp. Technol. Conf.*, June 1999, pp. 493-499.

[42] S. Pasha, A. C. Cangellaris, and J. L. Prince, "An all-purpose dispersive multiconductor interconnect model compatible with PRIMA," *IEEE Trans. Adv. Packag.* Vol. 24, pp. 126-130, May 2001.

[43] A. Dounavis, R. Achar, and M. S. Nakhla, "Efficient passive circuit models for distributed networks with frequency-dependent parameters," *IEEE Trans. Adv. Packag.*, vol. 23, pp. 382-392, Aug. 2000.

[44] A. Dounavis, R. Achar and M. Nakhla, "Passive macromodels for distributed high-speed networks," *IEEE Trans. Microwave Theory and Tech.* vol. 49, pp. 1686-1696, Oct. 2001.

[45] A. Dounavis, R. Achar, and M. Nakhla, "Addressing transient errors in passive macromodels of distributed transmission-networks," *IEEE Trans. Microwave Theory and Tech.*, vol. 50, pp. 2759-2768, Dec. 2002.

[46] G. Antonini, "A new methodology for the transient analysis of lossy and dispersive multiconductor transmission lines," *IEEE Trans. Microwave Theory and Tech.*, vol. 52, pp. 2227-2239, Sept. 2004.

[47] S. K. Lele, "Compact finite difference schemes with spectral-like resolution," *J. Comput. Phys.*, vol. 103, pp. 16-42, 1992.

[48] A. J. Gruodis, and C. S. Chang, "Coupled lossy transmission line characterization and simulation," *IBM J. Res. Dev.*, vol. 25, pp. 25-41, Jan. 1981.

[49] I. Elfadel, H. Huang, A. Ruehli, A. Dounavis, and M. Nakhla, "A comparative study of two transient analysis algorithms for lossy transmission lines with frequency-dependent data," *IEEE Trans. Adv. Packag.*, vol. 25, pp. 143-153, 2002.

[50] I. Elfadel, A. Dounavis, H. Huang, M. Nakhla, A, Ruehli, and R. Achar, "Accuracy and performance of passive transmission line macromodels based on optimal matrix rational approximations," in *Proc. 11th Topical Meeting on EPEP*, Oct. 2002, pp. 351-354.

[51] C. W. Ho, A. E. Ruehli, and P. A. Brennan, "The modified nodal approach to network analysis," *IEEE Trans. Circuits Syst.*, vol. 22, pp. 504-509, June 1975.

[52] L. Y. Li, G. E. Bridges, and I. R. Ciric, "Efficient simulation of interconnects networks with frequency-dependent lossy transmission lines," *IEEE Microwave and Wireless Components Letters,* vol. 12, pp. 131-133, Apr. 2002.

[53] B. D. Anderson and S. Vongpanitlerd, *Network analysis and Synthesis*. Englewood Cliffs, NJ, 1973.

[54] M. Celik and A. C. Cangellaris, "Efficient transient simulation of lossy packaging interconnects using moment-matching techniques," *IEEE Trans. Comp., Packag., Manufact. Tech. B*, vol. 19, pp. 64-73, Feb. 1996.

[55] M. Celik and A. C. Cangellaris, "Simulation of dispersive multiconductor transmission lines by Padé approximation via the Lanczos process," *IEEE Trans. Microwave Theory Tech.*, vol. 44, pp. 2525-2535, Dec. 1996.

[56] M. Celik and A. C. Cangellaris, "Simulation of multiconductor transmission lines using Krylov subspace order-reduction techniques," *IEEE Trans. Computer-Aided Design*, vol. 16, pp. 485-496, May 1997.

[57] H.D.Young, *Statistical Treatment of Experiment Data*, McGraw-Hill, New York, 1962.

[58] C. R. Paul, *Analysis of Multiconductor Transmission Lines*, New York: Wiley, 1994.

[59] R. Khazaka, E. Chiprout, M. Nakhla, and Q. J. Zhang, "Analysis of high-speed interconnects with frequency dependent parameters," in *Proc. Int. Symp. EMC*, Zurich, Switzerland, Mar. 1995, pp. 203-208.

[60] M. Celik, A. C. Cangellaris, and A. Deutsch, "A new moment generation technique for interconnects characterized by measured or calculated S-parameters," *in IEEE Int. Microwave Symp. Dig.*, June 1996, pp. 196-201.

[61] K. M. Coperich, J. Morsey, V. I. Okhmatovski, A. C. Cangellaris, and A. E. Ruehli, "Systematic development of transmission line models for interconnects with frequency-dependent losses," *IEEE Trans. Microwave Theory and Tech.*, vol. 49, pp. 1677-1685, Oct. 2001.

[62] K. Coperich, J. Morsey, V. Okhmatovski, A. C. Cangellaris, and A. Ruehli, "Systematic development of transmission line models for interconnects with frequency-dependent losses," in *Proc. 9th Topical Meeting on EPEP*, Oct. 2002, pp. 221-224.

[63] B. Gustavsen and A. Semlyen, "Rational approximation of frequency domain responses by vector fitting," *IEEE, Trans. Power Delivery*, vol. 14, pp. 1052-1059, July 1999.

[64] B. Gustavsen and A. Semlyen, " Simulation of transmission line transients using vector fitting and model decomposition," *IEEE Trans. Power Delivery*, vol. 13, pp. 605-612, April 1998.

[65] W. T. Beyene and J. E. Schutt-Aine, "Efficient transient simulation of high-speed interconnects characterized by sampled data," *IEEE Trans. Comp., Packag., Manufact. Technol. B*, vol. 21, pp. 105-113, Feb. 1998.

[66] W. T. Beyene and J. E. Schutt-Aine, "Accurate frequency-domain modeling and efficient simulation of high-speed packaging interconnects," *IEEE Trans. Microwave Theory Tech.*, pp. 1941-1947, Oct. 1997.

[67] R. Neumayer, F. Haslinger, A. Stelzer, and R. Weigel, "On the synthesis of equivalent circuit models for multiports characterized by frequency-dependent parameters," IEEE Trans. Microwave Theory and Tech., vol. 50, pp. 2789-2796, Dec. 2002.

[68] M. Elzinga, K. Virga, L. Zhao, and J. L. Prince, "Pole-residue formulation for transient simulation of high-frequency interconnects using householder LS curve-fitting techniques," *IEEE Trans. Adv. Packag.*, vol. 25, pp. 142-147, May 2000.

[69] M. Elzinga, K. L. Virga, and J. L. Prince, "Improved global rational approximation macromodeling algorithm for networks characterized by frequency-sampled data," *IEEE Trans. Microwave Theory and Tech.*, vol. 48, pp. 1461-1468, Sept. 2000.

[70] D. Woodford, *Introduction to PSCAD V3*, Manitoba Hydro Research Center Inc., Winnipeg, MB, 2001.

[71] The Manitoba HVDC Research Centre, Winnipeg, MB, PSCAD/EMTDC Power Systems Simulation Software, 1994.

[72] L. Y. Li, G. E. Bridges and I. R. Ciric, "Efficient simulation of multiconductor transmission lines using order-reduction techniques," in *Proc. ANTEM Symposium*, Winnipeg, Manitoba, Canada, Aug. 2000, pp. 265-269.

[73] L. Y. Li, G. E. Bridges and I. R. Ciric, "An efficient method for frequency-domain and transient analysis of interconnect networks," *2000 IEEE Antennas and Propag. Society International Symp.*, July 2000, pp. 132-135.

[74] L. Y. Li, G. E. Bridges, and I. R. Ciric, "Analysis of high-speed interconnects using efficient multipoint Padé approximation," *Electron Lett.*, vol. 37, pp. 874-875, July 2001.

[75] L. Y. Li, G. E. Bridges, and I. R. Ciric, "Efficient transient simulation of networks containing lossy frequency-dependent interconnects," in *Proc. ANTEM Symposium*, Montreal, Quebec, Canada, Aug. 2002, pp. 553-557.

[76] Ling Y. Li, G. E. Bridges, and I. R. Ciric, "Simulation of transient on frequency dependent transmission line using an improved multipoint Padé approximation technique," in *Proc. ANTEM Symposium*, Ottawa, Ontario, Canada, Aug. 2004, pp. 285-288.

[77] J. R. Carson, "Wave propagation in overhead wires with ground return," BSTJ, vol. 5, pp. 539-554, 1926.

[78] W. S. Meyer and H. W. Dommel, "Numerical modeling of frequency-dependent transmission line parameters in an electromagnetic transient program," *IEEE Trans. Power Apparatus and Systems*, vol. 93, pp. 1401-1409, Sept/Oct., 1974

[79] A. E. Ruehli, "Equivalent circuit models for three dimensional multicondutor systems," *IEEE Trans. Microwave Theory and Tech.* Vol. 22, pp. 216-221, March 1974.